Applied Catalysis B: Environmental 166–167 (2015) 603–643

Contents lists available at ScienceDirect

Applied Catalysis B: Environmental

journal homepage: www.elsevier.com/locate/apcatb

Review

Decontamination of wastewaters containing synthetic organic dyes by electrochemical methods. An updated review

Enric Brillas[a,*], Carlos A. Martínez-Huitle[b]

[a] Laboratori d'Electroquímica dels Materials i del Medi Ambient, Departament de Química Física, Facultat de Química, Universitat de Barcelona, Martí i Franquès 1-11, 08028 Barcelona, Spain
[b] Laboratório de Eletroquímica Ambiental e Aplicada, Instituto de Química, Universidade Federal do Rio Grande do Norte, Lagoa Nova CEP 59.072-900, RN, Brazil

ARTICLE INFO

Article history:
Received 28 August 2014
Received in revised form 29 October 2014
Accepted 8 November 2014
Available online 15 November 2014

Keywords:
Electrochemical oxidation
Hydroxyl radical
Active chlorine species
Electro-Fenton
Photoelectrocatalysis

ABSTRACT

As the environment preservation gradually becomes a matter of major social concern and more strict legislation is being imposed on effluent discharge, more effective processes are required to deal with non-readily biodegradable and toxic pollutants. Synthetic organic dyes in industrial effluents cannot be destroyed in conventional wastewater treatment and consequently, an urgent challenge is the development of new environmentally benign technologies able to mineralize completely these non-biodegradable compounds. This review aims to increase the knowledge on the electrochemical methods used at lab and pilot plant scale to decontaminate synthetic and real effluents containing dyes, considering the period from 2009 to 2013, as an update of our previous review up to 2008. Fundamentals and main applications of electrochemical advanced oxidation processes and the other electrochemical approaches are described. Typical methods such as electrocoagulation, electrochemical reduction, electrochemical oxidation and indirect electro-oxidation with active chlorine species are discussed. Recent advances on electrocatalysis related to the nature of anode material to generate strong heterogeneous •OH as mediated oxidant of dyes in electrochemical oxidation are extensively examined. The fast destruction of dyestuffs mediated with electrogenerated active chlorine is analyzed. Electro-Fenton and photo-assisted electrochemical methods like photoelectrocatalysis and photoelectro-Fenton, which destroy dyes by heterogeneous •OH and/or homogeneous •OH produced in the solution bulk, are described. Current advantages of the exposition of effluents to sunlight in the emerging photo-assisted procedures of solar photoelectrocatalysis and solar photoelectro-Fenton are detailed. The characteristics of novel combined methods involving photocatalysis, adsorption, nanofiltration, microwaves and ultrasounds among others and the use of microbial fuel cells are finally discussed.

Contents

* Corresponding author. Tel.: +34 93 4021223; fax: +34 93 4021231.
E-mail addresses: brillas@ub.edu (E. Brillas), carlosmh@quimica.ufrn.br (C.A. Martínez-Huitle).

http://dx.doi.org/10.1016/j.apcatb.2014.11.016
0926-3373/

1. Introduction

The contamination of water bodies by man-made organic chemicals is definitely a critical issue that the recent water framework directives are trying to address in order to ensure good water quality status and healthy ecosystems [1,2]. Although major attention is currently paid to persistent and emerging pollutants, especially if they are likely to endocrine disrupting activity, water pollution by synthetic dyes is also of great concern due to the large worldwide production of dyestuffs. Several studies have reported that there are more than 100,000 commercially available dyes with an estimated annual production of over 7×10^5 tons of dye-stuff [3]. Industries such as textile, cosmetic, paper, leather, light-harvesting arrays, agricultural research, photoelectrochemical cells, pharmaceutical and food produce large volumes of wastewater polluted with high concentration of dyes and other components [4]. The pollutants in these effluents include organic and inorganic products like finishing agents, surfactants, inhibitor compounds, active substances, chlorine compounds, salts, dyeing substances, total phosphate, dissolved solids and total suspended solids (TSS) [5]. However, coloring matter is the major problem because it creates an esthetic problem and its color discourages the downstream use of wastewater [6]. Esthetic merit, gas solubility and water transparency are affected by the presence of dyes even in small amount or concentrations [7].

Dyes can be classified as Acid, Basic, Direct, Vat, Sulfur, Reactive, Disperse, metal complexes, etc., including antraquinone, indigoide, triphenylmethyl, xanthene and phthalocyanine derivatives. This classification expresses a general characteristic property of the dye (see more information in Ref. [8]). For example, Acid means that it is negatively charged, Basic when it is positively charged, Reactive if it is an anionic dye used in the textile industry, Mordant if it contains a metallic ion, Vat when it derives of natural indigo, Disperse when it is a non-ionic dye used in aqueous dispersion and so on. This nomenclature, followed by the name of its color and an order number, gives the color index (C.I.) name of the dye [8].

According to Jin et al. [9] and Solís et al. [10], about 280,000 tons of textile dyes are currently discharged in effluents every year because large volumes of wastewaters are generated in various processes of this industry such as sizing, scouring, bleaching, mercerizing, dyeing, printing and finishing [11,12]. For example, Reactive dyes with good water solubility and easily hydrolyzed into insoluble forms are lost in about 4% during dyeing [4]. As a result, dye effluents contain chemicals that are toxic, carcinogenic, mutagenic or teratogenic to various fish species [7]. Azo dyes are the most widely used dyes and represent over 70% of their total production [2,4,10,13]. They are complex aromatic compounds with large structural diversity that always provide a high degree of chemical, biological and photocatalytic stability and breakdown resistance with time, exposure to sunlight, microorganisms, water and soap; in other words, they are resistant to degradation [14]. For this reason, many studies have been focused mainly on the removal of azo dyes from waters. Nevertheless, the introduction of synthetic fibers has led to the appearance of some niche markets that require the use of other classes of dyes, becoming a new great environmental problem.

An extensive literature has reported the characteristics and applications of most important methods for removing dyes from water [3,4,8,10,13,15–20]. Fig. 1 summarizes their main technologies classified as physicochemical, chemical, advanced oxidation processes (AOPs), biological and electrochemical. The mechanisms for color removal involve physical dye separation, breakdown of the dyes or decolorization by adsorption/biodegradation [3,5,8].

The physicochemical techniques include coagulation/flocculation, adsorption and membrane separation. In coagulation, Sulfur and Disperse dyes are removed from the electrostatic attraction between oppositely charged soluble dye and polymer molecule. Acid, Direct, Vat and Reactive dyes also coagulate but do

List of abbreviations

Acronyms

ACF	activated carbon fiber
AOP	advanced oxidation process
ABS^M	average absorbance
BDD	boron-doped diamond
CNT	carbon nanotube
DSA	dimensionally stable anode
EAOP	electrochemical advanced oxidation process
EO	electrochemical oxidation
EC	electrocoagulation
EF	electro-Fenton
ITO	indium tin oxide
MW	microwave
GC–MS	gas chromatography–mass spectrometry
HPLC	high-performance liquid chromatography
LC–MS	liquid chromatography–mass spectrometry
MFC	microbial fuel cell
MCE	mineralization current efficiency
PEC	photoelectrocatalysis
PEF	photoelectro-Fenton
PTFE	polytetrafluoroethylene
ROS	reactive oxygen species
RVC	reticulated vitreous carbon
SCE	saturated calomel electrode
SHE	standard hydrogen electrode
SPEC	solar photoelectrocatalysis
SPEF	solar photoelectro-Fenton
SS	stainless steel
US	ultrasound
UV	ultraviolet
UVA	ultraviolet A
UVB	ultraviolet B
UVC	ultraviolet C
UV–vis	ultraviolet–visible

Symbols

E_{anod}	anodic potential (V)
E_{cat}	cathodic potential (V)
COD	chemical oxygen demand (mg O_2 dm^{-3})
I	current (A)
j	current density (mA cm^{-2})
t	electrolysis time (s, min, h)
EC_{COD}	energy cost per unit COD mass (kWh $(g\,COD)^{-1}$)
EC_{TOC}	energy cost per unit TOC mass (kWh $(g\,TOC)^{-1}$)
EC	energy cost per unit volume (kWh m^{-3})
F	Faraday constant (96,487 C mol^{-1})
C_0	initial dye concentration (mg dm^{-3}, mM)
λ_{max}	maximum wavelength (nm)
E_{cell}	potential difference of the cell (V)
k_1	pseudo-first-order rate constant (s^{-1})
t_r	retention time (min)
k_2	second-order rate constant (M^{-1} s^{-1})
V_s	solution volume (dm^3)
Q	specific charge (Ah dm^{-3})
E°	standard redox potential (V/SHE)
TOC	total organic carbon (mg C dm^{-3})
TSS	total suspended solids (mg dm^{-3})
λ	wavelength (nm)

not settle, whereas cationic dyes do not coagulate. However, this approach generates large amounts of sludge and high content of dissolved solids remains in the effluent. Adsorption allows good removal of dyes from the effluent, but the adsorbent regeneration is expensive and involves the loss of adsorbent. The use of appropriate membranes is capable of removing all types of dyes, being a compact technology without generation of sludge. However, the high cost of membranes and equipment, the lowered productivity with time due to fouling of the membrane and the disposal of concentrates are the principal limitations [3,8,17].

Many biological treatments have been studied including anaerobic process, oxidation, trickling filters, activated sludge process and so on [3,8,10,18]. Microbial biomass is also commonly used for the treatment of industrial effluents. Microorganisms such as algae, fungi, bacteria and yeasts are capable to degrade certain type of dyes. Biological methods are environmentally friendly, produce less sludge than physicochemical systems and are relatively inexpensive. Nevertheless, their application is limited since biological treatment needs a large land area, has sensitivity toward toxicity of certain chemicals and treatment time is very high. Moreover, some dyes are generally toxic and are not easily biodegraded [16].

More powerful chemical methods such as ozonation and oxidation with hypochlorite ion, as well as AOPs such as Fenton's reagent and photocatalytic systems like TiO_2/UV, H_2O_2/UV and O_3/UV, provide fast decolorization and degradation of dyes. AOPs are environmentally friendly methods involving the on-site generation of highly reactive oxygen species (ROS) such as (primarily, but not exclusively) hydroxyl radicals ($^\bullet$OH) that control the degradation mechanism [2,20]. Nevertheless, the use of these methods is not currently well accepted because they are quite expensive and have operational problems [3,4,8,15,17].

Electrochemical technologies have emerged as novel treatment technologies for the elimination of a broad-range of organic contaminants from water. The environmental application of electrochemical approaches has been the topic of several books and reviews [4,11,15,19,21–37], summarizing and discussing their use for the prevention and remediation of pollution problems because the electron is a clean reagent. Several advantages include high energy efficiency, amenability to automation, easy handling because of the simple equipment required, safety because they operate under mild conditions (ambient temperature and pressure) and versatility. They can be applied to effluents with chemical oxygen demand (COD) from 0.1 to about 100 g dm^{-3} [33]. Among these technologies, electrochemical advanced oxidation processes (EAOPs) have received great attention, although other electrochemical approaches can also be effectively used for treating industrial effluents. The strategies of electrochemical technologies include not only the treatment of effluents and wastes, but also the development of new processes or combined methods with less harmful effects, often denoted as process-integrated environmental protection.

Before 2000, only a little number of studies was devoted to show the interest of electrochemical technologies for destroying dyes from wastewaters [3,15,17,23]. After that, many research groups have dedicated great efforts to propose EAOPs and other electrochemical approaches as potential alternatives for removing dyes from synthetic and industrial effluents. The significant development of emerging electrochemical technologies for the remediation of dyestuffs wastewaters up to the year 2008 has been appointed in our previous review [4]. The growing interest of academic and industrial communities in the applicability of electrochemical technologies for removing dyes, especially EAOPs, has been reflected in the last 5 years by a high number of publications in peer-reviewed journals, patents and international conferences.

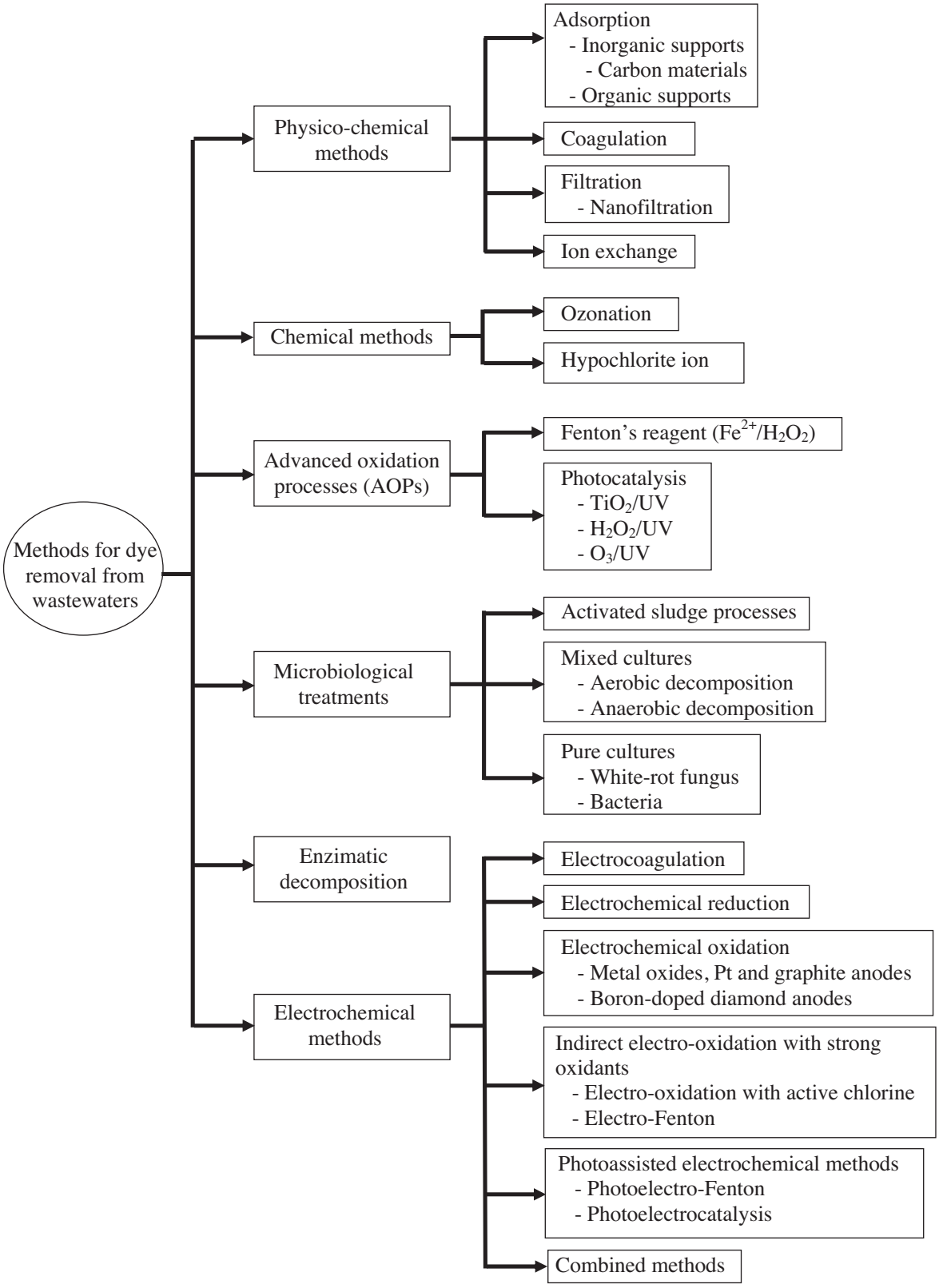

Fig. 1. Main methods applied to the removal of organic dyes from wastewaters.

Fig. 2 illustrates a general scenario of the papers published in the last 5 years over the treatment of dyes as a function of the electrochemical technology used, including several reviews describing the application of some of such methods [10,11,30,31,34–37]. As can be seen, the most popular method is electrochemical oxidation (EO), classified as an EAOP since heterogeneous •OH is generated at the anode surface. Other typical methods are electrocoagulation (EC) and indirect electro-oxidation with strong oxidants including electro-oxidation with active chlorine and electro-Fenton (EF). This latter method and photo-assisted electrochemical methods such as

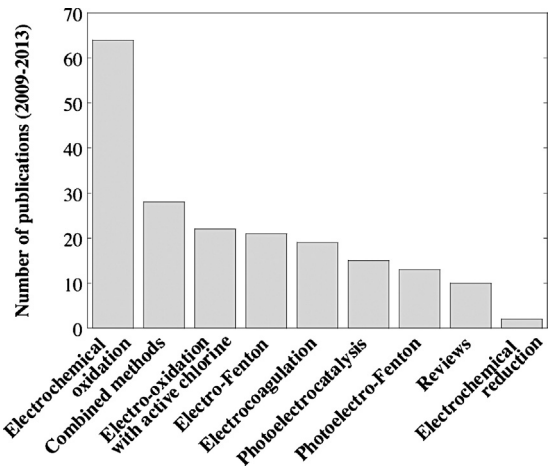

Fig. 2. Number of publications devoted to the electrochemical treatment of organic dyes in synthetic and real water effluents in the period 2009–2013.

photoelectrocatalysis (PEC) and photoelectro-Fenton (PEF) are well established EAOPs where dyes can be destroyed by heterogeneous •OH and/or homogeneous •OH produced in the solution bulk. Note the recent exposition of effluents to sunlight in the photo-assisted methods leading to solar PEC (SPEC) and solar PEF (SPEF). A large variety of combined methods have also been recently developed including the coupling of EAOPs with photocatalysis, adsorption, nanofiltration, microwaves (MW) and ultrasounds (US) among others and the use of microbial fuel cells (MFC). Conversely, studies on the possible application of electrochemical reduction have been very limited.

The present paper aims to increase the knowledge related to the most relevant applications of all the electrochemical approaches by reviewing lab and pilot plant experiments to treat synthetic and real effluents containing dyes from 2009 to 2013, as an update of our previous review up to the year 2008 [4]. Fundamentals of each technology are briefly discussed to better understand its advantages and limitations for the environmental prevention of pollution with special focus on the application of new interesting electrochemical technologies developed in the last years like SPEC, SPEF and many combined methods.

2. Decolorization, mineralization and energetic parameters

Schemes of relevant bench-scaled electrochemical systems used for EC, EO, EF, PEF and PEC are shown in Figs. 4, 5, 8a, 10, 25 and 30a of our previous review on dyes [4]. The decay in color of dyes wastewaters during electrochemical treatment is usually monitored from the decolorization efficiency or percentage of color removal by Eq. (1) [4]:

$$\text{Color removal}\,(\%) = \frac{{ABS_0}^{M} - {ABS_t}^{M}}{{ABS_0}^{M}} \times 100 \quad (1)$$

where ${ABS_0}^{M}$ and ${ABS_t}^{M}$ are the average absorbances before electrolysis and after an electrolysis time t, respectively, at the maximum visible wavelength (λ_{max}) of the wastewater determined from UV–vis spectrophotometry. The substitution of dye concentration by ABS^{M} in Eq. (1) is a typical mistake that should be avoided since it has been demonstrated that colored products with similar λ_{max} to the starting dye can also be produced, then prolonging the decolorization process [38,39].

The degradation process of dye-stuffs solutions can be monitored from the decay of their COD and/or total organic carbon (TOC). COD is related to the oxidation of organics, whereas TOC informs about their mineralization. These data allow calculating the percentages of COD and TOC removal (or decay) as follows [4]:

$$\text{COD removal}\,(\%) = \frac{\Delta\text{COD}}{\text{COD}_0} \times 100 \quad (2)$$

$$\text{TOC removal}\,(\%) = \frac{\Delta\text{TOC}}{\text{TOC}_0} \times 100 \quad (3)$$

where ΔCOD and ΔTOC are the experimental COD and TOC decays (in mg dm^{-3}), respectively, at electrolysis time t and COD_0 and TOC_0 are the corresponding initial values before treatment. The current efficiency can then be determined from ΔCOD (in g dm^{-3}) by Eq. (4) [4]:

$$\text{Current efficiency}\,(\%) = \frac{(\Delta\text{COD})FV_s}{8It} \times 100 \quad (4)$$

where F is the Faraday constant (96,487 C mol^{-1}), V_s is the solution volume (in dm^3), I is the applied current (in A), 8 is the oxygen equivalent mass (in g eq^{-1}) and t is the electrolysis time (in s). When TOC is measured, the mineralization current efficiency (MCE) at a given time t (in h) can be estimated from Eq. (5) [40,41]:

$$\text{MCE}\,(\%) = \frac{nFV_s(\Delta\text{TOC})}{4.32 \times 10^7 mIt} \times 100 \quad (5)$$

where n refers the number of electrons exchanged in the mineralization process of the dye, 4.32×10^7 is a conversion factor for units homogenization (=3600 s h^{-1} × 12,000 mg C mol^{-1}) and m is the number of carbon atoms of the dye.

Energetic parameters are essentials figures-of-merit to assess the viability of electrochemical treatments of dyes for industrial application. Operating at constant I (in A), the specific energy consumption per unit volume (EC), unit COD mass (EC_{COD}) and unit TOC mass (EC_{TOC}) are obtained from the following expressions [4,39]:

$$\text{EC}\,(\text{kWh m}^{-3}) = \frac{E_{cell}It}{V_s} \quad (6)$$

$$\text{EC}_{\text{COD}}\,(\text{kWh}\,(\text{g COD})^{-1}) = \frac{E_{cell}It}{(\Delta\text{COD})V_s} \quad (7)$$

$$\text{EC}_{\text{TOC}}\,(\text{kWh}\,(\text{g TOC})^{-1}) = \frac{E_{cell}It}{(\Delta\text{TOC})V_s} \quad (8)$$

where E_{cell} is the average potential difference of the cell (in V), t is the electrolysis time (in h), V_s is the solution volume (in L) and (ΔCOD) or (ΔTOC) are the corresponding experimental abatements of COD and TOC (in mg L^{-1}), respectively.

Note that high current efficiencies of MCE calculated from Eq. (4) or (5) and low specific energy consumptions determined from Eqs. (6) and (7) are preferable to be used in a given treatment to be useful in practice.

3. Electrocoagulation

In EC, Fe or Al anodes immersed in the polluted water are dissolved by the pass of a current to yield different Fe(II) (and/or Fe(III)) or Al(III)) species with hydroxide ions, respectively, depending on the effluent pH [25]. These species act as coagulant/flocculant for the separation of dyes and other charged pollutants from the wastewater. Moreover, electroflotation also takes place when the bubbles of H_2 gas evolved at the cathode can attach the coagulated particles to transport them to the solution surface where they are separated. Fig. 3 schematizes the different phenomena occurring in EC [42].

EC is more effective and yields more rapid dyes separation with smaller amount of produced sludge and lower operating costs than traditional coagulation [25,26], where Fe^{3+} or Al^{3+} ions, usually in the form of sulfate and chlorides salts, are directly added to the wastewater as coagulating agents of dyes. The displacement

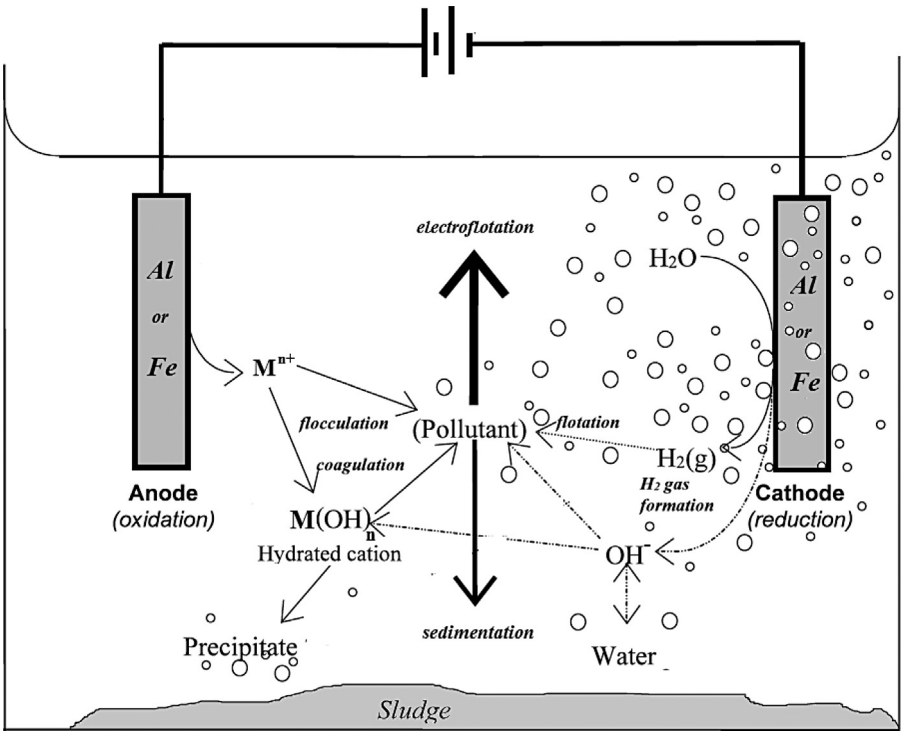

Fig. 3. Mechanism for electrocoagulation (EC).

Adapted from Ref. [42].

of anions and cations under the electric field applied to the electrodes in EC enhances the collision between charged particles, thereby increasing the efficiency of coagulation. However, anode passivation and sludge deposition on the electrodes, inhibiting the electrolytic process, as well as the production of high amount of iron and aluminum ions solved in the effluent, which need to be removed, are the main disadvantages of EC [25].

The characteristic behavior of EC for each sacrificial anode and recent applications to the treatment of dyeing solutions are presented in subsections below. Table 1 summarizes selected results reported for Fe or Al alone, as well as when both anodes were comparatively used.

3.1. EC with Fe anode

In EC, the oxidation of a sacrificial Fe anode yields the dissolution of Fe^{2+} in the effluent from reaction (9) with a standard potential $E^\circ = -0.44$ V/SHE, whereas OH^- and H_2 gas are formed at the cathode from reaction (10) with $E^\circ = -0.83$ V/SHE [43–45]:

$$Fe \rightarrow Fe^{2+} + 2e^- \quad (9)$$

$$2H_2O + 2e^- \rightarrow 2OH^- + H_{2(g)} \quad (10)$$

At pH > 5.5, $Fe(OH)_2$ precipitates by reaction (11) remaining in equilibrium with Fe^{2+} up to pH 9.5 or with monomeric species such as $Fe(OH)^+$, $Fe(OH)_2$ and $Fe(OH)_3^-$ at higher pH values. In the presence of dissolved O_2 gas, insoluble $Fe(OH)_{3(s)}$ is generated from Fe^{2+} oxidation via reaction (12) and released protons can be directly reduced to H_2 gas at the cathode by reaction (13) giving the total reaction (14) in the electrolytic cell.

$$Fe^{2+} + 2OH^- \rightarrow Fe(OH)_{2(s)} \quad (11)$$

$$4Fe^{2+} + 10H_2O + O_{2(g)} \rightarrow 4Fe(OH)_{3(s)} + 8H^+ \quad (12)$$

$$8H^+ + 8e^- \rightarrow 4H_{2(g)} \quad (13)$$

$$4Fe + 10H_2O + O_{2(g)} \rightarrow 4Fe(OH)_{3(s)} + 4H_{2(g)} \quad (14)$$

Note that $Fe(OH)_3$ coagulates from pH > 1.0, thereby being present in more acidic media than $Fe(OH)_2$. $Fe(OH)_3$ precipitate can be in equilibrium with soluble monomeric species like Fe^{3+}, $Fe(OH)^{2+}$, $Fe(OH)_2^+$, $Fe(OH)_3$ and $Fe(OH)_4^-$ depending on the pH range [4]. The insoluble flocs of $Fe(OH)_3$ can remove soluble dyes by surface complexation or electrostatic attraction [43]. In the former mechanism, the dye acts as ligand to bind a hydrous iron moiety of the floc that gives a surface complex as shown in reaction (15), whereas in the second one, the positive or negative charges of the flocs attract the opposite regions of the dyes. Coagulation of these flocs leads to particles that are further separated from the effluent by sedimentation or electroflotation.

$$Dye{-}H + (HO)OFe_{(s)} \rightarrow Dye{-}OFe_{(s)} + H_2O \quad (15)$$

Recent studies on the decolorization and decontamination of dyestuff solutions by this procedure have been carried out with bench-scaled tank reactors equipped with parallel monopolar electrodes operating in batch mode [44–48]. Each one of these electrodes is an electrical contact to the power supply and their two active faces have the same polarity. Table 1 highlights that the removal of dyes depends on operating parameters such as their concentration, electrolyte composition, solution volume and pH, stirring, electrolysis time and applied current density (j). Most of these trials were performed at pH 6–7 with low stirring since under these conditions, $Fe(OH)_3$ flocs were formed in larger proportion and the dye molecules and their oxidation products were rapidly removed by complexation or electrostatic attraction, followed by coagulation [4]. Low j values (<30 mA cm^{-2}) and either NaCl or Na_2SO_4 medium were also utilized. The former parameter allows controlling the generation rate of iron ions, the growth of $Fe(OH)_3$ flocs and the rate and size of H_2 bubbles evolved and consequently, it determines the electrolysis time and energy cost of the EC process of the dyestuff effluent. The use of NaCl as electrolyte makes feasible the anodic oxidation of Cl^- to active chlorine species like Cl_2, HClO and ClO^-, which can oxidize organics [44,46].

Table 1
Percentage of color removal and COD decay for the electrocoagulation with Fe and/or Al anodes of several synthetic dyes solutions containing NaCl or Na_2SO_4 under selected conditions at ambient temperature or 25 °C.

Dye[a]	Anode	Solution	Electrolytic system[b]	j[c] (mA cm^{-2})	% color removal	% COD decay	Ref.
Acid Black 1 Reactive Blue 4 Acid Red 87 (Eosin Yellow)	Fe	500 cm^3 of 100 mg dm^{-3} dye with 0.1 g dm^{-3} NaCl at natural pH (6.8, 3.8, and 5.8, respectively)	Stirred tank reactor with two monopolar plate electrodes in batch for 12 min	10.7	81[d] 84[d] 39[d]	27[d] 65[d] 26[d]	[44]
Acid Blue 113	Fe	200 cm^3 of 540 mg dm^{-3} COD of the dye with 2 g dm^{-3} NaCl at pH 6.5	Tank reactor with two monopolar plate electrodes in batch without stirring for 60 min	30	95[d]	91[d]	[45]
Reactive Black 5	Fe	500 cm^3 of 100 mg dm^{-3} dye in tap water with 2 g dm^{-3} NaCl or Na_2SO_4 at pH 6.6	Stirred tank reactor with two monopolar plate electrodes in batch for 20 min	7.5	82[e] 93[d]	–[f] –[f]	[46]
Acid Black 52 Acid Yellow 220	Al	250 cm^3 of 200 mg dm^{-3} dye with 2 g dm^{-3} NaCl at pH 5	Stirred tank reactor with two monopolar plate electrodes in batch for 7.5 min	4.0	90[d] 98[d]	–[f] –[f]	[50]
Acid Black 172	Al	2.5 dm^3 of 300 mg dm^{-3} dye with NaCl at pH 7	Stirred tank reactor with four monopolar plate electrodes in batch for 9.1 min	8.3	90[d]	–[f]	[51]
Basic Green 4	Al	1.5 dm^3 of 100 mg dm^{-3} dye with 1.5 g dm^{-3} NaCl at pH 6.2	Tank reactor with two monopolar plate electrodes in batch without stirring for 45 min	11.7	99[d]	82[d]	[52]
Acid Blue 19 (Alphazurine FG)	Fe Al	250 cm^3 of 50 mg dm^{-3} dye with Na_2SO_4 at pH 6.1	Stirred tank reactor with two monopolar plate electrodes in batch for 4 min	10	95[e] 29[e]	65[e] –[f]	[54]
Basic Violet 3 (Crystal Violet)	Fe Al	500 cm^3 of 200 mg dm^{-3} dye with 284 mg dm^{-3} Na_2SO_4 at pH 5.8	Stirred tank reactor with three monopolar anodes and four monopolar cathodes in batch for 5 min	2.8	95[e] 90[e]	98[e] 85[e]	[56]
Reactive Red 43	Fe Al	1.8 dm^3 of 50 mg dm^{-3} dye with 0.04 M NaCl at pH 6.5	Stirred tank reactor with two monopolar anodes and two monopolar cathodes in batch for24 min	2.5	99[d] 77[d]	97[d] 74[d]	[58]

[a] Color index (common) name.
[b] t_r is the retention time in batch operation mode.
[c] Applied current density.
[d] With NaCl.
[e] With Na_2SO_4.
[f] Not determined.

Figs. 4a and b show the fast decolorization that underwent 25 mg dm^{-3} of the azo dye Reactive Black 5 in tap water at pH 6.6 in the presence of 2 g dm^{-3} Na_2SO_4 or NaCl, respectively, using a stirred tank reactor equipped with a Fe anode and a stainless steel (SS) cathode, both of 44 cm^2 electrode area [46]. In both cases, the increase in j accelerated the removal of the dye, more rapidly in chloride than in sulfate medium. After 20 min of EC treatment, 93% and 82% of color removal were found in such media. The color removal decay obeyed a pseudo-first order reaction and the apparent rate constant (k_1) changed with initial pH, as presented in Fig. 4c. The authors demonstrated that the decolorization process involved the pre-eminent reduction of the azo bond with cleavage into benzenic and naphthalenic derivatives by Fe^{2+} compared to the coagulation of the dye with the $Fe(OH)_3$ flocs. The quicker color removal at neutral and alkaline media in the presence of chloride than sulfate (see Fig. 4c) can be due to the additional oxidation with ClO^-, which becomes less efficient in acidic medium probably because active chlorine species (Cl_2 and/or HClO) are destroyed by Fe^{2+} to yield Fe^{3+} and Cl^- [46].

As can be seen in Table 1, high percentages of color removal can be achieved for all dyes effluents by EC, whereas the percentage of COD decay was rather poor in many cases. This different behavior suggests a change in the mechanism of the decolorization process respect to the removal of organics, mainly when azo dyes are treated. While the former can be related to the rapid reductive cleavage of the dye with Fe^{2+}, the latter involved the slower adsorption–desorption of intermediates with $Fe(OH)_3$. These points were confirmed by Saravanan et al. [45] from the FTIR analysis of Acid Blue 113 solutions treated by EC in a Fe/SS cell.

3.2. EC with Al anode

This method involves the anodic reaction of Al to soluble Al^{3+} ($E^\circ = -1.66$ V/SHE) and the cathodic reduction of water to hydroxide ion and H_2 gas as follows [4,49,50]:

$$Al \rightarrow Al^{3+} + 3e^- \quad (16)$$

$$3H_2O + 3e^- \rightarrow 3OH^- + (3/2)H_{2(g)} \quad (17)$$

The metal ions and hydroxide ions generated at the electrode surfaces react in the bulk wastewater to form soluble monomeric species such as $Al(OH)^{2+}$, $Al(OH)_2^+$ and $Al(OH)_3$ in acidic medium and $Al(OH)_4^-$ in alkaline medium. The two former cations can also evolve to polymeric species such as $Al_2(OH)_2^{4+}$, $Al_6(OH)_{15}^{3+}$, $Al_7(OH)_{17}^{4+}$ and so on. All these species are also converted into insoluble $Al(OH)_{3(s)}$ via the following overall reaction:

$$Al + 3H_2O \rightarrow Al(OH)_{3(s)} + (3/2)H_{2(g)} \quad (18)$$

In alkaline medium, however, the Al cathode can be chemically attacked by OH^- generated from reaction (17) and dissolved in the form of soluble $Al(OH)_4^-$, leading to higher amount of aluminum ions in the wastewater than those expected from reaction (16) [4]. An excess of aluminum in solution is also feasible by anodic corrosion in the presence of Cl^- ions [49].

The large networks of Al—O—Al—OH in $Al(OH)_{3(s)}$ can remove dyes from wastewaters by surface complexation or electrostatic attraction [4,50]. The former mechanism involving hydrous aluminum moieties takes place according to reaction (19):

$$Dye—H + (HO)OAl_{(s)} \rightarrow Dye—OAl_{(s)} + H_2O \quad (19)$$

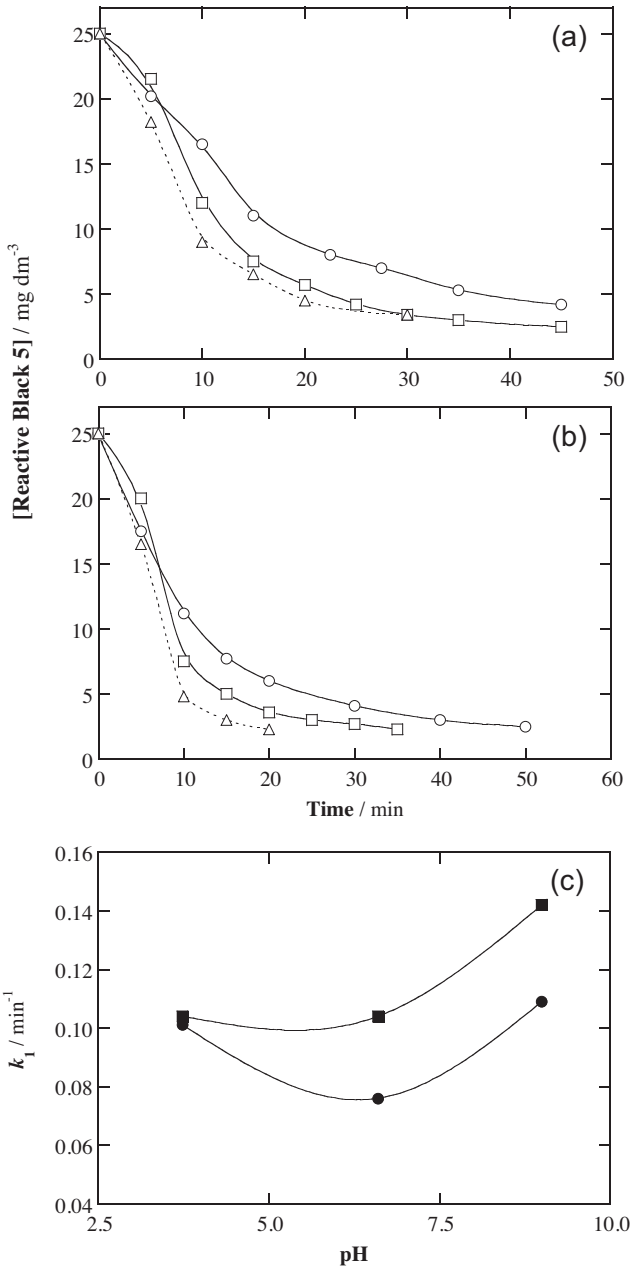

Fig. 4. Effect of current density on the decolorization of Reactive Black 5 with electrolysis time for the EC treatment of 500 cm^3 of a tap water with 25 mg dm^{-3} dye solution in 2 g dm^{-3} of (a) Na_2SO_4 and (b) NaCl at pH 6.6 using a tank reactor with a 44 cm^2 Fe anode. Current density: (○) 4.5 mA cm^{-2}, (□) 6.0 mA cm^{-2} and (△) 7.5 mA cm^{-2}. (c) Effect of initial pH on observed pseudo-first order decolorization rate constant in the presence of (●) Na_2SO_4 and (■) NaCl at 6.0 mA cm^{-2}. Adapted from Ref. [46].

The precipitation by neutralization of opposite charges predominates in acidic medium, taking place the reaction of dyes with monomeric species at pH < 5.0 from reaction (20) and with polymeric species at pH 5–6 from reaction (21). In contrast, the adsorption on $Al(OH)_3$ flocs followed by coagulation yields the sludge at pH > 6.5 via reaction (22).

$$\text{Dye} + \text{monomeric-Al} \rightarrow [\text{Dye—monomeric-Al}]_{(s)} \quad (20)$$

$$\text{Dye} + \text{polymeric-Al} \rightarrow [\text{Dye—polymeric-Al}]_{(s)} \quad (21)$$

$$\text{Dye} + Al(OH)_{3(s)} \rightarrow [\text{sludge}] \quad (22)$$

Moreover, the formed $Al(OH)_3$ flocs can adsorb soluble organics and/or trap colloidal particles, which can be in turn separated from the solution.

Although in EC with Al, dyes are only removed by pure adsorption and coagulation, the desorption of these compounds can produce low decolorization efficiencies and poor organic removal. Merzouk et al. [49] proposed a model to evaluate the decay in absorbance, turbidity, COD and TOC of single and mixed dye wastes just assuming an adsorption-desorption equilibrium between matter and $Al(OH)_{3(s)}$ via reactions (20)–(22). This model allowed explaining the EC treatment of 2 dm^3 of a real textile effluent of pH 7 using a flow plant equipped with a tank reactor containing two Al electrodes of 105 cm^2 area operating in batch between 4 and 20 mA cm^{-2} at liquid flow rate of 0.15 dm^3 min^{-1}. The amount of Al species dissolved in the effluent was the limiting factor of the process regardless of applied j and thus, about 65% color removal with ca. 70% COD and TOC decays, along with overall disappearance of turbidity, were obtained as maximal after producing 250–350 mg dm^{-3} of soluble aluminum.

Results of Table 1 confirm that EC with Al yielded excellent color removal, between 90% and 99%, for Acid Black 52 and Acid Yellow 220 [50], Acid Black 172 [51] and Basic Green 4 [52]. The decolorization efficiency of the two former dyes in single and binary solutions was followed by electrolyzing 250 cm^3 of 200–600 mg dm^{-3} of substrates up to 8 g dm^{-3} NaCl within pH range 2.5–10 between 1.0 and 12 mA cm^{-2} for 7.5 min. Similar color removal was found for single and binary solutions with dye contents <400 mg dm^{-3} at optimum pH 5 owing to the coagulation of the major part of monomeric-Al species from reaction (20). The increase in j accelerated the decolorization of both dyes because of the release of more soluble Al species, but higher amounts of NaCl caused primordially a rise in conductivity with a very low effect on color removal. For the EC process of Acid Black 172, Taheri et al. [51] applied the response surface methodology (RSM) to analyze the decolorization process with four independent variables like initial dye content up to 600 mg dm^{-3}, initial pH between 4 and 10, applied j between 2.1 and 14.5 mA cm^{-2} and electrolysis time between 3 and 15 min. The mathematical correlation of such variables with the percentage of color removal was developed using a central composite design consisting of 31 experiments with 16 factorial points, 8 axial points and 7 replicates at the central point. About 90% of correlation between experimental and model values was obtained and the optimized data determined by this procedure are collected in Table 1 [51]. In the case of Basic Green 4, Singh et al. [52] used the change in zeta potential with operating variables to find optimum values of 99% color removal and 82% COD and 63% TOC decays with 2.48 kWh (kg TOC)$^{-1}$ energy consumption when a 100 mg dm^{-3} dye solution at pH 6.2 was treated at 11.7 mA cm^{-2} for 45 min. Energy-dispersive X-ray spectroscopy (EDX) analysis revealed that the scum (produced as a layer of gas bubbles with floated particles) contained a more content of carbon, whereas the sludge contained larger proportion of aluminum. These findings were justified assuming that the EC process involves: (i) the generation of small organic products that are collected in the scum by electroflotation and (ii) the coagulation of longer organics with $Al(OH)_3$ in the sludge.

An interesting comparative study on the EO and EC treatments of 3 dm^3 of 75–200 mg dm^{-3} Acid Green 50 solutions in 0.5–2.0 g dm^{-3} NaCl within the pH interval 3–9 at j values between 1.1 and 7.0 mA cm^{-2} for 21 min has been reported by El-Ashtoukhy and Amin [53]. Experiments were performed in cylindrical plexiglass reactors equipped with 8 graphite rods of 1 cm diameter as anode (for generation of active chlorine species) and a stainless steel screen as cathode for EO and two cylindrical Al sheets as electrodes for EC. About 100% of color removal was reached more

rapidly by EC and in both systems, the decolorization increased at higher j and NaCl concentration, but it became slower with rising dye concentration. While no pH effect was observed for EO, an optimum pH of 6.9 was found for color removal by EC. At this pH, 100 mg dm^{-3} of Acid Green 50 in 1 g dm^{-3} NaCl electrolyzed at 3.5 mA cm^{-2} gave 68% and 87% COD removal for EO and EC, respectively, with corresponding energy consumptions of 5.73 and 3.82 kWh (kg COD)$^{-1}$. Although these results seem to indicate the superiority of EC over EO, more research with more potent oxidation anodes in the latter technique is needed to conclude a general comparative behavior.

3.3. Comparative EC behavior of anodes

Several comparative EC studies with Fe and Al anodes have been performed for synthetic Acid [54,55], Basic [56], Reactive [55,57–59] and Disperse [60] dyes used in the textile industry. For the three former kinds of dyes, selected data of Table 1 show that the use of Fe is advantageous compared to Al for decolorization, whereas the opposite behavior has been reported for Disperse Red 167 [60]. The superiority of Fe observed in most cases can be related to the reduction of dyes by Fe^{2+} ions supplied to the medium from reaction (9), a fact that not takes place using Al since dyes are only removed by pure adsorption and coagulation [46]. However, the decolorization process was significantly influenced by the anions of the solution. Fig. 5 exemplifies the evolution of decolorization efficiency for 1.8 dm^3 of 50 mg dm^{-3} Reactive Red 43 solutions in the presence of several common anions at neutral pH using an Al/Al cell at 2.5 mA cm^{-2} [57]. High percentages of color removal can be observed in the presence of Cl^-, which decreased considerably by raising Cl^- content and adding NO_3^- and SO_4^{2-} owing to the inhibition of Al^{3+} formed from reaction (16). Similar tests in a Fe/Fe cell revealed that the presence of NO_3^- caused a passive layer on the iron anode surface, which was destroyed by pitting corrosion when Cl^- was added. In the presence of this ion, greater decolorization efficiency was found and more quantity of Fe^{2+} was released by reaction (9), making the EC treatment with Fe more efficient than with Al [57].

Comparative studies carried out by EC demonstrated that this procedure is an easy, fast, effective and economical method for achieving almost total decolorization of chloride dyes wastewaters with both, Fe and Al anodes. In this process, reduction with Fe^{2+} and/or oxidation with active chlorine species (Cl_2/HClO/ClO^-) can play a role significant, apart from coagulation. In contrast, partial destruction of dyes by the above species and/or desorption of byproducts can account for by the poorer decontamination found in many cases.

A key parameter in EC is the solution pH, which is usually chosen near neutral or low alkaline values to favor the formation of coagulants. Low current densities and short decolorization times are commonly applied to obtain cost-effective processes. The cell configuration is other important operating variable that needs to be investigated in EC. Lemlikchi et al. [60] showed that the increase from 2 to 6 bipolar Fe or Al electrodes (with different polarity in their two faces) located in parallel between extreme monopolar Fe or Al, respectively, promoted gradually the percentage of color removal of 1 dm^3 of a 50 mg dm^{-3} Disperse Red 167 solution with 1 g dm^{-3} NaCl at pH 4.0–9.0 and 200 mA. This phenomenon can be related to the concomitant production of more coagulant with lowering j when more surface from bipolar electrodes is used. Unfortunately, no more publications in this way have been reported. On the other hand, it is also noticeable that operating cost for the decolorization process can be substantially reduced if a battery connected to a solar photovoltaic cell is employed as power supply [55].

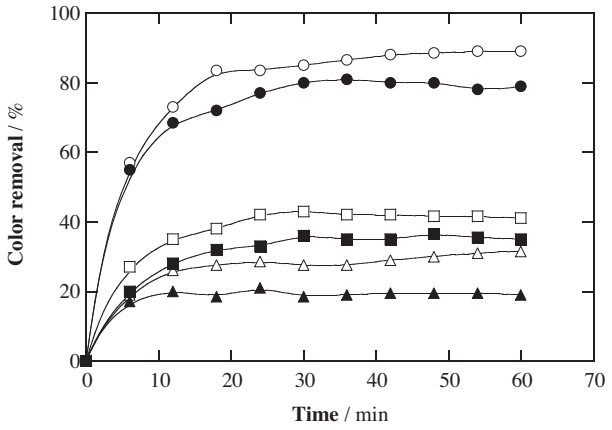

Fig. 5. Effect of anions on the decolorization efficiency of Reactive Red 43 vs. electrolysis time during the EC treatment of 1.8 dm^3 of 50 mg dm^{-3} dye solutions at pH ca. 6.5 using a stirred tank reactor with two Al electrodes of 50 cm^2 electrode area at 2.5 mA cm^{-2}. Electrolyte: (○) 0.02 M Cl^-, (□) 0.01 M Cl^- + 0.01 M NO_3^-, (△) 0.01 M Cl^- + 0.01 M SO_4^{2-}, (●) 0.04 M Cl^-, (■) 0.04 M Cl^- + 0.01 M NO_3^- and (▲) 0.04 M Cl^- + 0.01 M SO_4^{2-}.
Adapted from Ref. [57].

4. Electrochemical reduction

Direct electroreduction has lost the interest for the destruction of dyes in aqueous solution because it offers a very poor decontamination of wastewaters compared to other electrochemical treatments. This has been demonstrated recently by Méndez-Martínez et al. [61] who studied the decolorization and degradation of 80 mg dm^{-3} of the azo dye Reactive Black 5 in 0.1 M KOH under N_2 atmosphere using stirred undivided and divided tank reactors containing a Ni mesh anode and a Ni-polyvinylchloride composite cathode at constant anodic (E_{anod}) or cathodic (E_{cat}) potential. For the treatment of a 50 cm^3 solution in the undivided cell at E_{cat} = −3.0 V/SCE, total decolorization was achieved in 60 min with low COD (16%) and TOC (8%) removals. When the divided cell was employed, the anodic and cathodic compartments were filled with 100 cm^3 of the dye solution. The EO in the anodic compartment yielded a fast 90% decolorization after 38 min at E_{anod} = 2.0 V/SCE owing to the action of •OH formed at the Ni anode, whereas color was much more slowly removed in the cathodic compartment due to the electrochemical reduction of the dye, reaching 82% decolorization efficiency after 213 min at E_{cat} = −2.0 V/SCE. Analysis of aromatic intermediates by HPLC and LC–MS/MS revealed the formation of electroreduction products with m/z 200, 369.5 and 547 in the catholyte of the divided cell, but electro-oxidation products with m/z 201, 185 and 172 were detected in both, the anolyte of the divided cell and using the undivided one, as presented in Fig. 6. The quick formation of alkylsulfonylphenol derivatives by —N=N— cleavage under the latter conditions explained the large superiority of the EO of Reactive Black 5 compared to its direct reduction at the cathode.

On the other hand, Velazquez-Peña et al. [62] showed that small contents of dyes like Thionine, Methyl Orange and Methylene Blue accelerated the electrochemical reduction of Cr(VI) to Cr(III) at pH 2 with 0.01 M NaCl using a stirred tank reactor equipped with two BDD electrodes. The electrochemical reduction of 100 cm^3 of 50 mg dm^{-3} $K_2Cr_2O_7$ at 200 mA only gave 36% conversion to Cr(III) in 45 min. In contrast, by adding 50 μM Methyl Orange, 90% of Cr(VI) was reduced under the same conditions while 98% of dye was oxidized because it acted as mediated electron transfer in the solution by cleavage of its —N=N— bond.

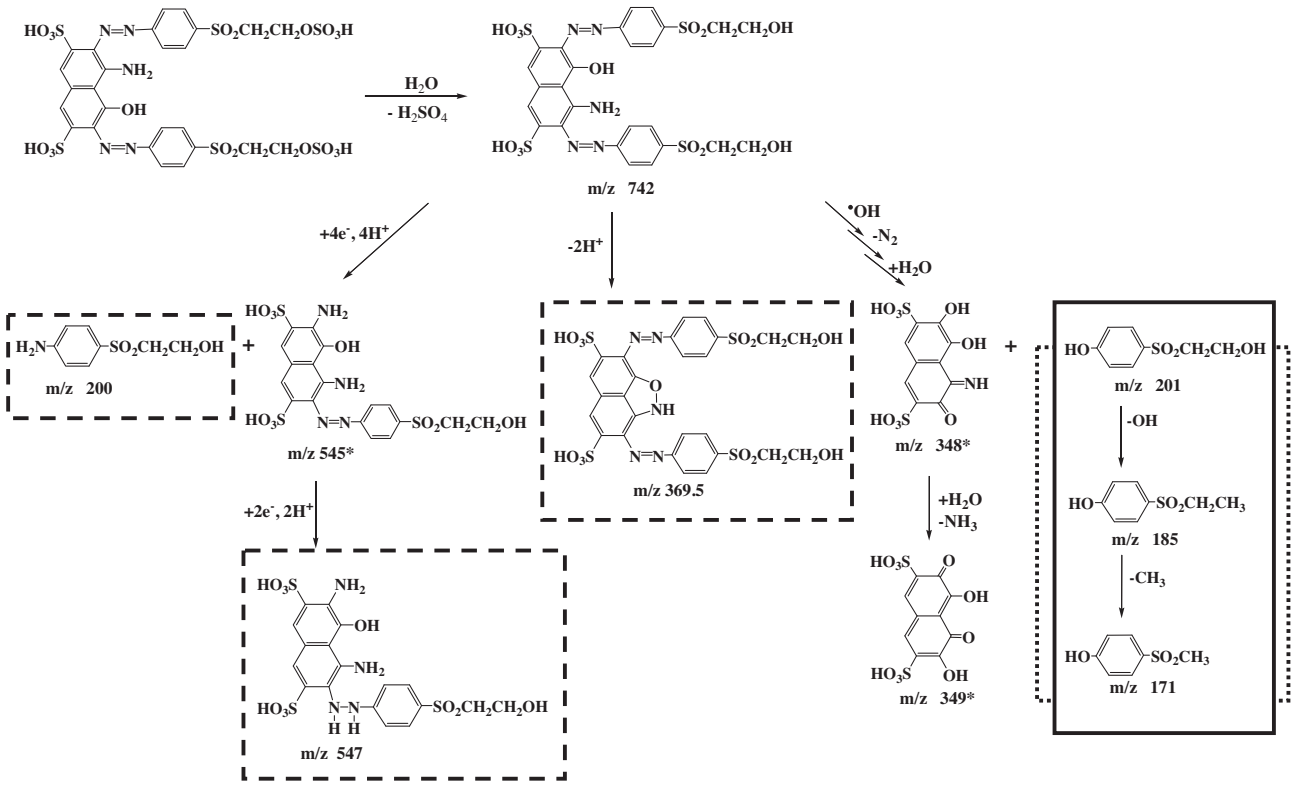

Fig. 6. Proposed degradation pathways for the electroreduction and electro-oxidation of Reactive Black 5 with Ni electrodes. By-products identified by LC–MS in (· · ·) an undivided cell, (—) the anodic compartment of a divided cell and (- - -) the cathodic compartment of a divided cell.
Adapted from Ref. [61].

5. Electrochemical oxidation

As can be seen in Fig. 2, over the last 5 years the decontamination of wastewaters containing dyes has been preferentially performed by using EO or electro-oxidation. In fact, this is the most popular electrochemical procedure for removing organic pollutants from wastewaters [4,26]. Starting from the beginning of the investigation of EO, pioneering studies by Dabrowski in the 70s, Kirk, Stucki, Kotz, Chettiar and Watkinson in the 80s, and Johnson, De Battisti and Comninellis in the 90s, allow the elucidation of the basic fundamentals of EO for its application as a promising alternative for treating wastewaters [28,30].

EO consists in the oxidation of pollutants in an electrolytic cell by [4]: (i) direct anodic oxidation at the electrode surface or direct electron transfer to the anode M, yielding very poor decontamination and (ii) chemical reaction with electrogenerated hydroxyl radicals from water discharge at the anode M such as chemisorbed "active oxygen" (oxygen in the lattice of a metal oxide anode MO) or physically adsorbed "active oxygen" (physisorbed M(•OH)).

The existence of different heterogeneous species formed from water discharge has allowed the proposal of two main approaches for EO [4,25,28,30,32]: (i) the electrochemical conversion method, where refractory organics are selectively transformed into biodegradable compounds like carboxylic acids with chemisorbed MO and (ii) the electrochemical combustion or electrochemical incineration method, in which organics are converted into dehydrogenated or hydroxylated derivatives with physisorbed M(•OH) up to mineralization to CO_2 and inorganic ions. In both cases, the oxidation of pollutants and production of oxidizing species depend on the potential difference of the electrochemical cell. The use of high E_{cell} values maintains the anode activity and promotes the simultaneous oxidation of pollutants and water. Conversely, when low E_{cell} values are applied, O_2 evolution is avoided causing the loss of anode activity because of the adsorption on its surface of intermediates formed from direct anodic oxidation, making this procedure not useful for wastewater remediation in practice.

The studies performed in the last 20 years [22–32] have highlighted the strong influence of the nature of the anode material on both, the selectivity and efficiency of EO. This behavior has been interpreted by a comprehensive model for organics destruction in acidic medium including the competition with O_2 evolution reaction, proposed by Comninellis [63]. The predictions of this model fit well with results obtained with diverse anodes (e.g., Pt, IrO_2, SnO_2, PbO_2 and conductive diamond electrodes, among others), which present different O_2 overpotential values.

5.1. Model for the organics oxidation with heterogeneous hydroxyl radical

Comninellis [63] proposed that selective oxidation of organics occurs with electrodes forming the so-called higher oxide MO (chemisorbed "active oxygen") while combustion takes place with electrodes in which M(•OH) radicals are accumulated onto its surface (physisorbed active oxygen). However, this model was partially modified when new assumptions were considered after the use of diamond electrodes such as BDD [64]. Then, the different behavior of anodes in EO was explained by considering two limiting cases in the schematic model of Fig. 7, the so-called "active" (Pt, IrO_2 and RuO_2) and "non-active" (PbO_2, SnO_2 and BDD) anodes. In the active anodes with low O_2-overpotentials, the chemisorbed "active oxygen" is the main oxidant favoring the electrochemical conversion of organics into carboxylic acids, whereas in the non-active

anodes with high O_2-overpotentials, the electrochemical combustion takes place since organics are mineralized to CO_2 under the action of M(•OH) radicals.

The proposed model of Fig. 7 considers that the initial reaction in both kinds of anodes M corresponds to the oxidation of water molecules leading to the formation of physisorbed hydroxyl radical M(•OH) by reaction (a). Both the electrochemical and chemical reactivity of heterogeneous M(•OH) are dependent on the nature of the electrode material. The surface of active anodes interacts strongly with •OH and a so-called higher oxide or superoxide MO may be generated following reaction (b). This occurs when higher oxidation states are available for a metal oxide anode, above the standard potential for O_2 evolution (E° = 1.23 V/SHE). The redox couple MO/M acts as a mediator in the oxidation of organics R by reaction (c), which competes with the side reaction of O_2 evolution via chemical decomposition of the higher oxide species from reaction (d). In contrast, the surface of a non-active anode interacts so weakly with •OH that organics can directly react with M(•OH) to yield fully oxidized products such as CO_2 by reaction (e), where R is an organic compound with m carbon atoms and without any heteroatom, which needs $a = (2m + n)$ oxygen atoms to be totally mineralized to CO_2. The oxidative reaction (c) with the surface redox couple MO/M is much more selective than the mineralization reaction (e) with M(•OH). The latter reaction also competes with the side reactions of this radical like direct oxidation to O_2 from reaction (f) or indirect consumption through dimerization to hydrogen peroxide by reaction (g).

A non-active electrode does not participate in the direct anodic reaction of organics and does not provide any catalytic active site for their adsorption from the aqueous medium. It only acts as an inert substrate and as a sink for the removal of electrons. In principle, only outer-sphere reactions and water oxidation are possible with this kind of anode. Hydroxyl radical produced from water discharge by reaction (a) is subsequently involved in the oxidation process of organics.

The aforementioned model presupposes a strong link of the electrochemical activity (related to the overpotential for O_2 evolution) and chemical reactivity (related to the rate of organics oxidation) of physisorbed M(•OH) to the strength of M–•OH interaction. Generally, the weaker the interaction, the lower the anode reactivity for organic oxidation with faster chemical reaction with M(•OH). The BDD electrode is the best non-active anode verifying this behavior [64], thereby being proposed as the preferable anode for EO. The electrogeneration of M(•OH) as mediated oxidant has permitted to consider EO as an EAOP. Note that a weaker oxidant as ozone can also been generated from water discharge at the anode (E° = −1.51 V/SHE) by reaction (h) in Fig. 7 [27,28,30]. Consequently, several reactive oxygen species (ROS) such as M(•OH) by reaction (a), H_2O_2 by reaction (g) and O_3 by reaction (h) are generated, although the former is the strongest oxidant of pollutants. This species, however, has so short lifetime that only acts while direct current is provided to the anode.

When BDD is used, other weaker oxidizing agents like peroxodisulfate, peroxodicarbonate and peroxodiphosphate can be also competitively formed with ROS from the anodic oxidation of bisulfate (or sulfate), bicarbonate and phosphate present in the electrolyte as follows [29]:

$$2HSO_4^- \rightarrow S_2O_8^{2-} + 2H^+ + 2e^- \quad (23)$$

$$2HCO_3^- \rightarrow C_2O_6^{2-} + 2H^+ + 2e^- \quad (24)$$

$$2PO_4^{3-} \rightarrow P_2O_8^{4-} + 2e^- \quad (25)$$

A very different behavior is found when chloride solutions are treated by EO, since active chlorine species like Cl_2, HClO and/or ClO^- formed from Cl^- oxidation at the anode can effectively mineralize the dyes and their by-products in competition with ROS. In this section, comparative degradation examples will be given to discuss the efficiency of different anode materials depending on supporting electrolyte used including Cl^-, although the characteristics of indirect electro-oxidation with active chlorine species will be extensively discussed in Section 6.1.

5.2. Anode materials, electrochemical systems and experimental parameters

The most important factor determining the extent of dyes mineralization by EO is obviously the anode material, as already established by Comninellis. The groups applying the EO approach for dyes degradation [66–129] have tested a large variety of electrodes including doped and undoped PbO_2 [66–72,126–128], mixed metal oxides of Ti, Ru, Ir, Sn and Sb [73–86,124,129], doped-SnO_2 [87,88], Ti/Pt and Pt [82,84,89–94,125,126], carbonaceous electrodes [95–100] and recently, three-dimensional electrodes [101,102]. However, synthetic BDD thin films are currently preferred as anodes [103–129] by their better oxidative performance. These works have utilized diverse electrochemical systems for the treatment of dyeing wastewaters by EO. Similar designs already reported in our previous review [4] like conventional three-electrode cells with two- or one-compartments and divided or undivided two-electrode cells or tank reactors have been frequently utilized [66,67,69–72,77,79,82–85,91,92,95–97,101,102,104,106,108,110–112,124,128]. These cells are equipped with monopolar and sometimes bipolar electrodes [73,119]. More relevant applications have been reported to treat synthetic and real effluents using flow cells with parallel electrodes and flow plants with a three-phase three-dimensional electrode reactor or a bipolar trickle tower reactor [79,80,87,88,102,103,105,106,114,115,120,127]. In flow cells with planar and monopolar electrodes in parallel plate configuration, hydrodynamic conditions can reduce the interelectrode gap increasing the oxidation rate of pollutants. A good design of these reactors then allows the optimization of the mass transport coefficient for a maximum current efficiency.

The characteristics of EO and its relevant application to dyes removal will be examined from a general classification of the anodes used.

5.3. Metal oxides electrodes

In the last 5 years, doped and undoped PbO_2 and mixed metal oxides of Ru, Ti, Sb, Sn and Ir, have been widely used as anodes for the EO of synthetic dyes [66–88,124,126–129]. Table 2 summarizes selected results for the treatment of chloride-free dyes solutions using these electrodes.

5.3.1. PbO_2 anode

Lead dioxide with high O_2-overpotential is among the most commonly used anodes to remove dyes because the rate of organic oxidation has proved to be higher than that of other traditional anodes. This effectiveness has been clearly confirmed by Carvalho et al. [66] when treated 500 cm^3 of 300 mg dm^{-3} Methyl Green solutions in 0.5 M H_2SO_4 with Ti/PbO_2 anode using a stirred two-electrode cell for studying the role of current density between 10 and 40 mA cm^{-2}, temperature from 25 to 60 °C at 10 mA cm^{-2} and agitation rate between 100 and 300 rpm at 10 mA cm^{-2}. About 90% color removal was obtained for all applied j, whereas increasing TOC reduction from 43% to 70% was found when current density rose owing to the production of more amounts of PbO_2(•OH). Higher TOC removal from 40 to 82% was also obtained when temperature increased from 25 to 60 °C by the concomitant increase in mass transport with acceleration of oxidation reactions, whereas color removal was superior to 90% in all cases. Higher stirring

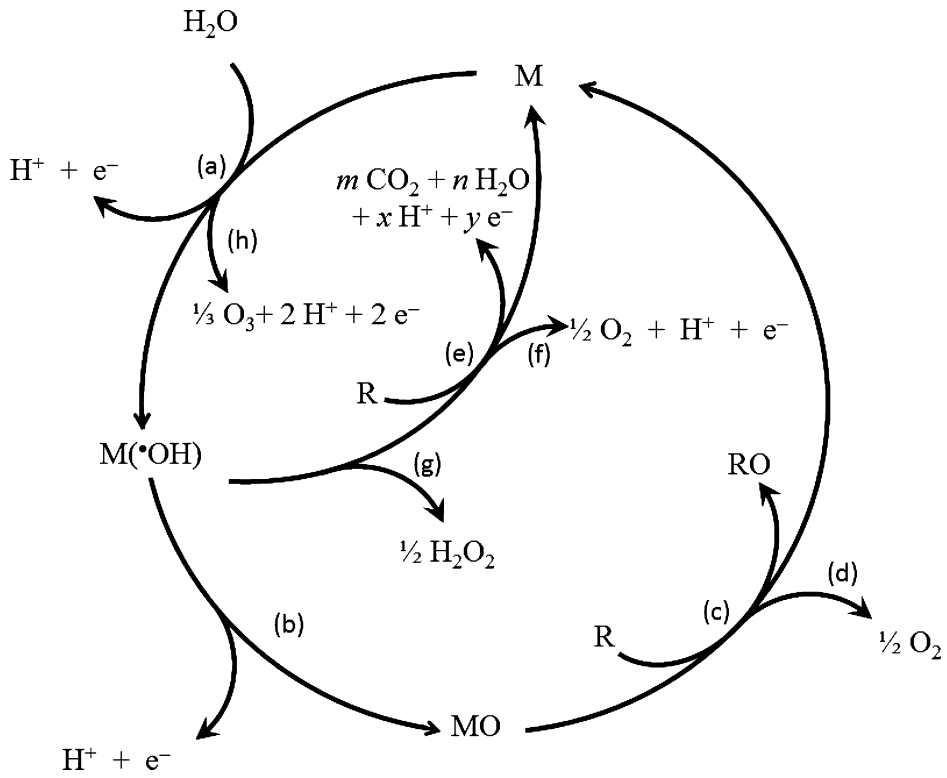

Fig. 7. Mechanistic scheme of anodic oxidation of organic compounds with simultaneous oxygen evolution on non-active anodes (reactions (a), (e) and (f)) and on active anodes (reactions (a), (b), (c) and (d)). (a) Formation of hydroxyl radical, M(•OH); (b) formation of the higher metal oxide, MO; (c) electrochemical conversion of the organic compound, R, via the higher metal oxide; (d) oxygen evolution by chemical decomposition of the higher metal oxide; (e) electrochemical combustion of the organic compound via hydroxyl radicals; (f) oxygen evolution by electrochemical oxidation of hydroxyl radicals; (g) hydrogen peroxide production via hydroxyl radicals and (h) production of ozone.

Adapted from refs. [63–65].

Table 2
Percentage of color and COD removals and energy cost for the electrochemical oxidation of selected chloride-free dyes solutions using metal oxides and Pt anodes, as well as with three-dimensional electrodes.

Dye[a]	C_0 (mg dm^{-3})	j[b] (mA cm^{-2})	Electrolysis time (h)	% color removal	% COD decay	Energy cost[c]	Ref.
PbO_2 anode							
Acid Orange 52 (Methyl Orange)	0.25[d]	0.6[e]	2	100	28[f]	–[g]	[72]
Basic Yellow 2 (Auramine-O)	150[h]	50	4	–[g]	68	26.4 kWh m^{-3}	[128]
Reactive Blue 194	30	150	0.5	90	24[f]	–[g]	[69]
Reactive Red 195	100	30	10	100	79[f]	–[g]	[67]
$Ti/Ru_{0.3}Ti_{0.7}O_2$ anode							
Acid Red 2 (Methyl Red)	11.4	30	2.5	100	100[f]	11.0 kWh m^{-3}	[77]
Acid Red 2 (Methyl Red)	100	60	6.5	95	35[f]	89.4 kWh m^{-3}	[82]
Acid Red 26 (Ponceau 2R)	50	200	2	100	11[f]	–[g]	[84]
Pt anode							
Acid Red 2 (Methyl Red)	100	60	6.5	100	52[f]	75.2 kWh m^{-3}	[82]
Acid Red 26 (Ponceau 2R)	50	200	2	100	15[f]	–[g]	[84]
Basic Blue 9 (Methylene Blue)	60	50	14	100	75	33.6 kWh m^{-3}	[91]
(Novacron Yellow)	250	60	6	92	40	163 kWh m^{-3}	[93]
(Remazol Red BR)	250	60	6	96	35	161 kWh m^{-3}	
Three-dimensional electrodes							
Acid Orange 52 (Methyl Orange)	1150	2[e]	0.67	–[g]	94	14.6 kWh (kg COD)$^{-1}$	[101]

[a] Color index (common) name.
[b] Applied current density.
[c] Different units reported.
[d] mM concentration.
[e] Current (A).
[f] Percentage of TOC decay.
[g] Not determined.
[h] Initial COD (mg dm^{-3}).

also caused a slight enhancement of the percentage of color and TOC removals as a result of the faster mass transfer toward the anode.

Hmani et al. [128] studied the EO of 200 cm^3 of 150 mg dm^{-3} COD of Auramine-O at pH 6.0 in a one-compartment Pyrex glass cell with a BDD or PbO_2 anode by applying 50 mA cm^{-2} and 30 °C. The lead dioxide was deposited by electrolysis of a lead nitrate aqueous solution onto a rectangular Ta plate. The oxidation rate and current efficiency of the dye for the BDD anode were greater than for PbO_2. At BDD, 95% COD removal was reached in 90 min, whereas at PbO_2 it hardly achieved 68%. Regarding the energy consumption, the use of BDD was more cost-effective. For example, to reach 95% COD removal, BDD and PbO_2 anodes consumed 11.33 and 26.13 kWh m^{-3}, respectively. This demonstrates that the oxidation ability of each anode depends on the different nature of the physisorbed BDD(•OH) and PbO_2(•OH) radicals generated on them. The high oxidation power of PbO_2 anode is due to its high O_2 overpotential. An inspection of Table 2 corroborates the great mineralization attained for other dyes by EO with PbO_2.

Despite the high overpotential of PbO_2 for O_2 evolution, this anode shows low durability by surface corrosion and sometimes, it generates highly toxic Pb^{2+} ion leading to serious secondary pollution [22,130]. New alternative preparations of undoped or doped PbO_2 electrodes have demonstrated to be more stable and active [68,70]. For this reason, the use of doped PbO_2 anodes for EO of dyes has received great attention in the last 5 years. For example, Weng et al. [68] prepared a novel lead-doped electrode with a typical rare earth (Ce) by thermal decomposition–electrodeposition technique to enhance the activity of the β-PbO_2 surface. They degraded solutions of 100 mg dm^{-3} of the cationic Turquoise Blue GB in 0.2 M Na_2SO_4 at 40 mA cm^{-2} and after 60 min, 97.9% dye removal and 64.3% COD decay were obtained with a Ce-doped PbO_2 anode, values much greater than 85.4% and 40.3%, respectively, found for an undoped β-PbO_2. Little effect on these parameters was observed when increasing concentrations of the electrolyte from 0.1 to 0.5 M Na_2SO_4 were used. For 100 mg dm^{-3} Turquoise Blue GB and using a Ce-doped PbO_2 anode, the dye and COD decays rose from 76.2% and 50.2% at 20 mA cm^{-2} to 97.9% and 64.3% at 40 mA cm^{-2} respectively, as expected for the concomitant increase of heterogeneous physisorbed hydroxyl radicals as oxidant. These results demonstrate that addition of a rare earth as Ce improves strongly the degradation of dye on β-PbO_2 surface. This assumption was confirmed by the overall mineralization of benzoic and acetic acids identified as intermediates by GC–MS, which attained a content of 110.23 and 124.65 mg dm^{-3} respectively, after 60 min of treatment. Other example is the fabrication of cerium-doped lead oxide anode on titanium dioxide nanotubes (TiO_2-NTs/Ce-PbO_2) used to remove Rhodamine B [70]. A conventional stirred three-electrode cell was used to treat a solution of 30 mg dm^{-3} Rhodamine B in 0.1 M Na_2SO_4 + 0.01 M NaCl at pH 5.2 and 50 mA cm^{-2}, always achieving 100% color removal in all cases while TOC was reduced from 63% to 82% when contents from 1 to 5 mM Ce were used to prepare TiO_2-NTs/Ce–PbO_2 anodes. Similar results in terms of decolorization and TOC removal were achieved for different Ce deposition times. Higher color removal and mineralization degree were also obtained by growing *j* from 10 to 50 mA cm^{-2} and pH from 2 to 12. However, it is important to note that the supporting electrolyte contained NaCl that favored the decolorization and mineralization rates due to the participation of active chlorine species formed at the anode surface.

Recent papers have also demonstrated that the fabrication of PbO_2 electrodes mixed with other metals or titanium dioxide nanotubes provides an enhancement in the mineralization with high current efficiency of Reactive Red 195, Reactive Blue 194 and Active Black 194 [67,69,71]. For example, the EO process of 160 cm^3 of 0.1 M Na_2SO_4 containing 100–400 mg dm^{-3} of Reactive Red 195 in a two-compartment cell with a Nafion-117 cation-exchange membrane was studied between 5 and 40 mA cm^{-2} with Ti/SnO_2–Sb/PbO_2 electrodes [67]. An increase in mineralization rate occurred when *j* varied in the range 30–40 mA cm^{-2}, reducing the electrolysis time. In acidic medium, the dye was rapidly removed from solution; whereas in alkaline medium it was more slowly destroyed because of the enhancement of O_2 evolution at the anode surface. This phenomenon reduced the diffusion rate of substances from the bulk towards the electrode, avoiding an efficient mineralization that attained only about 30% after 4 h of electrolysis. Regarding the variation of the initial dye concentration, TOC removal dropped from 80% to 53% when dye content rose from 100 to 400 mg dm^{-3} at pH 5.6 and 30 mA cm^{-2}. The poor oxidation action of physisorbed hydroxyl radicals •OH in sulfate medium was enhanced by adding 1–10 mM NaCl, which gave much better performance of >98% of dye and TOC removals in shorter electrolysis time by the additional oxidation of organics with active chlorine species. The role of these species was clarified from GC–MS analysis of treated solutions in the presence and the absence of chloride ions, confirming that they acted on the chromophore group stripping but they do not give the cleavage of the phenyl ring of aromatic intermediates. On the contrary, An et al. [69] reported modest performances using a Sb-doped SnO_2/PbO_2 electrodeposited on an ordered microstructured TiO_2-NTs template as anode for the EO of 100 cm^3 of 30–200 mg dm^{-3} Reactive Blue 194 in 0.1 M Na_2SO_4 using a stirred tank reactor at room temperature. The best conditions were found for 30 mg dm^{-3} dye at 150 mA cm^{-2}, where 90% decolorization and 24% TOC decay were achieved in 30 min (see Table 2). These authors indicated that the chemical structure of dye in acidic and alkaline media becomes a determining parameter because of the difficult oxidation of its protonated and unprotonated forms, respectively. The effect of chloride ions on the mineralization of Reactive Blue 194 was also investigated, showing no significant improvement when Cl^- ions in solution rose from 0.001 to 0.01 M. The low toxicity risk of the treated effluent was confirmed by the no detection of halogenated derivatives by GC–MS.

An improvement on degradation results have been reported for praseodymium (Pr) modified Ti/SnO_2–Sb/PbO_2 electrodes. He et al. [71] tested the treatment of 160 cm^3 of 100 mg dm^{-3} Acid Black 194 solutions with 0.1 M Na_2SO_4 using a stirred tank reactor with 6 cm^2 Ti/SnO_2–Sb/PbO_2 or Ti/SnO_2–Sb/PbO_2–Pr anode and a Pt sheet as cathode. The use of a Ti/SnO_2–Sb/PbO_2–Pr electrode resulted in a superior electrocatalytic degradation of Acid Black 194, increasing 1.5-fold the COD decay compared to the undoped one. This behavior was related to the structure of the PbO_2 electrode, being proposed that physisorbed hydroxyl radicals were localized in active centers promoted by Pr doping.

Other interesting results have been reported by Recio et al. [72] who prepared PbO_2 coatings on reticulated vitreous carbon (RVC) and titanate nanotubes (RVC/PbO_2/TiNT) to decontaminate synthetic wastewaters using a stirred tank reactor containing 275 cm^3 of 0.25 mM Methyl Orange solution in 0.05 M Na_2SO_4 by applying a constant current of 0.6 or 1 A. Both electrodes led to total decolorization of the solution in 60 min, reaching >95% of color removal at 30 min. At 60 min, 45% TOC was removed by the RVC/PbO_2/TiNT anode, whereas only 24% TOC decay was attained with RVC/PbO_2. These anodes minimized the mass transport limitations inherent to planar electrodes, increasing the poor stability of carbon against corrosion and producing high amounts of physisorbed hydroxyl radicals from water oxidation at high positive potentials. However, poor degradation was obtained using both anodes compared to doped PbO_2 electrodes [67,69,71].

5.3.2. DSA-type electrodes

Dimensionally stable anodes (DSA) are constituted of a Ti base metal covered by a thin conducting layer of metal oxide or mixed metal-oxides of Ti, Ru, Ir, Sn, Ta and Sb [4,26,28,30]. Many studies have been performed to find new coating layers for electrochemical applications [32]. However, these active anodes show a limited oxidation power to incinerate dyestuffs because of their low ability to electrogenerate M(•OH), as can be seen in Table 2. This was demonstrated by Panakoulias et al. [129], who reported much lower COD and TOC removals for Reactive Red 120 in 1 M $HClO_4$ using Ti/IrO_2–RuO_2 than Si/BDD. The former anode exhibited higher selectivity of organic intermediates, enhancing TOC removal from 10% at 25 °C to 40% at 80 °C. In contrast, the Si/BDD anode gave total mineralization. Both electrodes led to total decolorization, but requiring a specific charge of only 2 Ah dm^{-3} for BDD and a value as high as 25 Ah dm^{-3} for Ti/IrO_2–RuO_2. The maximum instantaneous current efficiency (ICE) was 45% for Si/BDD and 13% for Ti/IrO_2–RuO_2, indicating the lower efficiency of the DSA anode compared to the non-active one.

Synthetic dyes effluents with Reactive Black 5 [74,88], Orange II [75], Chrome Brown [76], Methyl Red [77,82], Reactive Blue 4 [78], Reactive Orange 16 [78], Indigo Carmine [80], Crystal Violet [81], Methyl Orange [83,86], Ponceau 2R [84], Malachite Green [85] and Reactive Orange 4 [87] have been degraded with metal-oxide anodes like Ti/CuO_x, TiNiO, Ti/CoO_x, Ti/AgO_x, Ti/RuO_x, Ti/$Ru_{0.3}Ti_{0.7}O_2$, Ti/$Ru_{0.3}Sn_{0.7}O_2$, Ti/$(RuO_2)_{0.7}(Ta_2O_5)_{0.3}$, Ti/$RuO_2$–$IrO_2$, Ti/$RuO_x$–$TiO_x$, Ti/$SnO_2$–Sb–Pt, Ti/$Ti_{0.7}Ru_{0.3}O_2$ and Ti/$Ir_{0.45}O_2$–Ta_2O_2. Real effluents have been treated with Ti/TiO_2–RuO_2–IrO_2 and Ti/RuO_x–TiO_x anodes [73,79].

Tavares et al. [82] utilized a stirred undivided cell with a 24 cm^2 Ti/$Ru_{0.3}Ti_{0.7}O_2$ or Ti/Pt anode for oxidizing 400 cm^3 of 100 mg dm^{-3} Methyl Red solutions in 0.25 M H_2SO_4 by applying 20–60 mA cm^{-2} at 25 °C. Complete decolorization was always achieved, although the color decayed more rapidly for Ti/Pt than Ti/$Ru_{0.3}Ti_{0.7}O_2$. Lower TOC removal was attained for the latter anode ranging from 10% to 35% as *j* increased. This behavior was ascribed to the fact that metallic cations in the oxide lattice may reach higher oxidation states under anodic polarization, followed by stabilization of the adsorbed M(•OH), thereby favoring O_2 evolution at the expense of the electrochemical incineration reaction. Conversely, at Ti/Pt anode TOC removal underwent a modest improvement up to about 50% under similar electrolytic conditions.

Oliveira Morais et al. [77] studied the behavior of Ti/$Ru_{0.34}Ti_{0.66}O_2$ as electrocatalytic material under soft oxidation conditions up to 30 mA cm^{-2}. A solution of 300 cm^3 of 11.4 mg dm^{-3} Methyl Red in 0.5 M H_2SO_4 was electrolyzed in a stirred tank reactor to clarify the fragmentation of the azo dye group and by-products formed. It was found that the process was initiated by the attack of Ti/$Ru_{0.34}Ti_{0.66}O_2$(•OH/MOx) radical on the —N=N— bond of Methyl Red giving benzoic acid and 4,4-*N*,*N*-dimethylaniline with loss of N_2 and NO_3^- ion. These compounds were transformed into aniline, nitrobenzene and benzene, releasing NO_2^- ion. The aromatic derivatives then suffered ring opening to produce a mixture of aliphatic acids, which were finally oxidized to CO_2. These authors reported higher TOC decays of 97%, 99% and 100% for 10, 20, and 30 mA cm^{-2}, respectively, than those given by Tavares et al. [82] using the same electrode and operating with higher *j* values.

Poorer mineralization has been reported for other mixed metal oxides of Ti–Ru and Ta–Ir when compared with Pt. For example, Ribeiro et al. [84] studied the EO degradation of 80 cm^3 of 50 mg dm^{-3} Ponceau 2R in 0.1 M $HClO_4$ in a stirred tank reactor equipped with a DSA electrode (Ti/$Ti_{0.7}Ru_{0.3}O_2$ and Ti/$Ir_{0.45}O_2$–Ta_2O_2) or Ti/Pt at different *j* values and room temperature. After 120 min of electrolysis, 100% color removal was always obtained for $j > 50$ mA cm^{-2}. In contrast, at 10 and 25 mA cm^{-2}, no more than 85% decolorization efficiency was achieved. Poor TOC removals of 7%, 11% and 15% were found for Ti/$Ir_{0.45}O_2$–Ta_2O_2, Ti/$Ti_{0.7}Ru_{0.3}O_2$ and Ti/Pt anodes, respectively, when 200 mA cm^{-2} were applied. The poor oxidation action of M(•OH) radicals in the above acidic medium can be ascribed to the promotion of side reaction of O_2 evolution as well as the production of intermediates, favoring the inactivation of electrodes and consequently, limiting the complete elimination of organic load.

Ruthenium-based oxide electrodes have also received great attention for treating synthetic effluents containing with dyes. The destruction of Chrome Brown [76], Reactive Blue 4 [78], Reactive Orange 16 [78], Methyl Orange [83,86,124] and Malachite Green [85] has been reported by EO with Ti/RuO_x–TiO_x anodes. Ternary oxide electrodes (Ti–Ru–Ir) have also been tested for Reactive Red 120 [129] and Crystal Violet [81]. The use of RSM giving the mathematical relationship between independent variables and COD has been investigated by Palani and Balasubramanian [83] and Soloman et al. [85] by using a Ti/RuO_x–TiO_x expanded mesh electrode. The effect of operating variables like current density from 4 to 22 mA cm^{-2}, electrolysis time from 9 to 60 min and Malachite Green concentration from 200 to 1200 mg dm^{-3} on 3.75–100% COD removal indicated that the highest COD removal was achieved for maximum *j*, the longest electrolysis time and minimum dye content [85]. However, the best COD values were obtained for 20.1 mA cm^{-2} applied during 40.53 min using 232.04 mg dm^{-3} of the dye. On the other hand, Palani and Balasubramanian [83] investigated the treatment of Methyl Orange solutions by using a novel rotating disk flow reactor with a 582 cm^2 Ti/RuO_x–TiO_x anode and found that COD reduction was significantly influenced by *j*, electrolyte flow, NaCl dosage and cathode rotation speed, reaching a 96% removal under optimum conditions.

A very limited number of papers has reported the use of SnO_2-doped electrodes during the EO of dyes. The electrochemical treatment of Reactive Orange 4 [87] and Reactive Black 5 [88] solutions was evaluated with a Ti/SnO_2–Sb–Pt anode in a filter-press reactor with divided [87,88] or undivided configurations [88]. The different aromatic compounds formed during the degradation of both dyes were identified by GC–MS to understand their oxidation and reduction processes.

5.4. Pt anode

The effective decolorization of dyes by EO with pure Pt [89,93,100,126] and Ti-supported Pt anodes [82,84,90,91,93,94,125] has been confirmed. Since the use of pure Pt anode results impracticable for industrial application due to its expensive cost, Pt-based anodes have been taken into consideration. Then, Pt-doped materials with different composition and preparation [82,84,87,89–91,93,94,100] have been tested to be applied to the EO of dyes.

Table 2 summarizes the percentages of color removal and COD decay for selected synthetic dyes wastewaters under optimized EO conditions with Pt anodes. Color, COD and TOC removal were mainly dependent on solution pH, temperature, stirring or flow rate and *j* or E_{cell} [82,84,89–94]. As explained in Section 5.3.2, total decolorization with 50% TOC decay were obtained in the degradation of a solution with 100 mg dm^{-3} Methyl Red and 0.25 M H_2SO_4 in a batch cell with a Ti/Pt anode [82]. A high decolorization efficiency, but with very low decontamination, is a result of the nature of Pt electrode, which is an active anode that accumulates small quantity of physisorbed Pt(•OH) on its surface during water discharge. This behavior is found for most dyes given in Table 2 [82,84,93] and in the literature [89,90,92,94,100,125,126], indicating that Pt anodes are efficient electrocatalytic materials to

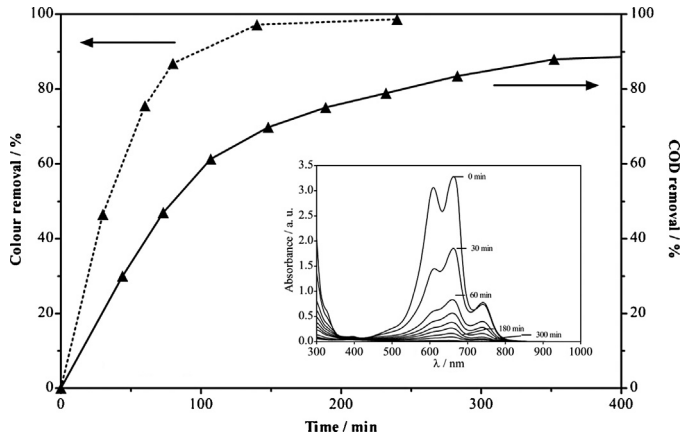

Fig. 8. Color and COD removals vs. electrolysis time during the EO of 350 cm^3 of 60 mg dm^{-3} Methylene Blue in 0.5 M H_2SO_4 at 25 °C using an undivided stirred tank reactor with a 15 cm^2 Ti/Pt anode and a 15 cm^2 Ti cathode at 50 mA cm^{-2}. The inset panel shows the change in the visible spectrum of the solution.
Adapted from Ref. [91].

remove color, but without a satisfactory removal of the organic matter. However, the poor oxidation action of Pt(•OH) in sulfate or acidic media [89–93,100,126] can be enhanced, in some cases, by using NaCl as supporting electrolyte [94,125] or by adding a known amount of NaCl to the solution [90], which gave much better performance due to the additional oxidation of organics with active chlorine species.

An inspection of Table 2 reveals the existence of a modest COD decay for Basic Blue 9 (Methylene Blue) using a Ti/Pt anode in front of a high decolorization efficiency under optimized conditions [91]. Fig. 8 illustrates the change of color and COD removals with electrolysis time during the EO treatment of 60 mg dm^{-3} of this dye in 0.5 M H_2SO_4 using a stirred tank reactor at 50 mA cm^{-2}. The maximum color removal of about ~99% was achieved after 200 min of electrolysis, with only 75% COD removal. This was attributed to the fast oxidation of the dye and its by-products with Pt(•OH) formed from reaction (a) in Fig. 7, but the subsequent formation of the higher oxide PtO following reaction (b) in Fig. 7 limited the oxidative power of this electrocatalytic material. Organic products could also be adsorbed at Pt surface to passivate it and as a consequence, lower organic matter can be removed. The latter behavior can be improved with increasing temperature, as found for the best decolorization efficiency of Methyl Red [82], Basic Blue 9 [91] and Reactive Orange 13 [91,94] when passing from 25 to 60–90 °C. In all cases, TOC decay was slightly increased between 5% and 16% respect to the values obtained at 25 °C.

Less is known about the influence of the chemical structure of the dye in the EO process with Pt. To clarify this, the comparative COD removal for 400 cm^3 of 200 mg dm^{-3} of four Reactive dyes in 0.1 M Na_2SO_4 using stirred divided and undivided batch cells was studied [92]. The influence of E_{cell} from 6 to 24 V and membrane division was examined during the degradation of Reactive Blue 52, which gave good COD removal >95% when 12 V were applied for 30 min with membrane division. Analogous experimental conditions were employed for Reactive Green 15 and Reactive Yellow 125, reaching COD decays up to 94% after 60 min of electrolysis with membrane division, whereas Reactive Black 5 only yielded 58% COD removal. These results confirm that not only the chemical structure affects the process, but also there exists a strong influence of the kind of substituent of the dye. Moreover, Jović et al. [92] reported the detection and identification of aliphatic carboxylic acids such as acetic, maleic and oxalic as final by-products of the treatment of Reactive Blue 52 solutions by means of HPLC analysis.

As active Pt anode shows a limited oxidation power to incinerate dyestuffs, several authors have compared its efficiency for removing dyes with other anodes [82,84,89,93,125,126]. It has been found that Pt can be more or less effective depending on the nature of the anode tested. For example, the EO of 100 cm^3 of a 100 mg dm^{-3} Alizarin Red solution with 0.05 M Na_2SO_4 at pH 7.0 and 25 °C was compared using Pt, PbO_2 and Si/BDD anodes at 100 mA cm^{-2} [126]. The mineralization ability of non-active PbO_2 and Si/BDD anodes was much greater than Pt. TOC was reduced by 90% and 98% for PbO_2 and Si/BDD, respectively, whereas only 28% TOC decay occurred for Pt. In contrast, Tavares et al. [82] reported a slightly better performance using Ti/Pt than the active $Ti/Ti_{0.3}Ru_{0.7}O_2$ anode for the EO of Methyl Red in 0.25 M Na_2SO_4, as pointed out in Section 5.3.2.

5.5. Carbonaceous and other anode materials

Electrode materials based on carbonaceous compounds have been widely applied in electrochemistry by their low resistivity and chemical inertness. Some papers have reported the use of anodes composed of carbonaceous materials for the EO of dyestuffs [95–102]. Anodes such as unmodified [95,96] and modified [99] graphite, carbon paper modified bimetallic platinum–bismuth [97], activated carbon fiber (ACF) [98] and activated carbon fabric [100] have been tested. Granular activated carbon [101,102] has been used as three-dimensional anode.

The EO of dyes like Vat Black 27 [95] and Reactive Black 5 [96] with graphite evidenced its low degradation ability. Kariyajjanavar et al. [95] studied the degradation of 50 mg dm^{-3} of Vat Black 27 in Na_2SO_4 or NaCl medium in a stirred tank reactor with a graphite anode. Bulk electrochemical incineration led decolorization efficiencies ranging from 5% to 99% and lower COD removals depending on electrolyte concentration (5–35 g dm^{-3}) after 240 min of electrolysis at 17 mA cm^{-2}. As expected, the increase in electrolyte concentration led to a drop in E_{cell} with minimum specific energy consumption of 15.20 kWh m^{-3}. When j rose to 42.5 mA cm^{-2}, a significant enhancement in the degradation of Vat Black 27 was found for 25 g dm^{-3} NaCl, attaining total decolorization and 83% COD removal in 240 min. Rivera et al. [96] used stirred cubic and cylindrical tank reactors with graphite electrodes when studied the electrochemical incineration of 70 mg dm^{-3} of Reactive Black 5 in several Na_2SO_4 aqueous solutions by applying 5 V at 25 °C. The degradation of the dye increased at higher electrolyte concentration as a result of the greater applied j and after 3 h of treatment, 80% color removal and total decolorization with TOC decays of 76% and 95% for the cubic and cylindrical cell configurations, respectively, were obtained. The better hydrodynamic conditions of the cylindrical cell enhancing the mass transport of reactants toward the electrode explain the higher performance of this common configuration to decolorize and decontaminate the dye solution.

Modified carbonaceous electrodes with metallic [98,100], bimetallic [97], nanotubes [99] and polymers [99] have used to degrade Methyl Orange [97], Acid Red 1 [98], Basic Blue 9 [99] and Amaranth [100]. Li et al. [97] considered the influence of modification of carbon paper with bimetallic nanostructures (platinum–bismuth) on the EO efficiency of 100 cm^3 of 20 mg dm^{-3} Methyl Orange in phosphate buffer using a three-electrode cell system with a Pt–Bi/C anode and a Ti mesh cathode of 5 cm^2 geometric areas. Higher dye degradation occurred when the Pt–Bi/C anode reached more positive E_{anod} values. Thus, over 74% dye abatement was found for decreasing times of 180, 143 and 90 min as rising E_{anod} values of 0.7, 1.1 and 1.5 V. These results are indicative of a high electrochemical activity the Pt–Bi/C anode even at low potential.

Two interesting studies of Liu et al. [101] and Zhao [102] were focused on the decolorization of dyes solutions using

three-dimensional electrode reactors containing granular activated carbon. Selected results listed at the end of Table 2 highlights the high degradation ability of these reactors. An undivided and cylindrical three dimensional electrode reactor with granular activated carbon as particle electrode, ACF/Fe as anode and ACF/Ti as cathode was used to treat a solution of 500 cm^3 with 300 mg dm^{-3} Acid Orange 7 and 3 g dm^{-3} of Na_2SO_4 at pH 3.0 and E_{cell} of 20 V [102]. After 60 min of treatment, TOC was removed up to 39.6% by oxidation and up to 20.7% by coagulation. The oxidation was mainly due to the direct destruction of the dye at the ACF/Fe anode and polarized graphite activated carbon particles along with mediated reaction with produced ROS (physisorbed •OH radicals and H_2O_2) and other oxidants. HPLC analysis revealed that Acid Orange 7 oxidation occurs via the cleavage of its —N=N— bond to give the aromatic amines sulfanilic acid and 1-amino-2-naphthol. The fact that sulfanilic acid concentration reached 23 mg dm^{-3} in 20 min to be gradually reduced until 2.0 mg dm^{-3} at 180 min, indicated that not only Acid Orange 7, but also their aromatic products, can be efficiently oxidized in the three-dimensional electrode reactor.

5.6. Boron-doped diamond electrodes

Over the last three decades, BDD thin films have been defined as non-active anodes since they do not provide any catalytically active site for the adsorption of reactants and/or products in aqueous media [4,26–34,36]. Physisorbed BDD(•OH) formed from water discharge on its surface by reaction (a) in Fig. 7 is then considered the responsible species for the electrochemical combustion of organic pollutants [32,33], although slower reactions with other ROS like H_2O_2 and O_3, and generated oxidants like active chlorine species, peroxodisulfate, peroxodicarbonate or peroxodiphosphate, are also feasible [28–33,131]. Many research groups have demonstrated that BDD allows total mineralization up to near 100% current efficiency of a large number of organics [4,28–31]. Many works have also been focused on the treatment of different dyes and the selection of experimental conditions to improve the performance of this technique [4,103–129]. This synthetic material deposited on several supports like Nb, Ti and Si has then been widely applied to dyestuff treatment. Although the significant employment and development of BDD-based electrochemical technology up to the year 2008 has been appointed in our previous review [4], it is noticeable that BDD thin films have been the most used anodes in different EAOPs for removing dyes from synthetic and industrial effluents in the last 5 years, as reflected by a high number of publications in peer-reviewed journals [103–129].

Although BDD deposits on Nb support [103,105,114,115,120,127] have been checked for dye treatment, the excessive high cost of this metallic substrate makes unfeasible its large-scale utilization in practice. Ti/BDD anodes with better requirements and small dimension have also been tested for the mineralization of several dyes [104,110]. However, these electrodes can present problems of cracking and detachment of the diamond film during long-term electrolysis. Si-supported BDD thin films have been widely used in the EO of dyes [106,108,111,113,116,117,119,121–126,128,129], in spite of their fragility and relatively low conductivity of the Si substrate.

The EO treatment by different BDD films has been studied for azo dyes (Reactive Black 5 [103], Reactive Orange 16 [104], Acidic Yellow 36 [107], Methyl Orange [107], Remazol Red [111], Novacron Blue [111], Reactive Red 147 [112], Acid Black 210 [113], Methyl Orange [115], Orange II [120], Rubin F-2B [121], Reactive Red 141 [122], Direct Black 22 [122], Disperse Orange 29 [122], Naphthalene Black 10B [123], Methyl Orange [124] and Reactive Red [129]), triphenylmethanes (Crystal Violet [110]), anthraquinones (Alizarin Blue Black B [119], Acid Blue 62 [122], Alizarin Red [126]), Auramine-O [128], Alphazurine A [117] and Basic Blue [114]. The influence of pH [103,111–113,119,123,124,128], dye concentration [103,105,107,112,114,115,117,119,124,125,128,129], j [103–129], temperature [106,108,111,114,116,117,127,128], supporting electrolyte [103,106,108,110,113,114,120–125,129], stirring rate [117] and flow rate [103,105,106,114,120] was investigated for optimizing degradation conditions. Many authors have examined the change of color removal, decay in COD and/or TOC, current efficiency and toxicity, which mainly depend on the above parameters. Also, identification of intermediates and energy requirements were determined when diamond anodes were utilized for the decontamination of synthetic dyes and real textile effluents. Only one work reported the effect of dye structure in EO with BDD [111].

Table 3 collects the excellent results obtained for the EO with BDD anodes of selected chloride-free dyes solutions considering the kind of support utilized. The characteristics of these processes are described and discussed below according to this classification, being the last subsection devoted to examine the papers related to BDD electrodes with unspecified support.

5.6.1. Ti/BDD electrodes

The effective EO of dyes with small Ti/BDD anodes has been demonstrated by Migliorini et al. [104] when degraded 400–450 cm^3 of 50 mg dm^{-3} Reactive Orange 16 in 0.1 M H_2SO_4 + 0.1 M K_2SO_4 using a polypropylene home-made single cell with a 4.15 cm^2 Ti/BDD anode and a Pt cathode of the same area by applying between 15 and 200 mA cm^{-2}. Two types of Ti/BDD anodes were synthesized with different boron doping to clarify the influence of boron content on dye degradation. For both anodes, color was reduced by 98% at 100–200 mA cm^{-2} and 25 °C in 90 min, being the process much more efficient than with lower j values because of the much higher production of BDD(•OH) at the Ti/BDD surface. For the Ti/BDD anode with 8.0×10^{21} atom cm^{-3} of boron, more than 95% color removal was achieved at 50 mA cm^{-2}, whereas only 55% decolorization efficiency was found for 25 mA cm^{-2}, similar to the results obtained for Ti/BDD with minor boron doping of 4.0×10^{21} atom cm^{-3}. However, TOC was reduced by 60% for the Ti/BDD with higher boron content, a value higher than 40% TOC removal determined for the anode with lower boron content. HPLC analysis of treated solutions revealed that aromatic intermediates were removed more rapidly in the former anode, making in evidence that boron content on Ti-support BDD thin films influences aromatic removal.

On the other hand, 150 cm^3 of 33–660 mg dm^{-3} Cristal Violet in sulfate media at pH 3–11 were degraded in a stirred tank reactor with a 4 cm^2 Ti/BDD anode at j values between 2.5 and 15 mA cm^{-2} [110]. The authors demonstrated that the largest enhancement of dye destruction via BDD(•OH) formed by water oxidation was obtained for 35.5 g dm^{-3} Na_2SO_4, neutral initial pH and 2.5 mA cm^{-2}. Under these conditions, the EO process completely oxidized the initial dye yielding 95% TOC reduction, without accumulation of side products.

5.6.2. Nb/BDD electrodes

Effective degradation of synthetic dye effluents containing Reactive Black 5 [103], Basic Blue 3 [114], Methyl Orange [115] and Orange II [102] has been demonstrated by using Nb/BDD anodes in a bipolar trickle tower reactor [103,114] and recirculation flow cells [102,115]. Few works have reported the treatment of real textile industry effluents with these electrodes [105,127]. An inspection of Table 3 corroborates the great decolorization attained for dyes (synthetic or real effluents) in EO with Nb/BDD, even when in some cases modest mineralization was attained. This behavior has been clearly confirmed by Ramirez et al. [115], who planned a 23 factorial design with j, dye concentration and electrolysis time as independent variables to oxidize Methyl Orange solutions in a pilot

Table 3
Per cent of color and COD decays and energy cost determined for the electrochemical oxidation of selected chloride-free dyes solutions using diamond anodes.

Dye[a]	C_0 (mg dm^{-3})	j[b] (mA cm^{-2})	Electrolysis time (h)	% color removal	% COD decay	Energy cost[c]	Ref.
Ti/BDD anode							
Reactive Orange 16	100	100	1.5	100	39[d]	–[e]	[104]
Basic Violet 3 (Crystal Violet)	250	2.5	2.25[f]	100	>95	–[e]	[110]
Nb/BDD anode							
Acid Orange 52 (Methyl Orange)	100	31	2.3	96	60	7.7 kWh m^{-3}	[115]
Acrylic fiber wastewater	723[g]	500[h]	2	–[e]	65	66 kWh m^{-3}	[105]
Textile wastewater	300	5	5[f]	95	>93	30 kWh m^{-3}	[127]
Si/BDD anode							
Acid Blue 7 (Alphazurine A)	500[g]	30	9	100	95	28.5 kWh (kg COD)$^{-1}$	[117]
Acid Blue 62	100	30	12[f]	100	100	60 kWh m^{-3}	[122]
Direct Black 22	100	30	23[f]	100	65	115 kWh m^{-3}	
Disperse Orange 29	100	30	62[f]	91	82	310 kWh m^{-3}	
Reactive Red 141	100	30	5[f]	100	100	25 kWh m^{-3}	
Basic Yellow 2 (Auramine-O)	150[g]	50	1.5	–[e]	95	11.3 kWh m^{-3}	[128]
Mordant Black 13 (Alizarin Blue Black B)	0.05[i]	40	3	94	65	2.3 kWh (g COD)$^{-1}$	[119]
(Novacron Blue C-D)	190	20	6[j]	100	93	16.2 kWh m^{-3}	[111]
(Remazol Red BR)	190	20	6[j]	100	94	20.7 kWh m^{-3}	

[a] Color index (common) name.
[b] Applied current density.
[c] Different units reported.
[d] Percentage of TOC decay.
[e] Not determined.
[f] Specific charge passed (Ah dm^{-3}).
[g] Initial COD.
[h] Current (mA).
[i] mM concentration.
[j] pH 4.5.

flow plant. For the best EO treatment for 3 dm^3 of 100 mg dm^{-3} Methyl Orange solutions in 0.05 M Na_2SO_4 at pH 3.0 and 25 °C with a 64 cm^2 Nb/BDD anode at 31 mA cm^{-2}, 94% decolorization efficiency was obtained after 138 min of electrolysis. Under these conditions, low TOC reduction of 60.3% with specific energy consumption of 7.7 kWh m^{-3} was determined. The low mineralization achieved proves that the reaction of generated BDD(•OH) with dye causes not only the cleavage of the chromophore system giving a large decolorization, but also the formation of several intermediates that are accumulated at long times diminishing TOC reduction. Another work has described similar results when the EO treatment of acrylic fiber wastewater was performed with a Nb/BDD anode [105]. It is reported that this BDD anode only allowed 65% COD removal, although this value was much higher than 18% found for a Ti/IrO_2–RuO_2 electrode. That confirms the stronger mineralization capacity of the Nb/BDD anode compared to the DSA one because of the higher oxidation power of BDD(•OH) radicals produced on its surface.

Other interesting results have been reported by Yavuz et al. [114] using a flow plant with a bipolar trickle tower reactor containing Rasching rings of Nb/BDD as anode with 352 cm^2 total area to decolorize Basic Blue 3 solutions. The rise of j from 0.500 to 0.875 mA cm^{-2} enhanced the color removal from 60% to 100% for 125 cm^3 of 20 mg dm^{-3} solutions of this dye in 0.01 M Na_2SO_4 at 30 °C and flow rate of 6.57 dm^3 min^{-1} at 30 °C. No influence on decolorization rate was observed by varying the flow rate and temperature from 25 to 45 °C. Conversely, increasing dye concentration from 10 to 40 mg dm^{-3} promoted slower decolorization prolonging the electrolysis time, due to the mass transport limitations at higher dye content in solution. For instance, from 18 to 60 min of electrolysis were required for complete decolorization at 0.875 mA cm^{-2}. Under the above optimum conditions with 20 mg dm^{-3} of Basic Blue and 0.875 mA cm^{-2}, 86.7% COD was reduced in 60 min. These authors used the same procedure to show that the color, COD and TOC of 100 mg dm^{-3} Reactive Black solutions in 0.2 M Na_2SO_4 at natural pH dropped in 97%, 51% and 24%, respectively, operating at 1 mA cm^{-2} and flow rate of 6.0 dm^3 h^{-1} for 60 min [103].

Nb/BDD films have also been compared with other electrode materials with high O_2-overvoltage that promote efficiently the overall electrochemical incineration of organics [105,127]. Relevant results have been published by Aquino et al. [127], who optimized the EO process for 400 cm^3 of a real textile effluent at 25 °C and 55 °C using a flow plant with a filter-press reactor containing either a 32.8 cm^2 Nb/BDD anode or a 5.9 cm^2 Ti–Pt/β-PbO_2 anode by varying j from 5 to 45 mA cm^{-2}. Fig. 9a shows that total COD abatement was not accomplished in the experiments carried out with Nb/BDD at 25 °C, only attaining about 90% COD decrease at 4 kA h m^{-3}. In contrast, Fig. 9c depicts that only 30–40% of COD was removed on Ti–Pt/β-PbO_2 anode at 25 °C between 15 and 45 mA cm^{-2}. Operating at higher temperature of 55 °C (see Fig. 9b), the best conditions were attained at the lowest j of 5 mA cm^{-2} for Nb/BDD, with 90% COD abatement at 2 kA h m^{-3} and total decontamination at 7 kA h m^{-3} with an specific energy consumption near 30 kWh m^{-3}. However, when 1.5 g dm^{-3} NaCl were added to the real effluent operating at 5 mA cm^{-2} and 55 °C, an unexpected outcome took place since no improvement in COD removal was observed. Although it is well-known that the mineralization by EO is facilitated by the addition of Cl^- ion since it produces active chlorine species, the effect of this ion using a BDD anode is not clear yet and sometimes, the expected improvement is not observed. For the Ti–Pt/β-PbO_2 anode at 55 °C, Fig. 9d highlights that COD decay was favored at the lowest j of 15 mA cm^{-2}, but the efficiency of this anode was much inferior to that of the Nb/BDD due to the higher oxidation power of the latter. In this case, Fig. 9d highlights that the addition of 1.5 mg dm^{-3} NaCl to the effluent using the Ti–Pt/β-PbO_2 anode at 15 mA cm^{-2} and 55 °C improved COD removal rate compared with the experiment without Cl^- addition, as reported for other anode materials [70,79].

5.6.3. Si/BDD electrodes

Si/BDD anode has been the most extensively used diamond material for EO of dyes [106,108,109,111,113,116,117,119,121–126,128,129]. The good performance for the remediation of dyes wastewaters with Si/BDD anodes can be deduced from

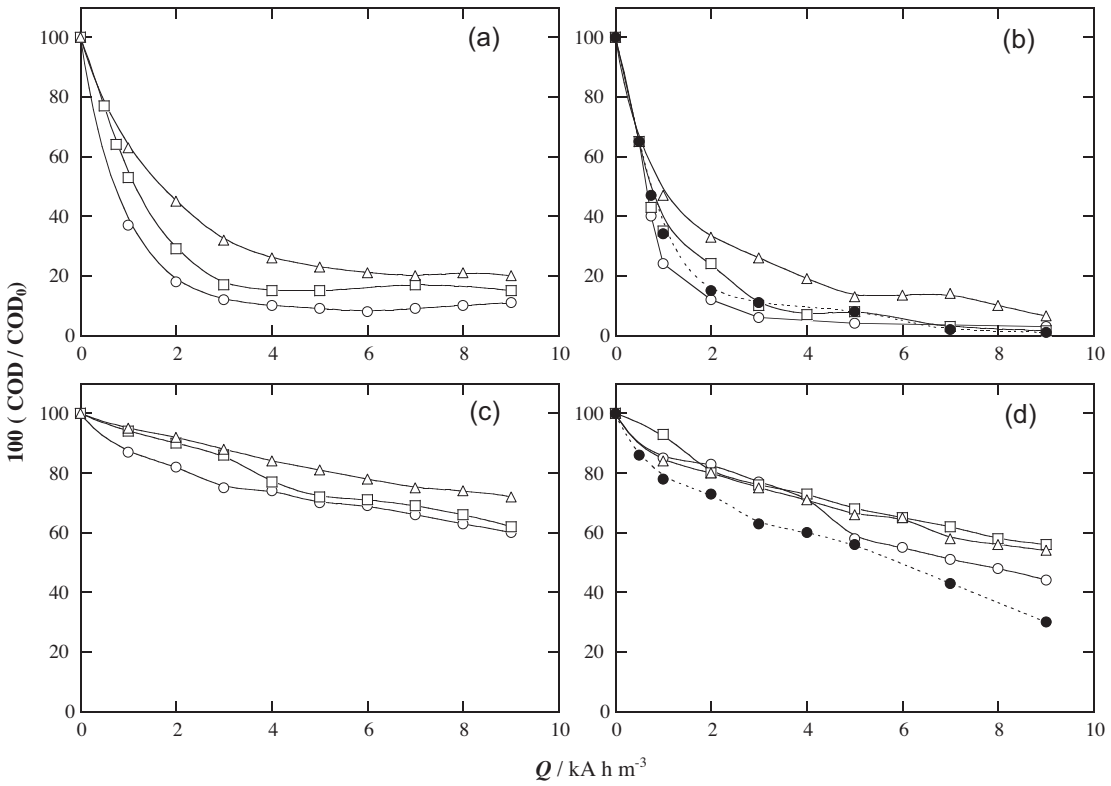

Fig. 9. Percentage of normalized COD vs. applied specific charge for 400 cm^3 of a real textile effluent, without and with NaCl, treated by EO using a filter-press flow plant containing either a 32.8 cm^2 Nb/BDD anode at (a) 25 °C and (b) 55 °C or a 5.9 cm^2 Ti–Pt/β-PbO_2 anode at (c) 25 °C and (d) 55 °C at liquid flow rate of 360 dm^3 h^{-1}. In (a) and (b): current density: (○) 5 mA cm^{-2}, (□) 10 mA cm^{-2}, (△) 20 mA cm^{-2} and (●) 5 mA cm^{-2} with addition of 1.5 g dm^{-3} NaCl. In (c) and (d): (○) 15 mA cm^{-2}, (□) 30 mA cm^{-2}, (△) 45 mA cm^{-2} and (●) 15 mA cm^{-2} with addition of 1.5 g dm^{-3} NaCl.
Adapted from Ref. [127].

the examples given at the end of Table 3. When Si/BDD has been compared with other materials [124,126,128,129], it leads to total decolorization and almost complete mineralization with higher current efficiency. These results are attributed to the efficient formation of BDD(•OH) and other electrogenerated oxidants present in a region close to the BDD surface and in the bulk. This behavior has been demonstrated by Zhou et al. [124] for the treatment of 200 cm^3 of a 50 mg dm^{-3} Methyl Orange solution in the presence of 14.2 g dm^{-3} Na_2SO_4 or 14.2 g dm^{-3} Na_2SO_4 + 3 g dm^{-3} NaCl in a stirred undivided tank reactor containing a Si/BDD or DSA anode and a SS plate cathode, all them of 3 cm^2 area. For the sulfate medium at pH 3.0, 100% color removal was found for the Si/BDD anode at 30 and 50 mA cm^{-2} with energy consumptions of 7 and 10 kWh m^{-3}, respectively; whereas no more than 20% color removal with similar energy requirements was achieved for the DSA electrode. At pH 10, only a significant rise in decolorization efficiency was observed for Si/BDD, ascribed to the change of the quinoid structure of the dye in acidic pH to its azo structure adopted in alkaline pH. Therefore, the dependence of Methyl Orange structure with solution pH and the nature of anode surface determine the reaction mechanism. Current efficiencies estimated in sulfate media were always superior for Si/BDD because the applied j was more efficiently used for organic degradation. Addition of 3 g dm^{-3} NaCl to the dye solution promoted the decolorization for both electrodes because of the additional formation of active chlorine species. Thus, total decolorization with BDD required the spent of only 1 kWh m^{-3}, whereas 60% color removal was attained using the DSA electrode.

The overall electrochemical incineration of Alizarin Red solution by Si/BDD has been reported by Ammar et al. [126], as explained in Section 5.4. These authors showed that Si/BDD and PbO_2 anodes were much more potent than Pt, as expected if in the two non-active anodes, the dye is incinerated pre-eminently by physisorbed M(•OH) and $S_2O_8^{2-}$ generated by reaction (a) in Fig. 7 and reaction (23), respectively. However, the treatment was largely prolonged by the gradual formation of short-linear aliphatic carboxylic acids that are more difficultly oxidizable with BDD(•OH) than aromatic pollutants. This was demonstrated by Rocha et al. [111] for the treatment of 400 cm^3 of 190 mg dm^{-3} Remazol Red BR and Novacron Blue C-D solutions in the presence of 71 g dm^{-3} Na_2SO_4 or 71 g dm^{-3} Na_2SO_4 + 10 g dm^{-3} NaOH using a one-compartment cell with a 10 cm^2 Si/BDD. These authors found total decolorization and 94% COD abatement after 250 min at 20 mA cm^{-2}, detecting maleic, acetic and oxalic acids as final by-products, the latter being the most persistent. It is important to remark that although Si/BDD anodes have been applied to the EO of many synthetic dyes, only some works have been devoted to the detection of by-products formed in chloride-free solutions [106,108,119].

Few papers have shown the applicability of EO with Si/BDD to the treatment of different dyes in real wastewaters [106,108,116]. For example, Martinez-Huitle et al. [106] have studied the degradation of 1 dm^3 of a real effluent of a Brazilian textile industry (650 mg dm^{-3} COD, 1204 HU (hazen units) of color, 2.70 mS cm^{-1} conductivity and pH 10.2) using an undivided flow cell with a 54.7 cm^2 Si/BDD anode considering the role of j between 20 and 60 mA cm^{-2}, temperature between 25 and 60 °C and addition of Na_2SO_4. About 50%, 95% and 100% of decolorization efficiency were achieved after 12 h at 20, 40 and 60 mA cm^{-2}, respectively. Additionally, COD was totally removed at 40 and 60 mA cm^{-2} in 19 and 17 h consuming about 350 and 400 kWh m^{-3}, respectively, but no complete COD decay was achieved at 20 mA cm^{-2} after 23 h of

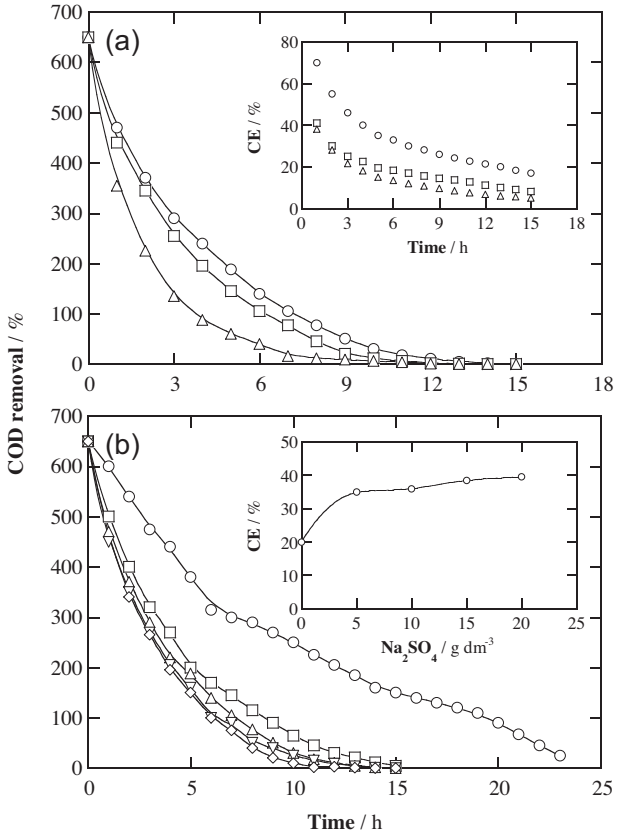

Fig. 10. (a) Influence of current density on the evolution of COD and current efficiency (inset), as a function of time, during the EO treatment of 1 dm^3 of an actual textile effluent with 5 g dm^{-3} Na_2SO_4 at 25 °C using a flow plant with a BDD anode and a Ti cathode, both of 54.7 cm^2 area, and liquid flow rate of 250 dm^3 h^{-1}. Current density: (○) 20 mA cm^{-2}, (□) 40 mA cm^{-2} and (△) 60 mA cm^{-2}. (b) Effect of Na_2SO_4 concentration on the change of COD and current efficiency at 5 h (inset), with time during the above EO treatments at 20 mA cm^{-2}. [Na_2SO_4] = (○) no addition, (□) 5 g dm^{-3}, (△) 10 g dm^{-3}, (▽) 15 g dm^{-3} and (◊) 20 g dm^{-3}.
Adapted from Ref. [106].

electrolysis with 200 kW h m^{-3} of specific energy consumption. The long time required for obtaining total color and COD was due to the low conductivity of the effluent and for this reason, known amounts of Na_2SO_4 were added to enhance the conductivity and promote the production of BDD(•OH) and peroxodisulfate via reaction (23). The larger action of these oxidants can be observed in Fig. 10a when the actual textile effluent was treated with 5 g dm^{-3} Na_2SO_4. COD was more quickly destroyed in 12–15 h, at slightly higher rate as *j* increased from 20 to 60 mA cm^{-2}, owing to the generation of more oxidants, and with lower energy requirements of 180 kW h m^{-3} as maximal. The inset panel of Fig. 10a shows a gradual drop of current efficiency at greater *j* as a result of the acceleration of waste reactions of BDD(•OH), mainly O_2 formation by reaction (f) in Fig. 7. The decolorization efficiency was also strongly enhanced reaching 95%, 100% and 100% after 12, 8 and 4 h at 20, 40 and 60 mA cm^{-2}, respectively. In contrast, Fig. 10b highlights that COD decay and efficiency did not improved significantly when Na_2SO_4 concentration increased up to 20 g dm^{-3}. Conversely, a rise in temperature had a strong positive effect on the oxidation rate at all *j* values.

Other interesting results have been reported by Sales Solano et al. [108] who decontaminate 500 cm^3 of a real textile wastewater with 1018 mg dm^{-3} COD, 7504 HU, 5.90 mS cm^{-1} and pH 12.4 using a stirred tank reactor with a 10 cm^2 Si/BDD anode in batch operation mode. At 60 mA cm^{-2}, 21% color removal and 12.6% COD decay were obtained in 12 h. Under similar conditions and adding Na_2SO_4, total decolorization and COD removal were achieved in 4 and 12 h, respectively. In the presence of NaCl, the electrolysis time was significantly reduced by the additional action of active chlorine species with a lower energy consumption of 36.96 kWh m^{-3} than 61.65 kWh m^{-3} needed for total decontamination with Na_2SO_4. A modest cost of approximately US$ 14.26 per m^3 of effluent was estimated. Other authors have also described the acceleration of real wastewater degradation by EO with a Si/BDD anode combined with addition of NaCl [116].

It is also noticeable the work of Alvarez-Guerra et al. [109] who used a photovoltaic solar-EO process to treat 1 dm^3 of a urban wastewater containing dyes with 80 mg dm^{-3} TOC and 1 mS cm^{-1} conductivity in a Diacell® filter-press reactor with a Si/BDD anode coupled with a photovoltaic module. These authors provided relevant information about the dimensions of electrochemical reactor and photovoltaic modules in terms of anode area and effectiveness, respectively. Input variables included the characteristics of the effluent (COD and TOC), flow rate, the required yield and the solar irradiance, and a real plant was designed to treat urban wastewater as a function of the number of habitants in the region and solar irradiance.

5.6.4. Diamond electrodes with unspecified support

The use of unspecified support diamond electrodes has given good performances for the remediation of dyes wastewaters [107,112]. An unspecified support diamond electrode was employed to mineralize a solution of Reactive Red 147 in 0.1 M Na_2SO_4 using a stirred tank reactor with different operating conditions such as *j*, pH and dye concentration [112]. Total decolorization was always achieved after 8 min of treatment, but color decay rate was dependent on the operating variables. Nevertheless, a synthetic solution with 50 mg dm^{-3} dye was not completely mineralized by BDD(•OH) and 77.2% TOC reduction was found as maximal at pH 5 and 10 mA cm^{-2}.

5.7. Comparative oxidation power of anodes

Many comparative studies with pure synthetic dyes of the textile industry have been performed to ascertain the best anodic material for EO, although no clear results have been obtained [78,89,92–94,98,111,122]. The De Andrade's group [78] reported the superiority of Ti/$Ru_{0.3}Sn_{0.7}O_2$ anode compared to Ti/$Ru_{0.3}Ti_{0.7}O_2$ and Ti$(RuO_2)_{0.7}(Ta_2O_5)_{0.3}$ ones for decolorizing Reactive Blue 4 against Reactive Orange 16, whereas the opposite tendency was found for the two latter anodes. When compared the EO process with Pt of Reactive Blue 52, Reactive Black 5, Reactive Green 15 and Reactive Yellow 125, higher performance was obtained for the former dye [92]. In contrast, the study made for the degradation of Amaranth and Procion Orange MX-2R revealed the same oxidation ability of Pt coated with polyaniline and disperse Pt nanoparticles as anodes [89], which was related to the oxidant or reductive characteristics of the Pt material.

More research efforts are then needed to better know what anode is preferable in EO as a function of the chemical structure and/or applicability of the dye, although the characteristics of the electrochemical system could also have a significant influence. For example, the treatment of 400 cm^3 of 190 mg dm^{-3} Remazol Red BR and Novacron Blue C-D solutions in Na_2SO_4 using a stirred tank reactor with a Si/BDD anode at 60 mA cm^{-2} yielded more than 95% color and COD reductions in 300 min with specific energy consumption ranging from 4.13 to 57.52 kWh m^{-3} depending on pH and dye structure [111]. When 1.5 dm^3 of 250 mg dm^{-3} of the same dyes were degraded in a flow reactor with either a Ti/Pt or Ti/Pt–SbSn anode at 60 mA cm^{-2} and flow rate of 160 dm^3 h^{-1} [93], 91% color removal and only 34% COD reduction were found for both dyes using the former anode, whereas the values of these parameters differed for both dyes with the latter anode. These findings

indicated that dye structure, batch or flow operating mode and anode material play an important role to decide the optimum operating parameters to apply the EO approach.

An inspection of data of Tables 2 and 3 shows that most anodes tested in EO for treating chloride-free dyes wastewaters provide high decolorization efficiency because they can easily destroy the different chromophore groups of dyestuffs. In contrast, aromatics and short aliphatic carboxylic acids formed during the process can only be largely mineralized by non-active anodes and conducting diamond electrodes, whereas they are inefficiently removed from solutions by metal, metal oxide and carbonaceous electrodes. The implementation of electrochemical systems like used by Ferreira et al. [93] with both, an active and non-active anode could be a suitable solution to increase the efficiency of the EO process.

Due to its non-active nature, diamond electrodes seem preferable to be utilized thanks their greater ability to completely mineralize dyes solutions with acceptable energy consumption at least at lab scale. Nevertheless, a set of experiments has shown that the conductive layer characteristics such as sp^3/sp^2 ratio [132], boron content [110,121,132] and BDD layer-thickness [132], as well as substrate properties like resistivity and roughness of the surface, have an important influence on bulk electrolysis results. Conversely to the lab scale, the viability of EO with diamond electrodes for industrial application is not well established yet and more research efforts are needed to clarify several fundamental aspects involving the production of desired or undesired oxidants, service lifetime of large-scale BDD electrodes, a total economic study of the process for real wastewaters, the optimization of electrolytic reactors and so on. Regarding the oxidants produced on the BDD surface, the greater oxidation power of BDD(•OH) and other ROS from water discharge could be improved by the additional generation of weaker peroxoderivative oxidants from oxidation of bisulfate, bicarbonate and phosphate of the electrolyte to favor the electrochemical combustion of pollutants in chloride-free solutions. In the presence of chloride ions, active chlorine species are easily produced at all anodes, accelerating the destruction of dyes and strongly enhancing the oxidation ability of the electrolytic system in most cases. Some comparative studies with different electrolytes reported in this section have shown the fastest destruction of several dyestuffs in chloride-containing effluents. In the next section, the electrochemical degradation of these solutions will be examined in more detail.

6. Indirect electro-oxidation with strong oxidants

Synthetic dye solutions or real textile industry effluents can be completely decontaminated by indirect electro-oxidation methods involving the homogeneous reaction of organic pollutants with strong oxidants generated during electrolysis. Two approaches are mainly utilized: (i) the electro-oxidation with active chlorine, so-called "indirect oxidation" [28,30] or "Cl^--mediated oxidation" [108], where anodic oxidation of Cl^- present in the effluent yields active chlorine species (dissolved Cl_2, HClO and/or OCl^-) and chlorite, chlorine dioxide, chlorate and perchlorate that can oxidize organic pollutants in the bulk [4,28,30,32] and (ii) the EF process in which organics can be destroyed with homogeneous •OH formed from Fenton's reaction between added catalytic Fe^{2+} and H_2O_2 electrogenerated from O_2 reduction at a suitable cathode [31].

In both cases, dyes are also competitively destroyed by direct anodic oxidation and by reaction with heterogeneous M(•OH) and other ROS and weaker oxidants produced from oxidation of water and anions of the electrolyte (see Section 5.1). In this section, the applicability of these mediated electro-oxidation methods to the decolorization and degradation of synthetic organic dyes is examined, making especial emphasis in the use of electrode materials favoring the generation of chlorine active species or H_2O_2. Other proposed indirect procedures will also be briefly described.

6.1. Electro-oxidation with active chlorine

Chlorine and chlorine–oxygen species like HClO and ClO^- are traditionally used for treating industrial wastewaters [24,25] and are also widely employed in the disinfection of drinking water [131]. The main difference of Cl^--mediated oxidation from EO is the on-site production of active chlorine species during electrolysis of contaminated chloride-containing solutions. The applicability of this approach is thanks to their advantages [24,131,133] such as: (i) the transport and storage of dangerous chlorine for water treatment is avoided, (ii) faster destruction of organic matter than in chemical oxidation and (iii) much lower total costs than conventional chemical technology. Nevertheless, important disadvantages have been described [116,131,134,135]: (i) the formation of undesirable toxic chloro-organic derivatives such as chloroform and (ii) the electrogeneration of chlorine–oxygen by-products such as chlorite, chlorate and perchlorate, which have a high health risk for living beings.

Particular attention in the fundamentals and experimental observations regarding their applications must be taken into consideration before or during the use of this mediated electro-oxidation method for the treatment of synthetic and real dyeing wastewaters, as discussed in detail in subsections below.

6.1.1. Electrogeneration of active chlorine species

Based on existing literature [136–142], the electrolysis of chloride aqueous solutions in an undivided cell involves the direct oxidation of chloride ion at the anode to yield soluble chlorine:

$$2Cl^- \rightarrow Cl_{2(aq)} + 2e^- \quad (26)$$

and the reduction of water at the cathode giving hydroxide ion and hydrogen gas from reaction (10).

If the local concentration of dissolved chlorine exceeds its solubility, then supersaturation drives the formation of bubbles of chlorine gas. Since electrogenerated chlorine diffuses from the anode toward the solution, it can react with chloride ion to form trichloride ion from reaction (27) or it is rapidly hydrolyzed to hypochlorous and chloride ion:

$$Cl_{2(aq)} + Cl^- \rightleftarrows Cl_3^- \quad (27)$$

$$Cl_{2(aq)} + H_2O \rightleftarrows HClO + Cl^- + H^+ \quad (28)$$

In the bulk solution this acid is in equilibrium with ClO^- ion with $pK_a = 7.55$ [137,143]):

$$HClO \rightleftarrows ClO^- + H^+ \quad (29)$$

The action of active chlorine species is dependent on the solution pH [4,143]. At pH ca. 4.0, Cl_3^- is formed in very low concentration, whereas until pH near 3.0, the predominant species is $Cl_{2(aq)}$. Meanwhile, the preferential species in the pH range 3–8 and for pH > 8.0 are HClO and ClO^-, respectively. Then, Cl^--mediated oxidation of dyes with these species is expected to be faster in acidic than in alkaline media because of the higher standard potential of $Cl_{2(aq)}$ ($E^\circ = 1.36$ V/SHE) and HClO ($E^\circ = 1.49$ V/SHE) than ClO^- ($E^\circ = 0.89$ V/SHE) [4]. Since most electrolyses in undivided cells are treated in alkaline medium, the mineralization of organic dyes is commonly ascribed to the chemical action of ClO^- as follows [136–138]:

$$Dye + ClO^- \rightarrow CO_2 + H_2O + Cl^- \quad (30)$$

The ClO^- concentration can be limited by its anodic oxidation to ClO_2^- ion from reaction (31) and consecutive oxidation of

this species to ClO_3^- and ClO_4^- ions from reactions (32) and (33), respectively [136–142]:

$$ClO^- + H_2O \rightarrow ClO_2^- + 2H^+ + 2e^- \quad (31)$$

$$ClO_2^- + H_2O \rightarrow ClO_3^- + 2H^+ + 2e^- \quad (32)$$

$$ClO_3^- + H_2O \rightarrow ClO_4^- + 2H^+ + 2e^- \quad (33)$$

The loss of ClO^- is also feasible by reduction to Cl^- ion at the cathode from reaction (34) and from the waste reactions (35)–(37) in the solution bulk:

$$ClO^- + H_2O + 2e^- \rightarrow Cl^- + 2OH^- \quad (34)$$

$$2HClO + ClO^- \rightarrow ClO_3^- + 2Cl^- + 2H^+ \quad (35)$$

$$2ClO^- \rightarrow 2Cl^- + O_2 \quad (36)$$

$$ClO^- + H_2 \rightarrow Cl^- + H_2O \quad (37)$$

The rates of electrode reactions (26) and (31)–(34) are a function of the electrocatalytic activity of the anode, Cl^- concentration, salt cation, stirring or flow rate, temperature and j [138,120]. In contrast, the homogeneous chemical reaction (30) depends on the diffusion rate of organics into the solution regulated by the stirring or flow rate, temperature and pH [138], whereas chemical waste reactions (35)–(37) are strongly enhanced with rising temperature [144].

6.1.2. Experimental systems

Similar electrochemical systems to those reported above for EO (see Section 5.2) are utilized for Cl^--mediated oxidation of dyeing solutions or real effluents. Conventional three-electrode cells with one- or two-compartment two-electrode cells or tank reactors have been frequently utilized [79,82,126,153,136]. Several papers have reported the use of flow reactors to treat dye effluents [79,127,138,120,147,152].

Regarding the anode material, its non-active or active nature is an important parameter that determines the predominant category of oxidants produced during the electrolysis of chloride solutions. Non-active anodes like BDD are not useful for indirect electrooxidation with active chlorine since they form largely ROS and other oxidants like peroxodisulfate, peroxodicarbonate or peroxodiphosphate [28–33,131]), avoiding a good generation of active chorine species. Nevertheless, some authors [108,116,124,125,145–147] have described the acceleration in dyes destruction with BDD anodes from chloride solutions in comparison to other electrolytes, whereas few works have considered negligible the generation of active chlorine [127]. For example, the degradation of 600 cm^3 of a 100 mg dm^{-3} Reactive Red 141 solution in 0.1 M Na_2SO_4 with a filter-press flow cell with a 78 cm^2 Si/BDD anode was optimized by RSM with a central composite design based on 4 independent variables like j between 10 and 50 mA cm^{-2}, pH between 3 and 11, addition of NaCl up to 2.34 g dm^{-3} and temperature between 15 and 55 °C [147]. Complete decolorization at 6 min and 100% of COD and 90% of TOC removals at 90 min were obtained under optimum conditions. The lowest specific charge for 90% decolorization was reached at pH < 4 with NaCl contents >1.5 g dm^{-3}, where generated HClO acts as main oxidant. COD decay was practically not affected by the solution pH, but it increased with raising NaCl concentration up to 1.5 g dm^{-3}. Temperatures higher than >40 °C diminished COD reduction, as a consequence of faster side reactions like O_2 and Cl_2 evolution. High TOC abatement was reached only with strong oxidants like •OH and HOCl when Cl^- content was <0.7 g dm^{-3} in acidic solutions to avoid the formation of ClO_3^- and ClO_4^-. Other authors have also reported excellent performances when treating real effluents with Si/BDD [108,125] and Tb/BDD [127] anodes. However, contradictory results on the role of oxidizing agents over dyestuffs have been described by these authors. Solano et al. [108] found that the mediated oxidation occurred via •OH plus $S_2O_8^{2-}$ in 0.070 M Na_2SO_4 or active chlorine species in 0.170 M NaCl. Nevertheless, in sulfate solution, no toxic intermediates were identified, whereas chloroform was produced in Cl^- solution. Conversely, no organochloride derivatives were detected by Aquino et al. [127] during the treatment of a real effluent after adding NaCl.

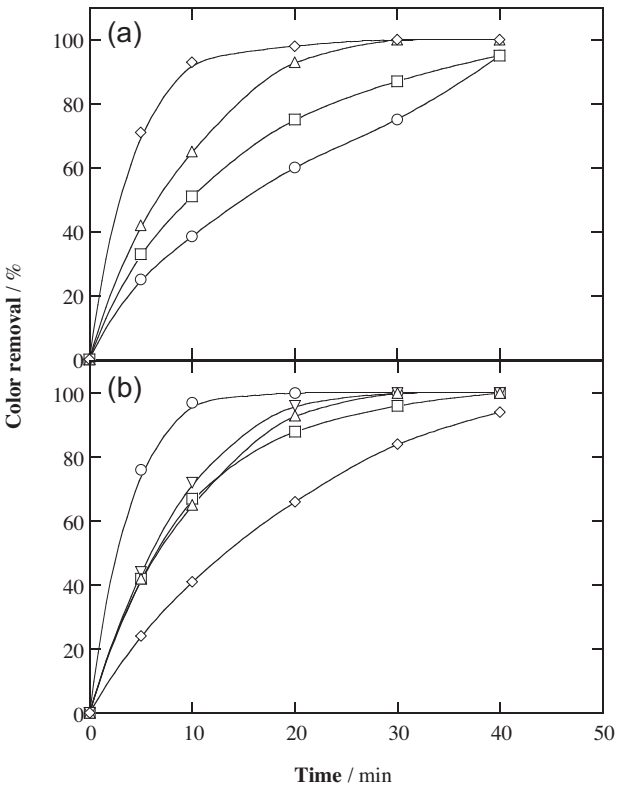

Fig. 11. Dependence of the percentage of color removal on electrolysis time for the EO treatment of 200 cm^3 of 50 mg dm^{-3} Acid Orange II using a flow plant with a Nb/BDD anode and a Nb/Pt cathode, both of 77.4 cm^2 area, at 200 mA, 20 °C and liquid flow rate of 400 cm^3 min^{-1}. In plot (a), KCl concentration: (○) 1.0 mM, (□) 3.0 mM, (△) 5.0 mM and (◊) 10 mM. In plot (b), 5.0 mM concentration of: (○) HCl, (□) LiCl, (△) KCl, (▽) NaCl and (◊) NH_4Cl.
Adapted from Ref. [120].

Other important parameter, usually disregarded in Cl^--mediated oxidation studies, is the cation of the chloride salt. This influence is illustrated in Fig. 11 for the treatment of 200 cm^3 of 50 mg dm^{-3} Acid Orange II using a flow plant with a 77.4 cm^2 Nb/BDD anode at 200 mA [120]. Fig. 11a shows a faster decolorization as more Cl^- concentration is added to the solution until 10 mM. Increasing j also causes the same effect, accelerating dye mineralization by the concomitant rise in rate of all electrode reactions to produce more amount of oxidizing species. Fig. 11b highlights that using different cations in the chloride solution, the color removal drops in the sequences: $H^+ > NH_4^+ > Na^+ \sim K^+ \sim Li^+$ at 0.65 mA cm^{-2}, $H^+ > Na^+ \sim K^+ \sim Li^+ \sim NH_4^+$ at 1.29 mA cm^{-2} and $H^+ > Na^+ \sim K^+ \sim Li^+ > NH_4^+$ at 2.58 mA cm^{-2}. These outcomes for HCl are in consistence with the ability of producing active chlorine species with higher oxidizing power like Cl_2 and HClO at low pH. The similar impact of LiCl, NaCl and KCl for all j values suggests the production of analogous amounts of active chlorine species, whereas the variable effect of NH_4Cl is difficult to interpret.

The use of PbO_2 provides a considerably [67,70,148–151] or slightly [127] enhancement for dyestuffs degradation in chloride solutions, despite this electrode is considered as a non-active anode. Conversely, active anodes have much higher electrocatalytic power for oxidizing chloride ion than for generating ROS, as found

for DSA-type [152], Pt [137,138,153,154] and graphite [136,155] electrodes. The destruction of Acid Blue 62, Disperse Orange 29, Remazol Brilliant Blue R, Direct Yellow 86 and Reactive Red 141 [144,148–151] has been studied by Cl^--mediated oxidation at PbO_2 anodes. It is noticeable the work of Mukimin et al. [151] who described a higher electrocatalytic power of synthesized PbO_2 from an alkaline than an acidic solution to degrade 50 cm^3 of Remazol Brilliant Blue R solutions in the presence of 4 g dm^{-3} NaCl at pH 5–10 by applying 5 V for 60 min, achieving total decolorization and 67–72% COD decay. The performance of the oxidation process was influenced by the equilibrium reaction between the Cl_2/HClO/ClO^- oxidizing species within the pH region of 5–10.

Comparison of Tables 2 and 4 evidences the higher efficiencies for color and COD removals found for Cl^--mediated oxidation than for EO with chlorine-free solutions when the same type of anode is employed. Although there is not enough comparative data in the literature to can establish the best kind of anode for the former technique, DSA-type electrodes are usually preferred due to their high stability and larger production of active chlorine species.

6.1.3. DSA-type electrodes

RuO_2- and IrO_2-based anodes are active anodes with excellent electrocatalytic activity for O_2 and Cl_2 evolutions. IrO_2 is one of the cheapest DSA electrodes with enhanced catalytic activity for such reactions and stability against corrosion compared to RuO_2 [156]. Both anodes produce so low amounts of physisorbed M($^\bullet$OH) that cause poor mineralization of organics. In contrast, their low Cl_2 overpotential favors the large formation of active chlorine species. Addition of NaCl to wastewaters improves the oxidation ability of Ti/IrO_2, Ti/RuO_2 and Ti/IrO_2–RuO_2 anodes [156].

In the last years, a limited number of papers have compared the treatment of some dyes with active chlorine produced at DSA-type anodes. Following the study on a stirred undivided cell with a Ti/$Ru_{0.3}Ti_{0.7}O_2$ or Ti/Pt anode to degrade 400 cm^3 of solutions of 100 mg dm^{-3} of Methyl Red in 0.25 M H_2SO_4 at 20–60 mA cm^{-2} and 25 °C (see Section 5.3.2), Tavares et al. [82] reported an increase in oxidation when low NaCl concentrations up to 0.8 g dm^{-3} were introduced in the dye solution. The EO treatment with 0.25 M H_2SO_4 + 0.2 g dm^{-3} NaCl at 40 mA cm^{-2} showed a strong influence of the nature of electrode material on the mineralization process because 96% TOC decay was attained after 360 min of electrolysis with Ti/$Ru_{0.3}Ti_{0.7}O_2$, but only 83% TOC removal was achieved for the Ti/Pt electrode. These authors assumed that $Cl_{2(aq)}$, HClO and/or ClO^- depending of pH checked were the oxidizing agents during indirect electro-oxidation.

The degradation of Indigo Carmine in a filter-press type FM01-LC reactor with Sb_2O_5-doped Ti/IrO_2–SnO_2 or BDD anode was investigated by Rodríguez et al. [80]. Micro- and macro-electrolyses were carried out using solutions of 0.8 mM dye in 0.05 M NaCl. Micro-electrolysis results showed an improvement of dye degradation by active chlorine species generated on DSA anode surface. In the case of BDD, however, more oxidizing species were formed improving the mineralization efficiencies. The geometry, flow pattern and mass transport of the FM01-LC reactor used in macroelectrolysis trials affected the hydrodynamic conditions on the Cl^--mediated degradation rate. Reynolds number (Re) values of 93, 371, 464 and 557 were tested between 5 and 20 mA cm^{-2}. The degradation rate was Re independent at the lowest j of 5 mA cm^{-2}, but it varied with Re at the highest j of 20 mA cm^{-2}. This behavior highlights the key importance of Re and j to assess the mass transport as well as the reactor design parameters. Lower energy consumption of 2.02 kWh m^{-3} for complete decolorization and 9.04 kWh m^{-3} for COD removal were obtained for the DSA electrode at 5 mA cm^{-2}. No chlorinated organic products were detected.

Relevant results have been published by Basha et al. [79] who studied the electrochemical degradation of a textile dyeing effluent (a mixture of reactive hydrolyzed dyes with 5800 mg dm^{-3} COD, 181 mg dm^{-3} BOD and 40 g dm^{-3} Cl^-) in batch and flow reactors using Ti/RuO_x–TiO_x. The EO process for 300 cm^3 of the effluent in the batch reactor was optimal for 40 mA cm^{-2}, giving 99.2% COD removal with specific energy consumption of 35.6 kWh (kg COD)$^{-1}$ in 8 h. Best results were found by treating 1.5 dm^3 in the flow reactor at flow rate of 100 dm^3 h^{-1} since 93% COD decay and 1.98 kWh (kg COD)$^{-1}$ were obtained after 6 h at 25 mA cm^{-2}. Under these conditions, the oxidation via physisorbed M($^\bullet$OH) was not relevant because the high concentration of Cl^- in solution promoted an effective oxidation mainly by active chlorine species, being more effective with increasing j, as expected if greater concentrations of such strong oxidants are gradually produced.

More results are then needed to ascertain the relative electrocatalytic activity of the large variety of DSA-type electrodes available for the electro-oxidation of organic dyes mediated with active chlorine and mainly, to determine if the use of DSA anodes could favor the production of organochloride compounds during electrochemical treatment.

6.1.4. Metal anodes

The use of metals such as Ti/Pt [137], pure Pt [138], Ir, Pd, Ni, Co and Ag [153] in indirect electro-oxidation with active chlorine can also yield rapid decolorization and large decontamination of highly concentrated dyes effluents. This has been shown by Gomes et al. [138] following the degradation of Reactive Orange 16 in NaCl effluents, as illustrated in Fig. 12. A flow cell containing a 2 cm^2 pure Pt anode was utilized to treat 100 dm^3 of 35 mg dm^{-3} of this dye in NaCl concentration ranging from 0.25 to 1 g dm^{-3} to investigate the influence of E_{cell}, flow rate and pH. Decolorization efficiencies for 1 g dm^{-3} NaCl ranged at 2.2 V from 80% to 96% when flow rate varied from 0.6 to 1.5 dm^3 h^{-1}. When the variation of NaCl content and E_{cell} was examined, 62% color removal was only achieved after 60 min at 1.8 V with 1 g dm^{-3} of NaCl (see Fig. 12a), whereas insignificant color decay was found for lower Cl^- concentrations. In contrast, when E_{cell} was increased to 2.2 V, about 93% decolorization efficiency was obtained at 60 min with 0.75 and 1.00 g dm^{-3} of NaCl (see Fig. 12b). This behavior is a clear synergistic effect of Cl^- oxidation toward O_2 evolution reaction with production of a greater amount of active chlorine species. The use of a membrane in the cell at 2.2 V caused a rapid decay in decolorization rate because of the drop in j. Fig. 12c and d highlights that the increase in NaCl content enhanced TOC removal and dropped the energy per order, respectively. From these results, the authors inferred that this procedure can only be attractive for decolorizing dyeing effluents because conventional biological treatment is unable to completely remove organic load satisfactorily. In a similar way, Mijin et al. [137] proposed the application of mediated electro-oxidation with a Ti/PtO_x anode to decolorize Basic Yellow 28 wastewaters with high Cl^- content as pre-treatment technology. They suggested optimum conditions for ~20 g dm^{-3} NaCl by applying 150 mA to remove 10–70 mg dm^{-3} of Basic Yellow 28 with a specific energy consumption of around 1.1 kWh m^{-3}. TOC analysis demonstrated that no complete mineralization was achieved, but only the partial degradation of amino group.

A very limited number of papers has reported some information on the intermediates formed during the Cl^--mediated oxidation of dyes on Pt. Puttappa et al. [154] detected the formation of several aromatic compounds, which evolved to aliphatic acids such as acetic, maleic and oxalic as final by-products, when 100 mg dm^{-3} of Acid Blue 193 were degraded in an undivided cell with a Pt foil anode. Tavares et al. [82] proposed possible fragmentation products of Methyl Red after short electrolysis times by means of GC–MS analysis when a Ti/Pt anode was used.

Table 4
Percentage of color and COD removals and energy cost for the indirect electro-oxidation with active chlorine of selected dyes in chloride solutions using DSA-type electrodes, metals and graphite as anodes at 20–30 °C.

Dye[a]	C_0 (mg dm^{-3})	Experimental conditions	j[b] (mA cm^{-2})	% color removal	% COD decay	Energy cost (kWh m^{-3})	Ref.
PbO_2 anode							
Acid Blue 62	100	1.75 g dm^{-3} NaCl, pH = 5.5, for 30 min	125	–[c]	71	2.1[d]	[144]
Disperse Orange 29	100	1.51 g dm^{-3} NaCl, pH = 6.5, for 2 h	74	100	100	35	[149]
Reactive Blue 19 (Remazol Brilliant Blue R)	–[e]	4 g dm^{-3} NaCl, pH = 5–10, for 1 h	5[f]	100	67–72	–[c]	[151]
Reactive Red 141	100	1.17 g dm^{-3} NaCl, pH = 5.0, for 30 min	75	100	100	3.1[d]	[150]
Ti/TiO_2-RuO_2-IrO_2 anode							
Acid Blue 74 (Indigo Carmine)	0.8[g]	0.05 M NaCl, pH = 6.27, for 5 h	10	100	100	15.6	[80]
Pt anode							
Basic Yellow 28	50	20 g dm^{-3} NaCl, pH = 5.2, for 1 h	150[h]	98	–	1.1	[137]
Acid Blue 193 (Luganil blue N)	100	2.0 g dm^{-3} NaCl, pH = 6.0, for 30 min	50	100	80	–[c]	[154]
Reactive Orange 16	35	1.0 g dm^{-3} NaCl, pH = 1.6, for 1 h	1.8[f]	61	57[i]	–[c]	[138]
Graphite anode							
(Novacron Deep Red C-D)	50	7 g dm^{-3} NaCl,	17	99	88	2.2	[155]
(Novacron Orange C-RN)	50	pH = 3.0, for 20 min	17	97	82	2.2	
Nb/BDD anode							
Acid Orange 7 (Orange II)	50	2.5 mM NaCl, pH = 7.6, for 1 h	2.58	94	–[c]	–[c]	[120]
Si/BDD anode							
Reactive Red 141	100	1.17 g dm^{-3} NaCl, pH = 1.6, for 6 min	30	100	100, 90[i,j]	–[c]	[147]

[a] Color index (common) name.
[b] Applied current density.
[c] Not determined.
[d] Data at 90% decolorization.
[e] Not specified.
[f] Applied cell voltage (V).
[g] mM concentration.
[h] Current (mA).
[i] Percentage of TOC decay.
[j] At 90 min.

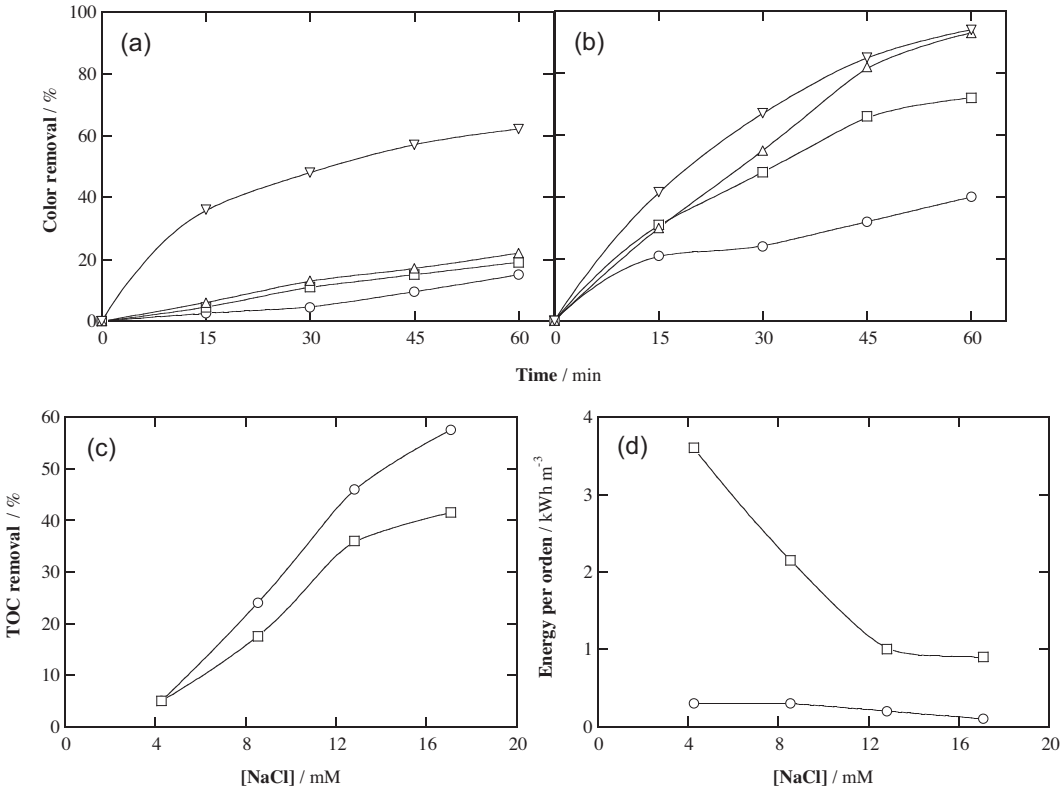

Fig. 12. Decolorization efficiency with electrolysis time for the EO with active chlorine of 50 cm^3 of 35 mg dm^{-3} Reactive Orange 16 in 0.5 M H_2SO_4 using a flow cell with a 2 cm^2 Pt anode and a 2 cm^2 stainless steel cathode by applying an anode potential of: (a) 1.8 and (b) 2.2 V vs. SHE at 25 °C and 1.24 dm^3 h^{-1}. NaCl concentrations of (◯) 0.25, (□) 0.50, (△) 0.75 and (▽) 1.00 g dm^{-3}. (c) TOC removal and (d) energy per order as a function of NaCl concentration at anode potential of (◯) 1.8 V and (□) 2.2 V vs. SHE. Adapted from Ref. [138].

More recently, the performance of different metals like Pt, Ir, Pd, Ni, Cu, Co and Ag as anodes was examined in a stirred tank reactor cell for the decolorization of 50 cm^3 of a 1000 mg dm^{-3} Reactive Blue 109 solution with 5.8 g dm^{-3} NaCl at pH 4 by applying 10 V [153]. Although the dye solution was completely decolorized with all electrodes, Ag, Co, Ni and Cu were completely corroded. For the stable Pt, Ir and Pd anodes, COD removals of 94%, 81% and 73% were found, respectively. The best performance for Pt anode can be related the enhancement of reactions (26), (28) and (29) favoring the dye oxidation with HClO at pH 4 instead of its slower reaction with ClO^- taking place in alkaline medium. Under the optimum conditions of 5.8 g dm^{-3} of NaCl and pH 4, the treatment of a real effluent at 20 mA cm^{-2} for 75 min led to 96% of color and COD removals, whereas slightly lower reductions were obtained for BOD, TOC and surfactant removals.

6.1.5. Graphite anode

The indirect electro-oxidation with active chlorine performed with a graphite anode has been focused to characterize the decolorization process of Reactive Blue 109 [153], Reactive Orange 107 [136], Novacron Deep Red C-D and Novacron Orange C-RN [155]. The two latter, for example, exhibited a fast color removal that increased with raising Cl^- concentration from 1 to 9 g dm^{-3} and j from 8.5 to 42.5 mA cm^{-2} as well as decreasing pH from 11 to 3, as expected if they react with $Cl_{2(aq)}$, HClO and/or ClO^- (see Section 6.1.3) with small participation of direct anodic oxidation on graphite. This behavior also affected the specific energy consumption of the process, which dropped with rising NaCl concentration and dropping pH. It is also noticeable the optimization study reported by Rajkumar and Muthukumar [136] for the treatment of 250 cm^3 of 0.3 g dm^{-3} Reactive Orange 107 solutions using a stirred graphite/graphite cell with 71.5 cm^2 electrodes by RSM. About 98% color removal and 90% COD decay were obtained for optimum conditions of 4.64 g dm^{-3} NaCl, pH 7.4, 35 mA cm^{-2} and electrolysis time of 16 min. This corroborates again the feasibility of using mediated oxidation with electrogenerated active chlorine as a very attractive method for an efficient and low cost color removal of dyeing wastewaters.

6.2. Electro-Fenton

EF is an indirect electro-oxidation method based on the production of homogeneous •OH radical from Fenton's reaction between Fe^{2+} ion initially present (or added) in the medium and H_2O_2 generated at a suitable cathode, with a second-order rate constant (k_2) of 63 M^{-1} s^{-1} [4,31,157]:

$$Fe^{2+} + H_2O_2 \rightarrow Fe^{3+} + {}^{\bullet}OH + OH^- \quad (38)$$

It is well-known that H_2O_2 can be produced in aqueous medium by the two-electron reduction of injected O_2 gas (pure or from air) at a carbonaceous cathode with high surface area like carbon felt, reticulated vitreous carbon (RVC), carbon-polytetrafluoroethylene (PTFE) and even BDD, according to the following reaction with E° = 0.68 V/SHE [31]:

$$O_{2(g)} + 2H^+ + 2e^- \rightarrow H_2O_2 \quad (39)$$

The loss of product or lowering of current efficiency can take place by parasitic reactions such as electrochemical reduction at the cathode surface from reaction (40) and disproportion in the bulk from reaction (41). Moreover, when an undivided cell is used, H_2O_2 is oxidized to O_2 via hydroperoxyl radical ($HO_2^{\bullet}$), a weaker oxidant than •OH, from reactions (42) and (43) [31]:

$$H_2O_2 + 2e^- \rightarrow 2OH^- \quad (40)$$

$$2H_2O_2 \rightarrow O_{2(g)} + 2H_2O \quad (41)$$

$$H_2O_2 \rightarrow HO_2^{\bullet} + H^+ + e^- \quad (42)$$

$$HO_2^{\bullet} \rightarrow O_{2(g)} + H^+ + e^- \quad (43)$$

Addition of a low catalytic concentration of Fe^{2+} to the acidic dyestuff solution then produces the strong oxidant •OH from Fenton's reaction (38). This reaction is catalytic because Fe^{2+} is continuously regenerated from Fe^{3+} reduction at the cathode (E° = 0.77 V/SHE) from reaction (44) or in the solution primordially by generated H_2O_2 from Fenton-like reaction (45) with $k_2 = 8.4 \times 10^{-6}$ M^{-1} s^{-1}. [4,157]. Nevertheless, the EF system loses efficiency due to the consumption of a part of homogeneous •OH by waste reactions involving, for example, its reaction with Fe^{2+} by reaction (46) with $k_2 = 3.2 \times 10^8$ M^{-1} s^{-1} and H_2O_2 from reaction (47) with $k_2 = 2.7 \times 10^7$ M^{-1} s^{-1}, whereas in an undivided cell, Fe^{2+} is also oxidized at the anode by reaction (48) [4]. The rate of reactions (46) and (47) is very low in EF compared to classical Fenton's reagent because of the smaller content of H_2O_2 accumulated in the medium and the weaker Fe^{2+} concentration used in the EF process. The efficient action of reaction (44) makes feasible the direct addition of Fe^{3+} to the medium [4,157].

$$Fe^{3+} + e^- \rightarrow Fe^{2+} \quad (44)$$

$$Fe^{3+} + H_2O_2 \rightarrow Fe^{2+} + H^+ + HO_2^{\bullet} \quad (45)$$

$$Fe^{2+} + {}^{\bullet}OH \rightarrow Fe^{3+} + OH^- \quad (46)$$

$$H_2O_2 + {}^{\bullet}OH \rightarrow HO_2^{\bullet} + H_2O \quad (47)$$

$$Fe^{2+} \rightarrow Fe^{3+} + e^- \quad (48)$$

In EF, organics are assumed to be destroyed solely by homogeneous •OH formed from Fenton's reaction (38). However, heterogeneous •OH produced at the anode in an undivided cell can also degrade the pollutants, primordially using BDD because of the high oxidation ability of BDD(•OH) [4,31]. Parallel slower destruction of organics with other weaker ROS like H_2O_2, $HO_2^{\bullet}$ and O_3, as well as with weaker oxidants like $S_2O_8^{2-}$ when using BDD (see Section 5.1), is feasible. The generation of final Fe(III)-carboxylate complexes, hardly mineralized with •OH, prolongs the duration of EF and sometimes, yields poor decontamination [2,4,31,38–41].

The use of EF presents important advantages compared to the traditional Fenton's reagent method, including: (i) easy regulation of the on-site H_2O_2 production, (ii) higher degradation rate of organic pollutants due to the quicker regeneration of Fe^{2+} at the cathode and (iii) lower operating cost if experimental variables are optimized [4]. Nevertheless, two main disadvantages are emphasized: (i) its application to acidic wastewaters in the pH interval 2–4 and (ii) the consumption of large amounts of chemicals needed to acidify effluents before treatment and/or to neutralize degraded solutions before disposal.

Recent studies on the EF treatment of dyeing solutions have confirmed the viability of the method to decontaminate synthetic effluents at lab scale [38,158–176]. Key parameters are H_2O_2 generation, solution pH, applied j or E_{cat}, and iron and dye concentrations. The maximum H_2O_2 accumulation is achieved by injecting O_2 or air to the solution or feeding a gas-diffusion cathode with an excess of such gases. The optimum pH is typically near 3.0, close to the optimum value of 2.8 for Fenton's reaction (38) [31], thereby producing the maximum amount of homogeneous •OH, which also depends on applied current as well as iron and dye contents.

Table 5 collects selected results for the EF degradation of synthetic organic dyes in chloride free solutions using undivided two-electrode cells. High decolorization efficiency along with great mineralization degree can be observed in most cases. Comparison of Tables 3–5 allows inferring that the degradation performance of EF is analogous to EO with diamond anodes, but much superior to indirect electro-oxidation with active chlorine and thus, EF prevents the generation of undesirable toxic chlorinated derivatives.

Table 5
Per cent of color removal and TOC decay for the electro-Fenton treatment of synthetic organic dyes in chloride-free solutions using different undivided two-electrode cells.

Dye[a]	C_0 (mg dm^{-3})	Treated solution	Current (mA)	Electrolysis time (h)	% color removal	% TOC decay	Ref.
RuO_2/ACF cell							
Acid Red 14	200	500 cm^3, 1 mM Fe^{2+}, pH 3.0, room temperature	360	6	–[b]	70	[158]
Basic Red 46 (Cationic Red X-GRL)	150	1 dm^3, 5 mM Fe^{2+}, pH 3.0, room temperature	800	4	75	42	[159]
Pt/RVC cell							
Acid Red 112 (Ponceau S)	0.30[c]	400 cm^3, 0.1 mM Fe^{3+}, pH 2,5, room temperature	−1.0[d]	2	100	98[e]	[160]
Pt/graphite-felt cell							
Mordant Red 11 (Alizarin Red)	200	250 cm^3, 0.2 mM Fe^{2+}, pH 3.0, room temperature	300	3.5	100	95	[163]
BDD/air-diffusion cell							
Acid Orange 7	1.0[c]	100 cm^3, 0.5 mM Fe^{2+}, pH 3.0, 35 °C	100	0.33	80	–[b]	[38]
Acid Red 151	0.5[c]		100	0.33	76	–[b]	
Direct Blue 71	0.2[c]		100	0.33	75	–[b]	
Direct Yellow 4	200	100 cm^3, 0.5 mM Fe^{2+}, pH 3.0, 35 °C	200	4	100	85	[173]
BDD/BDD cell							
Acid Yellow 36	80	100 cm^3, 1.0 mM Fe^{2+}, pH 3.0, room temperature	30	0.84	96	–[b]	[175]
Acid Orange 52 (Methyl Orange)	100	3 dm^3, 1.0 mM Fe^{2+}, pH 3.0, 25 °C	500	1	72	–[b]	[176]

[a] Color index (common) name. In the cells, ACF, activated carbon fiber; RVC, reticulated vitreous carbon.
[b] Not determined.
[c] mM concentration.
[d] Cathode potential (V vs. SCE).
[e] Percentage of COD decay.

Several authors have applied the EF process with active anodes like RuO_2 [158,159], Pt [160–166] and graphite [167,168]. Wang et al. [158] utilized an undivided cell equipped with a 57 cm^2 Ti/RuO_2 mesh anode and a 20 cm^2 activated carbon fiber (ACF) cathode to degrade 500 cm^3 of an O_2-saturated solution containing 200 mg dm^{-3} Acid Red 14 in 0.05 M Na_2SO_4 with 1.0 mM Fe^{2+} at pH 3.0 and 360 mA. After 360 min, about 70% TOC was removed (see Table 5), a value much greater than ca. 50% found under treatment of the same solution by Fenton's reagent after adding 98 mM H_2O_2, thus corroborating the superiority of EF. The BOD_5/COD ratio of the Acid Red 14 solution also rose from near 0.0 to 0.4 at 360 min, indicating that EF can be appropriate as pretreatment for subsequent biological treatment. Poorer results have been reported for the degradation of 1 dm^3 of 150 mg dm^{-3} of the cationic azo dye Basic Red 46 in 0.05 M Na_2SO_4 at pH 3.0 using the same electrodes of 90 cm^2 area [159]. Operating at 800 mA (where a steady 0.25 mM H_2O_2 was accumulated in the medium without iron ions) and a high Fe^{2+} content of 5 mM, 75% decolorization efficiency and 42% TOC reduction were achieved in 240 min. The authors also reported an enhancement of the decolorization process when 5 mM Cu^{2+} or Mn^{2+} instead of 5 mM Fe^{2+} were alternatively added to the cationic dye solution. This behavior was related to the generation of $^{\bullet}OH$ from the catalytic Cu^{2+}/Cu^{+} pair as follows:

$$Cu^{2+} + R \rightarrow Cu^{+} + R^{-} \quad (49)$$

$$Cu^{+} + H_2O_2 \rightarrow Cu^{2+} + {}^{\bullet}OH + OH^{-} \quad (50)$$

or the Mn^{2+}/Mn^{+} one by the following reactions:

$$Mn^{2+} + R \rightarrow Mn^{+} + R^{-} \quad (51)$$

$$Mn^{+} + H_2O_2 \rightarrow Mn^{2+} + {}^{\bullet}OH + OH^{-} \quad (52)$$

where R can be, for example, the generated radical $HO_2^{\bullet}$ [4].

The studies performed with a Pt anode gave deeper information over the influence of the experimental variables on the degradation ability of EF. Thus, El-Desoky et al. [160] described the use of a Pt/RVC cell to treat 400 cm^3 of O_2-saturated solutions of the diazo dye Ponceau S in 0.05 M Na_2SO_4 with 0.1 mM Fe^{3+} by applying E_{cat} = −1.0 V/SCE. The method was so effective that complete color removal of 0.05, 0.1 and 0.3 mM Ponceau S was achieved after 30, 60 and 90 min of electrolysis, respectively, due to the rapid cleavage of the —N=N— bonds, whereas about 98% mineralization was found for the same solutions in only 40, 60 and 120 min. However, the presence of 0.1 M NaCl or 0.1 M KCl in the medium decelerated the process due to the consumption of $^{\bullet}OH$ from its parasitic reaction with Cl^{-}.

The reactivity of homogeneous $^{\bullet}OH$ has been clarified using undivided cells of 225–250 cm^3 capacity equipped with a Pt anode and a 60 cm^2 carbon-felt [162] or graphite felt [163] cathode. For O_2-saturated solutions with 0.1 mM Acid Orange 7 in 0.05 M Na_2SO_4 at pH 3.0 and 60 mA [162], Fig. 13a shows the quickest and total disappearance of the dye by adding 0.10–0.20 mM Fe^{3+}, whereas the gradual presence of more Fe^{3+} caused inhibition of dye decay as a result of the loss of $^{\bullet}OH$ by the concomitant increase in rate of reaction (46). The quickest mineralization was found for 0.1 mM Fe^{3+}, as can be seen in Fig. 13b, attaining 93% TOC removal in 8 h. This slow TOC abatement was explained by the large persistence of generated carboxylic acids like glyoxylic, malonic, formic, acetic and primordially oxalic. Fig. 13c highlights that all these acids were slowly removed for 480 min at 100 mA owing to the hard attack of $^{\bullet}OH$ on their Fe(II) complexes. Under these conditions, Fig. 13d presents the gradual conversion of initial N of Acid Orange 7 into 80% of NH_4^{+} ion and 20% of NO_3^{-} ion, as well as of initial S into 94% of SO_4^{2-} ion. On the other hand, Fig. 14a depicts the gradual fast abatement of 200 mg dm^{-3} Alizarin Red with 0.2 mM Fe^{2+} at pH 3.0 when I rose from 100 to 300 mA [163]. These concentration decays always obeyed a pseudo-first-order reaction, as shown in the inset panel of this figure, and the increase in their slope (apparent rate constant k_1) with increasing I can be ascribed to the acceleration of H_2O_2 generation by reaction (39) producing higher amounts of oxidant $^{\bullet}OH$ via Fenton's reaction (38). At 300 mA, Fig. 14b highlights that while the dye disappeared in 120 min and the maximum accumulation of intermediates took place in about 60 min, 95% TOC removal was reached at 210 min (see Table 5). Its inset panel reveals the progressive drop in mineralization current efficiency from 54% to 29% due to the loss of organic matter and the formation of more recalcitrant intermediates [30].

Zhang et al. [164] utilized a heterogeneous iron oxyhydroxide (nano-FeOOH) catalyst to degrade 80 mg dm^{-3} amaranth in 0.2 M Na_2SO_4 at pH 4.0 using a divided Pt/graphite-felt cell at E_{cat} = −0.64 V/SCE. Total decolorization of 300 cm^3 of catholyte with 100 g dm^{-3} catalyst was achieved in 240 min, but only about 50% TOC was removed in 360 min. Amaranth was adsorbed onto the

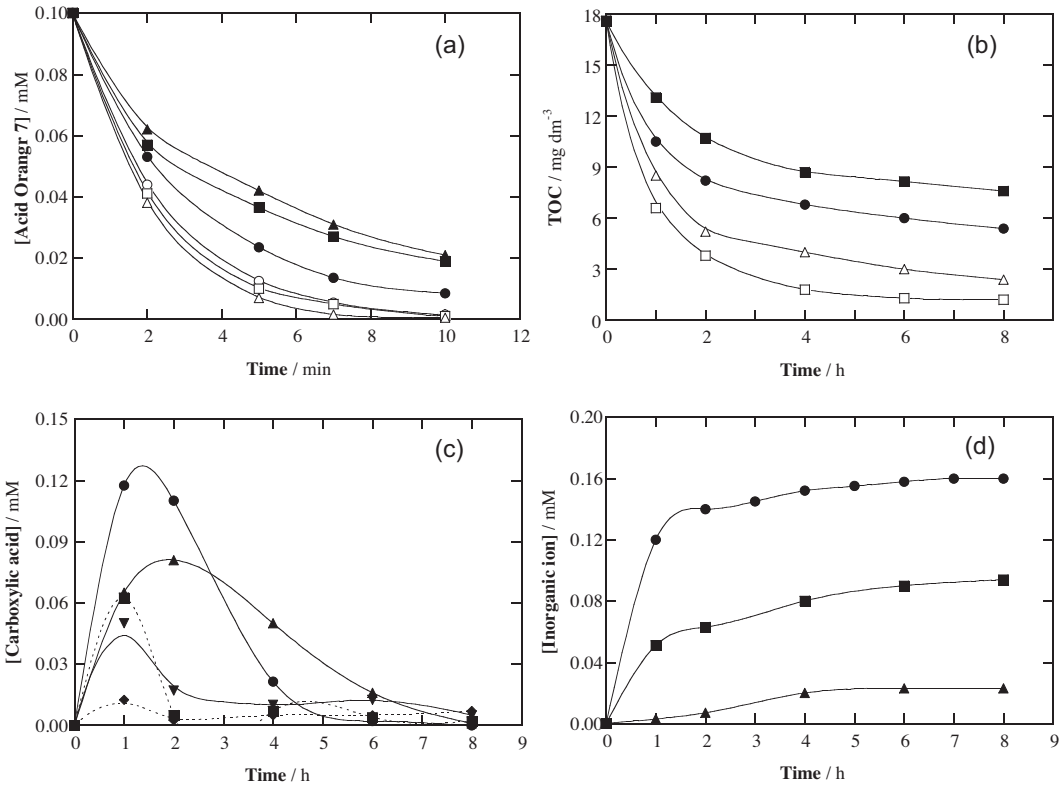

Fig. 13. (a) Degradation kinetics and (b) TOC decay of 225 cm^3 of 0.1 mM Acid Orange 7 in 0.05 M Na_2SO_4 of pH 3.0 by electro-Fenton (EF) using a stirred tank reactor equipped with a Pt anode and a 60 cm^2 carbon-felt cathode at 60 mA and room temperature. $[Fe^{3+}]_0$: (○) 0.05 mM, (□) 0.10 mM, (△) 0.20 mM, (●) 0.50 mM, (■) 1.00 mM and (▲) 2.00 mM. (c) Time-course of the concentration of (●) oxalic, (■), glyoxylic, (▲) malonic, (▼) formic and (♦) acetic acids detected during the EF process at 100 mA. (d) Evolution of the concentration of (▲) nitrate, (■) sulfate and (●) ammonium ions concentration released during the last EF treatment. Adapted from Ref. [162].

heterogeneous catalyst and efficiently degraded through: (i) heterogeneous Fenton's reaction on the catalyst and (ii) homogeneous Fenton's reaction (38) by the electrochemical reductive liberation of iron species under the applied electric field. On the other hand, Kayan et al. [165] demonstrated that 500 mg dm^{-3} Acid Red 97 underwent more than 94% TOC decay using either wet oxidation or EF. The former method became more efficient by adding oxidants in the order: H_2O_2 < bromate < persulfate < periodate, whereas the latter one was slower by treating a 200 cm^3 solution in 0.1 M $LiClO_4$ with 0.2 mM Fe^{2+} using a Pt/carbon-felt cell at 300 mA. In both methods, intermediates like 1,2-naphthalenediol, 1,1-biphenyl-4-amino-4-ol, 2-naphthalenol, phthalic anhydride, phthaldehyde, 3-hydroxy-1,2-benzenedicarboxylic acid and 4-aminobenzoic acid, along with oxalic acid, ammonium and nitrate ions, were identified.

The Sanromán's group has reported the decolorization of Lissamine Green B, Methyl Orange, Reactive Black 5 and Fuchsin Acid [167] and Azure B [168] by EF with a stirred tank reactor equipped with two graphite electrodes. It is noticeable the study performed on the optimization of Azure B by means of RSM. A 2^4 central composite face-centered design involving 30 experiments were made to treat 150 cm^3 of O_2-saturated dye solutions with 0.53 mM Fe^{2+} at pH 2.0, obtaining a maximum decolorization efficiency of 99.86% for 4.83 mg dm^{-3} Azure B, 15 cm^2 electrode area, E_{cell} = 14.19 V and 34.58 min of electrolysis time.

The EF process has also been developed with non-active anodes like PbO_2 [170] and BDD [38,171–176]. Lei et al. [170] utilized a flow plant for the treatment in batch mode of 800 cm^3 of an O_2-saturated solution with 123 mg dm^{-3} of the azo dye Reactive Brilliant Red X-3B, 0.05 M Na_2SO_4 and 0.1 mM Fe^{2+} at pH 3.0 with liquid flow rate of 15 cm^3 min^{-1}. The plant contained a trickle bed reactor consisting of a 30 cm^2 Ti/PbO_2 anode, a porous nylon diaphragm and a cathode frame with carbon-PTFE-coated graphite chips of 60 mm × 50 mm × 14 mm in dimension. The large volume of this 3D cathode yielded a high H_2O_2 concentration with 60% current efficiency operating at 300 mA, thus favoring a rapid decolorization efficiency of the dye solution, reaching 97% in 20 min, as well as a quick mineralization of 87% in 180 min.

The Brillas' group has explored the degradation behavior of 100 cm^3 of several azo dye solutions in 0.05 M Na_2SO_4 with 0.5 mM Fe^{2+} of pH 3.0 by EF using a stirred tank reactor equipped with a 3 cm^2 BDD anode and a 3 cm^2 carbon-PTFE air-diffusion cathode [38,171–174]. The main advantages of this cathode are: (i) high H_2O_2 production because air feeding is directly injected to the face opposite of the effluent without being dissolved in the medium and (ii) dyes are reduced in very low extent on its surface and hence, they are preferentially oxidized by generated hydroxyl radicals. In this sense, the combination of heterogeneous BDD(•OH) and homogeneous •OH is potent enough to quickly degrade dyeing solutions. Figs. 15a, 15b and 15c depict the influence of j between 8.3 and 100 mA cm^{-2} on the decolorization efficiency of solutions with 0.400 mM of azo bonds of monoazo Acid Orange 7, diazo Acid Red 151 and triazo Direct Blue 71, respectively [38]. In all cases, this parameter increased gradually with rising j up to 66.7 mA cm^{-2} due to the production of more amounts of BDD(•OH) at the anode surface and •OH in the bulk that destroy the —N=N— bonds, but at higher j it remained practically invariant suggesting a limitation by the mass transfer of dyes. This agrees with the pseudo-first-order decay found for all azo dyes under such conditions. Fig. 15a–c also highlights a deceleration in decolorization efficiency when the number of —N=N— bonds in the dye increased, as can be observed in Table 5 for 100 mA (33.3 mA cm^{-2}). That means that the attack of hydroxyl radicals becomes slower when

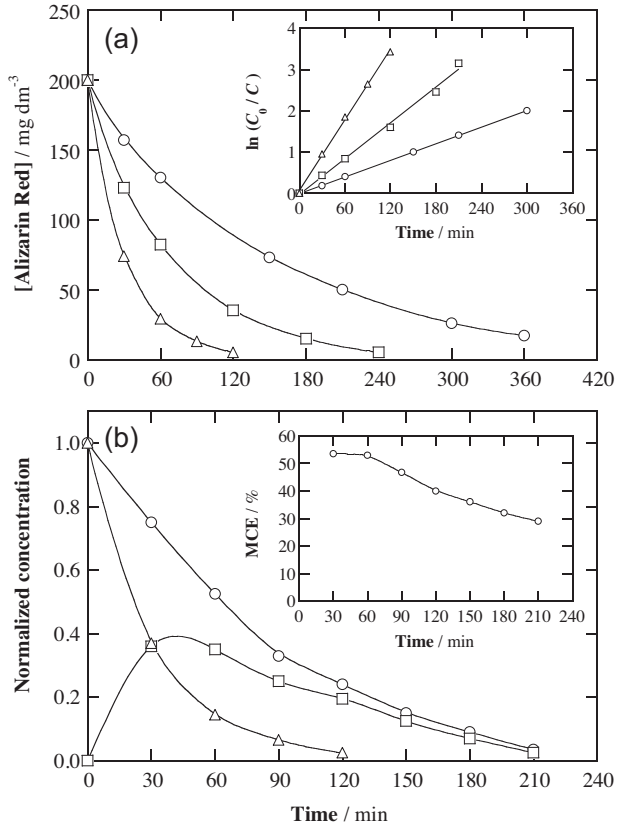

Fig. 14. (a) Effect of applied current on the degradation kinetics of 250 cm^3 of 200 mg dm^{-3} Alizarin Red with 0.2 mM Fe^{2+}, adjusted to pH 3.0 with sulfuric acid, using a stirred tank reactor with a Pt anode and a 60 cm^2 graphite-felt cathode at 25 °C. Current: (○) 100 mA, (□) 200 mA and (△) 300 mA. The inset panel presents the corresponding kinetics analysis assuming a pseudo-first-order reaction. (b) Evolution of the normalized concentration of (△) Alizarin Red, (□) intermediates and (○) TOC during the above EF treatment at 300 mA. The inset panel shows the trend of the mineralization current efficiency.
Adapted from Ref. [163].

the molecule contains more —N=N— bonds, although a significant mineralization can be always attained. For the diazo dye Direct Yellow 4, for example, 100% color removal and 85% mineralization were obtained for a 200 mg dm^{-3} dye solution operating at 200 mA (66.7 mA cm^{-2}) for 240 min (see Table 5) [173]. Oxalic and oxamic acids were detected as final carboxylic acids, which persisted long time during EF because they form Fe(III) complexes that are slowly mineralized preferentially with BDD(•OH). On the other hand, the decolorization and mineralization of the monoazo dye Sunset Yellow FCF were comparatively studied by different EAOPs to clarify the effect of generated oxidizing agents [174]. Fig. 16 shows that the TOC of a 290 mg dm^{-3} dye solution was reduced by 82% after 360 min of EF at 33.3 mA cm^{-2}, whereas it only attained 65% reduction under the same conditions by electrochemical oxidation with electrogenerated H_2O_2 (EO-H_2O_2). This corroborates the superiority of EF over EO-H_2O_2 because the combined attack of BDD(•OH) and •OH in the former process destroys more rapidly the organic pollutants than BDD(•OH) only produced in the latter one.

The use of a BDD/BDD cell for EF treatment has been introduced by the Peralta-Hernández's group [175,176]. A first study was centered on the decolorization of 100 cm^3 of O_2-saturated solutions containing the azo dye Acid Yellow 36 and 0.05 M Na_2SO_4 at pH 3.0 in a stirred tank reactor with two BDD electrodes of 2 cm^2 area [175]. The process was assessed by RSM on the basis of a 2^4 factorial design taking 60–80 mg dm^{-3} of dye, 0.1–0.3 mM of Fe^{2+}, 8–23 mA cm^{-2} of current density and 10–50 min of electrolysis time as independent variables. A good correlation between experimental and predicted data was obtained and the optimized values to yield 96% decolorization efficiency are reported in Table 5. A second study of this group was performed with a flow plant (see Fig. 17a [176]) equipped with a filter-press BDD/BDD cell of 64 cm^2 electrode area (see Fig. 17b [177]). With this system, 3 dm^3 of Methyl Orange solutions in 0.05 M Na_2SO_4 and 0.3 mM Fe^{2+} of pH 3.0 were degraded by EF at 500 mA and liquid flow rate of 12 dm^3 min^{-1} [176]. Fig. 17c shows a slow and progressive removal of the dye up to about 75% decay in 60 min regardless of its concentration between 100 and 200 mg dm^{-3}. That means that higher amount of Methyl Orange reacted with more hydroxyl radicals as concentration increases, indicating the inhibition of wasting reactions like reactions [46] and [47] by the presence of more organic matter. Small quantities of carboxylic acids like ascorbic, citric, maleic and oxalic were rapidly accumulated in the effluent, as detected by ion-exclusion HPLC.

6.3. Other indirect electrochemical techniques

Several studies have reported the mediated oxidation of dyes in plasma produced by very high potentials at bench scale [178,179]. The main drawback of these methods is the excessive energy requirements for industrial application. Wang [178] studied the degradation of 150 cm^3 of 50 mg dm^{-3} of the azo dye Polar Brilliant Blue with different electrolytes of 6.4 mS cm^{-1} conductivity at neutral pH in the anodic compartment of a stirred divided cell containing a Pt anode of 6 mm diameter and a 7 cm^2 SS cathode, thermostated at 25 °C. After 50 min of applying 500 V and 100 mA, about 80% decolorization efficiency was found for Na_2SO_4 and Na_2HPO_4 media where •OH was the main oxidant. The dimerization of this radical yielded the accumulation of high H_2O_2 contents. In contrast, overall decolorization was reached using a NaCl medium under the same conditions owing to the additional oxidation with active chlorine species (Cl_2/HClO/ClO^-) and oxygen singlet ($^1O_2$) formed from reaction between generated HClO and H_2O_2. In Na_2SO_4 medium, the potent action of •OH caused a quick reduction of 75% TOC in 60 min and final carboxylic acids like formic and oxalic and the release of NH_4^+, NO_3^- and Cl^- ions were detected. On the other hand, Magureanu et al. [179] utilized a high voltage electrode composed of 13 copper wires, which was placed at 5 mm of 35 cm^3 of a 50 mg dm^{-3} Methyl Orange solution in NaCl (250 μS cm^{-1} conductivity) of pH 6, contained in an insulating vessel with an Al counter-electrode at its bottom. The electrodes generated non-thermal plasma with oxidizing ROS (•OH, •O, O_3 and H_2O_2) by means of a pulsed corona discharge of 17 kV with a repetition rate of 27 Hz. H_2O_2 was accumulated up to 200 mg dm^{-3} after 30 min of plasma treatment, while the Methyl Orange solution was totally decolorized in 10 min, showing the effectiveness of the process. The release of nitrate, formate, sulfate and chlorine ions was detected, which caused an increase in conductivity and a drop in pH of degraded solution.

7. Photo-assisted electrochemical methods

Photo-assisted electrochemical methods such as PEC and PEF are emerging EAOPs based on the additional destruction of organic pollutants from waters by •OH radicals generated by an incident UV light on the electrolytic system and/or the quick photolysis of intermediates in the treated solution. The incident light can be provided by different artificial lamps supplying UVA (λ = 315–400 nm), UVB (λ = 285–315 nm) or UVC (λ < 285 nm) light [4,31,36,37]. The main drawback of these processes is the high energy cost of the artificial light irradiating the solution and for this reason, direct exposition at natural solar light (λ > 300 nm) has been recently utilized as

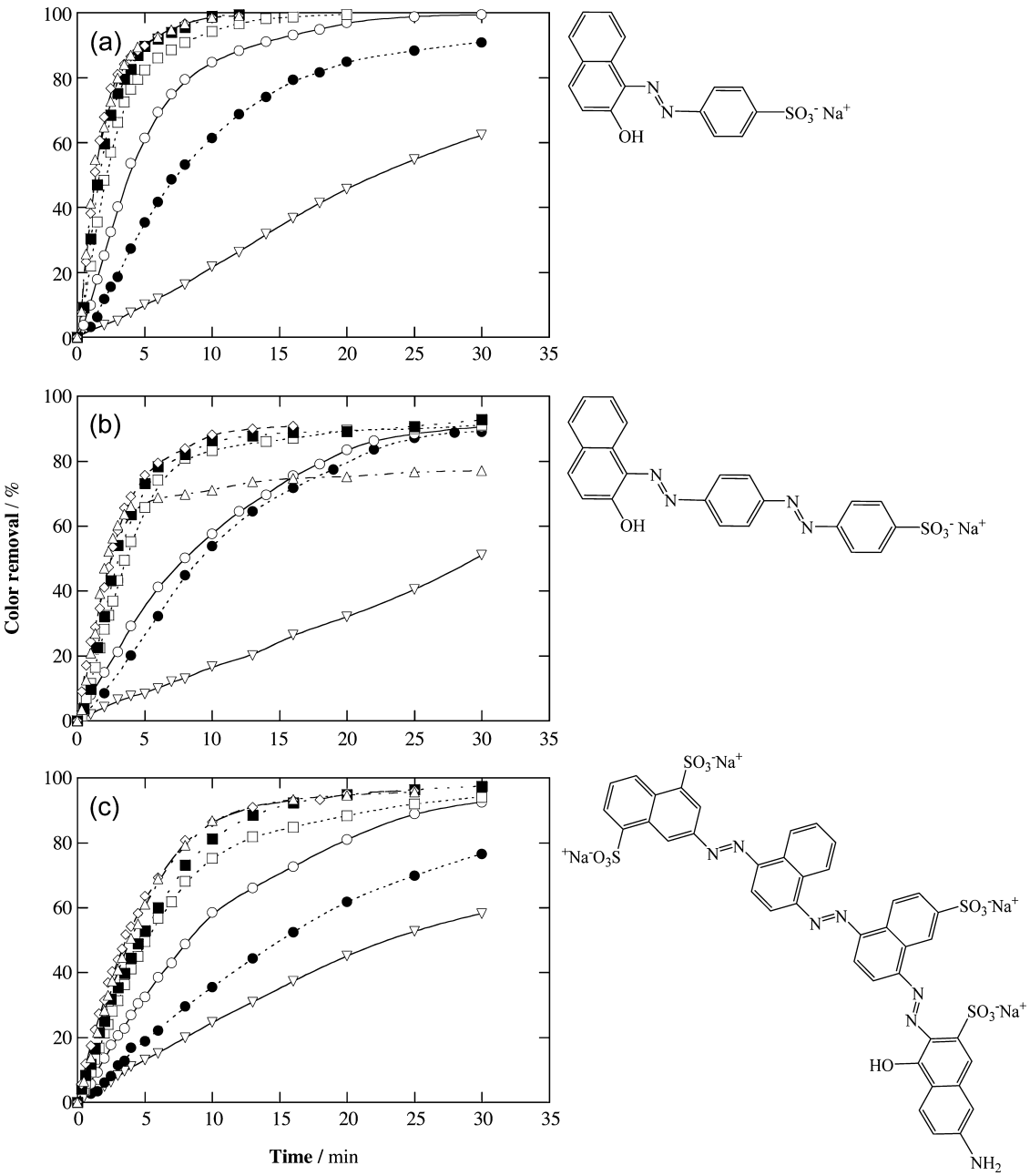

Fig. 15. Effect of current density on the percentage of color removal vs. electrolysis time for the EF treatment of 100 cm^3 of solutions containing 0.400 mM of initial azo bonds of (a) monoazo Acid Orange 7, (b) diazo Acid Red 151 and (c) triazo Direct Blue 71 in 0.05 M Na_2SO_4 with 0.5 mM Fe^{2+} at pH 3.0 and 35 °C using a stirred tank reactor with a BDD anode and an air-diffusion cathode, both of 3 cm^2 area. Current density: (▽) 8.3 mA cm^{-2}, (●) 16.7 mA cm^{-2}, (○) 33.3 mA cm^{-2}, (□) 50 mA cm^{-2}, (■) 66.7 mA cm^{-2}, (◊) 83.3 mA cm^{-2} and (△) 100 mA cm^{-2}. The molecular formula of each dye is also shown.
Adapted from Ref. [38].

inexpensive and renewable energy source, giving rise to the derived SPEC and SPEF methods.

The main characteristics of recent PEC [180–191], SPEC [192], PEF [38,174,193–199] and SPEF [2,39,174,200,201] treatments of dyeing solutions are described below. These works have shown excellent performance for photo-assisted electrochemical methods, as can be deduced from selected degradation results collected in Table 6.

7.1. Photoelectrocatalysis

Photocatalysis consists in the illumination of a stable semiconductor anode with an UV light to induce the oxidation of organics in wastewaters. The key property of a semiconductor material for this application is the band gap between its valence and conduction bands. The value of this gap has to be equal to the energy of the incident photon for exciting an electron (e^-_{CB}) from the valence to the conduction band generating a positively charged vacancy or hole (h^+_{VB}) [36,37]. The material more extensively used is the anatase crystalline form of TiO_2 as nanoparticles in suspension for photocatalysis as well as deposited onto a metal for PEC and SPEC, being an active photoanode with low cost, low toxicity, high stability and wide band gap of 3.2 eV. This allows the generation of e^-_{CB}–h^+_{VB} pairs via reaction (53) under irradiation with UV photons of $\lambda < 380$ nm. Organic pollutants can then be oxidized by h^+_{VB} and/or by heterogeneous •OH formed from reaction (54) between the hole and adsorbed water. Moreover, other ROS like $O_2^{\bullet -}$, $HO_2^\bullet$ and H_2O_2,

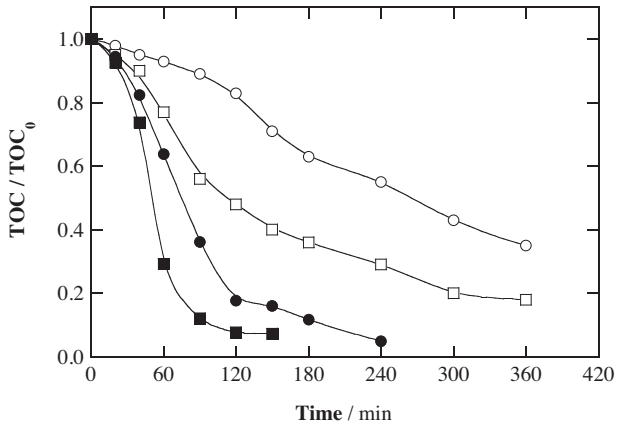

Fig. 16. Variation of normalized TOC with electrolysis time for the treatments of 100 cm^3 of 290 mg dm^{-3} Sunset Yellow FCF solutions in 0.05 M Na_2SO_4 at pH 3.0 and 35 °C using a stirred tank reactor with a 3 cm^2 BDD anode and a 3 cm^2 air-diffusion cathode at 33.3 mA cm^{-2}. Method: (○) Electrochemical oxidation with electrogenerated H_2O_2 (EO-H_2O_2), (□) EF, (●) photoelectro-Fenton (PEF) with 6 W UVA light of λ_{max} = 360 nm and (■) solar photoelectro-Fenton (SPEF). In the three latter methods, 0.5 mM Fe^{2+} was added to the solution.
Adapted from Ref. [174].

and even more •OH, can be produced from reactions (55)–(58) [36,37].

$$TiO_2 + h\nu \rightarrow e^-_{CB} + h^+_{VB} \quad (53)$$

$$h^+_{VB} + H_2O \rightarrow {}^\bullet OH + H^+ \quad (54)$$

$$e^-_{CB} + O_2 \rightarrow O_2^{\bullet -} \quad (55)$$

$$O_2^{\bullet -} + H^+ \rightarrow HO_2^\bullet \quad (56)$$

$$2HO_2^\bullet \rightarrow H_2O_2 + O_2 \quad (57)$$

$$H_2O_2 + O_2^{\bullet -} \rightarrow {}^\bullet OH + OH^- + O_2 \quad (58)$$

However, the recombination of e^-_{CB} with h^+_{VB} represents the major loss in efficiency of photocatalysis [4,36]. This problem is solved in PEC and SPEC by using an electrolytic system with a thin-film active photoanode subjected to UV illumination in which a constant bias potential to the anode (E_{anod}), a constant E_{cell} or a constant j is applied to promote the extraction of photoinduced electrons by the external electrical circuit, thus yielding an efficient separation of the e^-_{CB}–h^+_{VB} pairs. This inhibits reactions (55)–(58) and enhances the generation of higher quantity of holes by reaction (53) and heterogeneous •OH by reaction (54) with acceleration of organics oxidation compared to classical photocatalysis.

The electrochemical systems for PEC are stirred tank or flow reactors constituted of two- or three-electrode cells equipped with an immersed UV lamp or a quartz window to permit the UV irradiation to the anode surface. As can be seen in Table 6, low E_{anod}, E_{cell} or j values were applied to photoanodes such as TiO_2 alone [180–183,192] and doped with metals like Ni [194], Co [194], and Zn [185] or Cu^{2+} ion [186], as well as novel Ti/TiO_2/WO_3 [187], $TiNbO_5$ [188] and $TaWO_6$ [189] electrodes, due to their low electrical stability. In contrast, DSA-type materials of TiO_2–RuO_2 presented much larger stability and permitted the use of higher j values [190,191].

Shang et al. proposed the improvement of the PEC process of the dye Rhodamine B by using an indium tin oxide (ITO)/TiO_2/ITO photoanode instead of an ITO/TiO_2 one [180] and with a half-wave pulsed direct current instead of a direct current at constant E_{cell} [181]. Trials were carried out with a stirred quartz beaker of 220 cm^3 capacity containing up to 20 mg dm^{-3} of the dye in NaCl medium with two parallel electrodes of 16.6 cm^2 under illumination with an immersed 8 W UVC lamp. In a first work [180], a higher decolorization rate was found for 10 mg dm^{-3} Rhodamine B

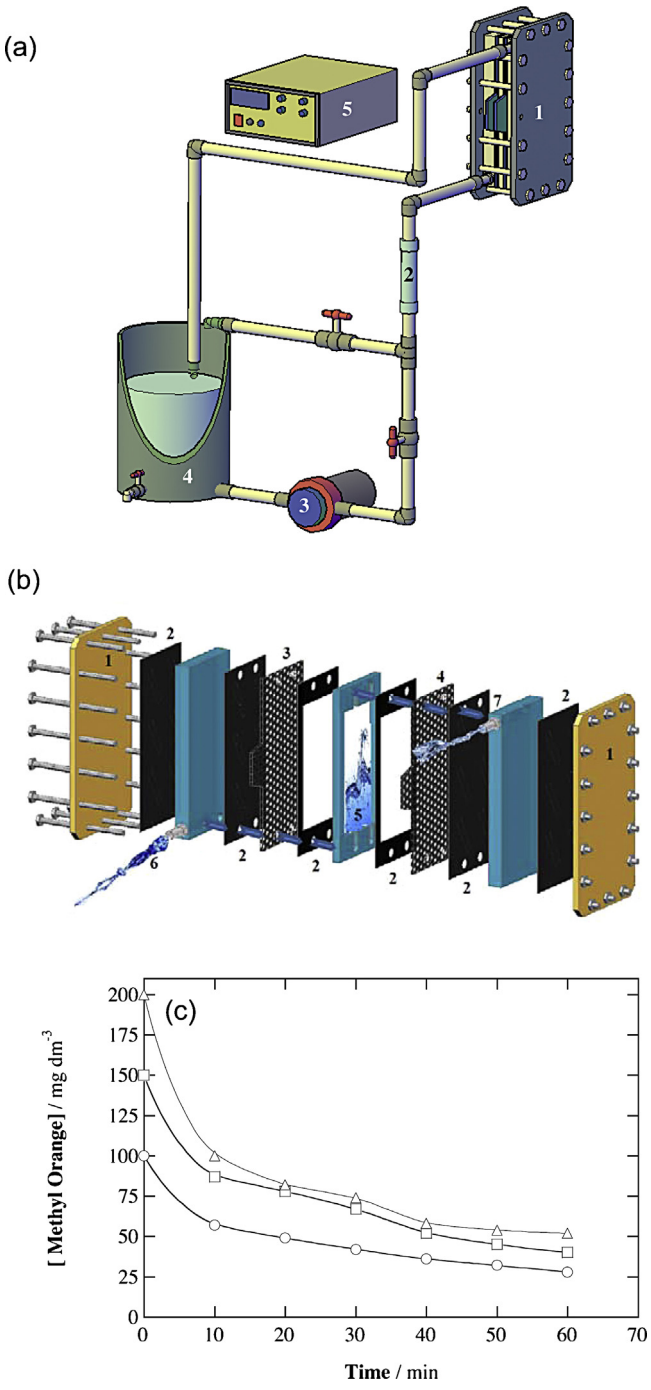

Fig. 17. (a) Experimental setup of a 3 dm^3 flow plant used for the EF treatment with a BDD/BDD cell. (1) Flow cell, (2) flowmeter, (3) peristaltic pump, (4) reservoir and (5) power supply. (b) Sketch of the electrochemical filter-press cell: (1) end plate, (2) gasket, (3) 64 cm^2 BDD anode, (4) 64 cm^2 BDD cathode, (5) liquid compartment, (6) liquid inlet and (7) liquid outlet. (c) Effect of dye concentration on its removal with electrolysis time for the EF degradation of Methyl Orange solutions in 0.05 M Na_2SO_4 with 0.3 mM Fe^{2+} at pH 3.0 using the above flow plant at 500 mA and liquid flow rate of 12 dm^3 min^{-1}. Dye content: (○) 100 mg dm^{-3}, (□) 150 mg dm^{-3} and (△) 200 mg dm^{-3}.
Adapted from Refs. [176,177].

in 1.5 M NaCl at E_{cell} = 1.5 V using two electrodes of ITO/TiO_2/ITO as a result of the enhancement of reaction (53) in the TiO_2 thin film area lying between the two ITO electrodes, because electrons can be more rapidly extracted by the two ITO/TiO_2 interfaces, thus producing more amount of oxidant holes. Moreover, the presence of Cl^- ions accelerated dye removal by the additional oxidative action

Table 6
Percentage of color removal and TOC decay determined for removing synthetic organic dyes from wastewaters under selected photoelectrocatalytic and photoelectro-Fenton conditions.

Dye[a]	C_0 (mg dm^{-3})	Experimental conditions	j[b] (mA cm^{-2})	% color removal	% TOC decay	Ref.
Photoelectrocatalysis						
SnO_2:Sb-TiO_2 photoanode						
Acid Orange 7 (Orange II)	15	640 cm^3, 0.05 M Na_2SO_4, pH 3, 21 W cm^{-2} UVC light, for 1 h				[183]
		External illumination	1.0	50	25	
		Internal illumination	1.0	50	28	
$TiNbO_5$ nanosheet multilayer photoanode						
Basic Violet 10 (Rhodamine B)	5[c]	0.05 M Na_2SO_4, 150 W UVC (for positive potential) or 300 W Xe (for negative potential) lamp, for 1 h	0.4[d]	57	–[e]	[188]
			−0.4[d]	52	–[e]	
$TaWO_6$ nanosheet photoanode						
Basic Violet 10 (Rhodamine B)	5[e]	0.01 M Na_2SO_4, 300 W Xe lamp for 1 h	0.4[d]	62	–[e]	[189]
			−0.4[d]	75	–[e]	
Ti/TiO_2–$(TiO_2)_{0.25}$ $(RuO_2)_{0.75}$ photoanode						
Vat Blue 4 (Indanthrene blue)	60	250 W UV lamp, for 3 h				[191]
		−0.03 M Na_2SO_4 at pH 6.77	100	27	–[e]	
		−0.05 M NaCl at pH 6.43	100	89	–[e]	
Solar photoelectrocatalysis						
TiO_2 coating/air-diffusion cell						
Acid Orange 7	15	100 cm^3, 0.05 M Na_2SO_4, pH 7.0, 35 °C, sunlight (31 W m^{-2}), for 4 h	1.0	100	40	[192]
Photoelectro-Fenton						
BDD/air-diffusion cell						
Acid Red 29	244	100 cm^3, 0.05 M Na_2SO_4, 0.5 mM Fe^{2+}, pH 3.0, 35 °C, 5 W m^{-2} UVA light, for 1 h	100	100[f]	87	[195]
Solar photoelectro-Fenton						
BDD/air-diffusion cell						
Acid Red (AR88)	119	2.5 dm^3, 0.05 M Na_2SO_4 with	50	100	94	[200]
Acid Yellow (AY9)	127	0.8 mM Fe^{2+} for AR88 or 0.1 M Na_2SO_4 with 0.5 mM Fe^{2+} for AY9, pH 3.0, 35 °C, solar light (∼17 W m^{-2}), for 6 h	50	100	>95	
Disperse Red 1	100[g]	2.5 dm^3, 0.1 M Na_2SO_4, 0.5	50	100	>95	[201]
Disperse Yellow 3	100[g]	mM Fe^{2+}, pH 3.0, 35 °C, sunlight (31 W m^{-2}), for 4 h	50	100	>95	

[a] Color index (common) name.
[b] Applied current density.
[c] μM concentration.
[d] Electrode potential (V vs. Ag/AgCl).
[e] Not determined.
[f] Data at 30 min.
[g] Initial TOC.

of active chlorine species (Cl_2/HClO/ClO^-) formed from •Cl radical, previously produced as follows [180]:

$$TiO_2(h^+_{VB}) + Cl^- \rightarrow TiO_2 + {}^\bullet Cl \quad (59)$$

$$Cl^- + {}^\bullet OH \rightarrow {}^\bullet Cl + OH^- \quad (60)$$

In a second work of these authors [181], the cell was equipped with an ITO/TiO_2 photoanode and a Pt cathode to comparatively decolorize 10 mg dm^{-3} Rhodamine B in 0.5 M NaCl at a E_{cell} = 1.40 V using either a half-wave pulsed direct current between 5 and 50 Hz of frequency or a direct current. The half-wave pulsed direct current yielded quicker decolorization due to a more efficient transport of electrons through the TiO_2 thin film enhancing reaction (53) and then, dye oxidation.

Esquivel et al. [182] synthesized a TiO_2 electrode by electrophoretic deposition on a SnO_2:Sb layer painted onto an optical fiber as light distributor. This novel photoanode of 13 cm^2 was mounted over an internal UVC lamp of 21 W cm^{-2} and placed in a flow cell with a carbon cloth cathode of the same area and an external UVC lamp of the same potency, through which 640 cm^3 of 15 mg dm^{-3} Orange II in 0.05 M Na_2SO_4 at pH 3.0 and liquid flow rate of 80 dm^3 h^{-1} were circulated. After 60 min at 1 mA cm^{-2}, 50% color removal and 25–28% TOC abatement were obtained by operating with internal or external UVC illumination (see Table 6). These findings demonstrated that similar amount of h^+_{VB} was produced in both cases and hence, the TiO_2 modified optical fiber photoanode with internal UV illumination can be useful for the treatment of dyes effluents. Based on the generation of H_2O_2 in the system from dimerization of heterogeneous •OH formed from water oxidation at the TiO_2 anode, 0.2 mM Fe^{2+} was added to the solution to produce more potent homogeneous •OH from Fenton's reaction (38) under internal UVC illumination. The PEC/EF process thus applied had much higher oxidation ability than single PEC, leading to 98% decolorization efficiency and 57% TOC reduction of the Orange II solution after 60 min at 1 mA cm^{-2}. A recent paper of the same authors [184] reported an enhancement of the decolorization of a 50 mg dm^{-3} Orange II solution in 0.05 M Na_2SO_4 at pH 3.0 when the TiO_2 photoanode was doped with 20% of Co or Ni under an UVA irradiation. In this way, Frade et al. [185] described the preparation of a 0.8 cm^2 photoanode composed of Zn doped TiO_2 nanocomposites that yielded an efficient 40% color removal of a 5 mg dm^{-3} Acid Orange 7 solution in 0.035 M Na_2SO_4 at pH 6.2 treated in a 100 cm^3 stirred tank reactor at E_{anod} = 1.0 V vs. Ag/AgCl for 120 min under UVA illumination. This was related to the formation of e^-_{CB}–h^+_{VB} pairs by reaction (53) not only on the TiO_2 surface but also on the surface of ZnO nanoparticles generated from the metallic Zn matrix during the calcination step of nanocomposites preparation. On the other hand, Zhang et al. [186] reported that the PEC treatment at E_{anod} = 1.0 V/SCE of 6 mg dm^{-3} Methylene Blue or Methyl Orange solution in 0.1 M Na_2SO_4 was enhanced using a Cu^{2+}-doped

TiO_2 film photoanode under visible light irradiation compared to a TiO_2 film photoanode illuminated with UVA light. This behavior was related to the fact that electron excitation and charge separation involve the transition from the TiO_2 valence band to the Cu^{2+} impurity states, needing less energetic photons.

Novel electrodes like $TiNbO_5$ nanosheet multilayer [188] and TaW_6 nanosheet [189] films developed for PEC by the Lin's groups have shown their dual ability to decolorize 5 μM Rhodamine B solutions by applying either a positive (E_{anod} = 0.4 V vs. Ag/AgCl) or negative (E_{cat} = −0.4 V vs. Ag/AgCl) potential, as can be seen in Table 6. Trials were performed in a conventional three-electrode undivided quartz glass cell with a 2.25 cm^2 nanosheet film working electrode, a Pt wire counter-electrode and a reference electrode of Ag/AgCl, filled with 0.05 or 0.01 M Na_2SO_4 as supporting electrolyte at pH = 2.5 and room temperature. When the positive potential was applied to the photoanode, it can be illuminated with a 150 W UVC or 300 W Xe lamp with a 420 nm filter to generate holes from reaction (53) that oxidize the dye. In contrast, when the negative external potential was imposed to the working electrode, it behaved as a cathode and the irradiation with the 300 W Xe lamp was more effective. To explain this, a dye-sensitized mechanism was proposed in which: (i) the photoexcited Rhodamine B molecule transferred an electron into the conduction band of the nanosheet semiconductor to give its cation radical, (ii) the outer circuit also injected electrons to the conduction band and (iii) the adsorbed O_2 onto the film surface captured the electrons to yield $O_2^{\bullet -}$, which is converted into $^\bullet$OH that oxidizes the dye.

Robust and highly stable DSA-type photoanodes of $Ti/TiO_2–(TiO_2)_x–(RuO_2)_{1-x}$ have been synthesized and applied to the decolorization of 60 mg dm^{-3} Indanthrene Blue solutions in 0.03 M Na_2SO_4 at pH 6.77 or 0.05 M NaCl at pH 6.43 by PEC [191]. The cell was a stirred tank reactor with a Pt cathode and an immersed UV light of 250 W to illuminate the photoanode. The best decolorization efficiency was found for the $Ti/TiO_2–(TiO_2)_{0.25}–(RuO_2)_{0.75}$ electrode, with the highest prepared RuO_2 content, at a j value as high as 100 mA cm^{-2} owing to the parallel oxidation of the dye by the holes formed at TiO_2 surface from reaction (53) and by heterogeneous $^\bullet$OH generated at RuO_2 surface from water oxidation. Moreover, color removal was strongly enhanced in chloride compared to sulfate medium (see Table 6) because of the additional attack of the dye by active chlorine species formed from Cl^- oxidation, as stated above.

An interesting paper of Garcia-Segura et al. [192] described the decolorization and mineralization of the azo dye Acid Orange G by SPEC using the photoelectrochemical system schematized in Fig. 18a. A 5 cm^2 TiO_2 photoanode was synthesized by atmospheric plasma spray technology, being composed of 29% rutile, 9% anatase and 62% Ti_7O_{13} on SS support. SEM images of the initial TiO_2 powder and the microparticulated TiO_2 coating prepared are depicted in Figs. 18b and 18c, respectively. The treatment of 100 cm^3 solutions with 0.05 M Na_2SO_4 at 35 °C was examined at pH between 3.0 and 11.0, azo dye content up to 45 mg dm^{-3} and anodic current density up to 2.0 mA cm^{-2}. Fig. 18d highlights the quickest percentage of color removal attained for a 15 mg dm^{-3} Acid Orange 7 solution of pH 7.0 by SPEC compared to solar photocatalysis, as expected for the efficient separation of e^-_{CB} and h^+_{VB} from the applied current. An increase in decolorization rate with anodic current density can be observed up to 1.0 mA cm^{-2} because of the greater production of photogenerated holes by the faster extraction of photoinduced electrons. The same behavior was found for the azo dye decay determined by reversed-phase HPLC, but in this case the kinetic process was progressively enhanced up to 2.0 mA cm^{-2} (see Fig. 18e) and it always obeyed a pseudo-first-order reaction (see Fig. 18f). Comparison of Fig. 18d and e evidences a slower decolorization of the solution, which was associated with the formation of colored aromatic products that are more slowly destroyed than the parent azo dye. The best operating variables for SPEC were 15 mg dm^{-3} Acid Orange 7, pH 7.0 and 1.0 mA cm^{-2}, conditions under which the solution was completely decolorized in 120 min, although only 40% mineralization was attained in 240 min (see Table 6). Accumulation of persistent carboxylic acids like phthalic, tartaric, succinic, acetic and oxamic was detected by ion-exclusion HPLC. The initial N of the azo dye was mineralized pre-eminently as NH_4^+ ion and, in smaller proportion, as NO_3^- ion.

7.2. Photoelectro-Fenton

In PEF and SPEF, the contaminated solution degraded under EF conditions is simultaneously submitted to UVA and sunlight illumination, respectively, to accelerate the mineralization rate of the dye. The positive action of light can be explained by: (i) the quicker Fe^{2+} regeneration and higher generation of homogeneous $^\bullet$OH from photoreduction of $Fe(OH)^{2+}$, the pre-eminent Fe^{3+} species at pH near 3, by photo-Fenton reaction (61) and/or (ii) the photolysis of Fe(III) complexes with generated carboxylic acids according to the generic reaction (62) [4,38,174].

$$Fe(OH)^{2+} + h\nu \rightarrow Fe^{2+} + {}^\bullet OH \quad (61)$$

$$Fe(OOCR) + h\nu \rightarrow Fe^{2+} + CO_2R^\bullet \quad (62)$$

When the treated solution is exposed to a more energetic UVC irradiation, direct photolysis of organic pollutants, along with the production of homogeneous $^\bullet$OH from photodecomposition of electrogenerated H_2O_2 via reaction (63), also take place [4].

$$H_2O_2 + h\nu \rightarrow 2{}^\bullet OH \quad (63)$$

Several authors have emphasized the superiority of PEF over EF for dye removal [173,193–199]. Thus, following the EF degradation of Direct Yellow 4 in a stirred BDD/air-diffusion cell described in Section 6.2, Garcia-Segura et al. [173] reported an almost total mineralization (97% TOC abatement) for 100 cm^3 of 200 mg dm^{-3} dye solution in 0.05 M Na_2SO_4 and 0.5 mM Fe^{2+} at pH 3.0 by PEF with a 6 W UVA light at 200 mA for 240 min, much higher than 85% TOC reduction determined for the comparable EF process (see Table 5). The higher mineralization degree achieved by PEF was accounted for by the quick photolysis of Fe(III) complexes of final oxalic and oxamic acids by reaction (62), much more slowly destroyed by heterogeneous BDD($^\bullet$OH) and homogeneous $^\bullet$OH in EF, as confirmed by ion-exclusion HPLC. Based on this behavior, the authors proposed a novel photo-assisted EF process, where the above EF treatment was carried out for 120 min, after which the current was stopped and only UVA light was irradiated to the solution up to 240 min. TOC decayed at similar rate in both, photo-assisted EF and PEF treatments during 120 and 240 min, indicating that the main mineralization process involved the photolysis of accumulated Fe(III)-carboxylate complexes. The photo-assisted EF treatment can then be envisaged as a more suitable process for dye treatment than PEF, having similar performance and being more cost-effective because electrical current and UVA light are partially applied.

The photodecarboxylation of final Fe(III)–carboxylate complexes, which explains the long time required for PEF treatment, has been reported by other authors [194,195]. For example, 100% color removal at 30 min and 87% TOC decay were reached in the PEF degradation with 6 W UVA light of 100 cm^3 of 244 mg dm^{-3} of the azo dye Acid Red 29 in 0.05 M Na_2SO_4 and 0.5 mM Fe^{2+} at pH 3.0 using a stirred BDD/air-diffusion reactor of 3 cm^2 electrode area at 100 mA cm^{-2} [195] (see Table 6). Oxidation products and released inorganic ions were quantified at 33.3 mA cm^{-2} by chromatographic techniques. Fig. 19a depicts the evolution of the aromatic tetrahydroxy-*p*-benzoquinone that disappears completely in 100 min. In contrast, the detected carboxylic acids

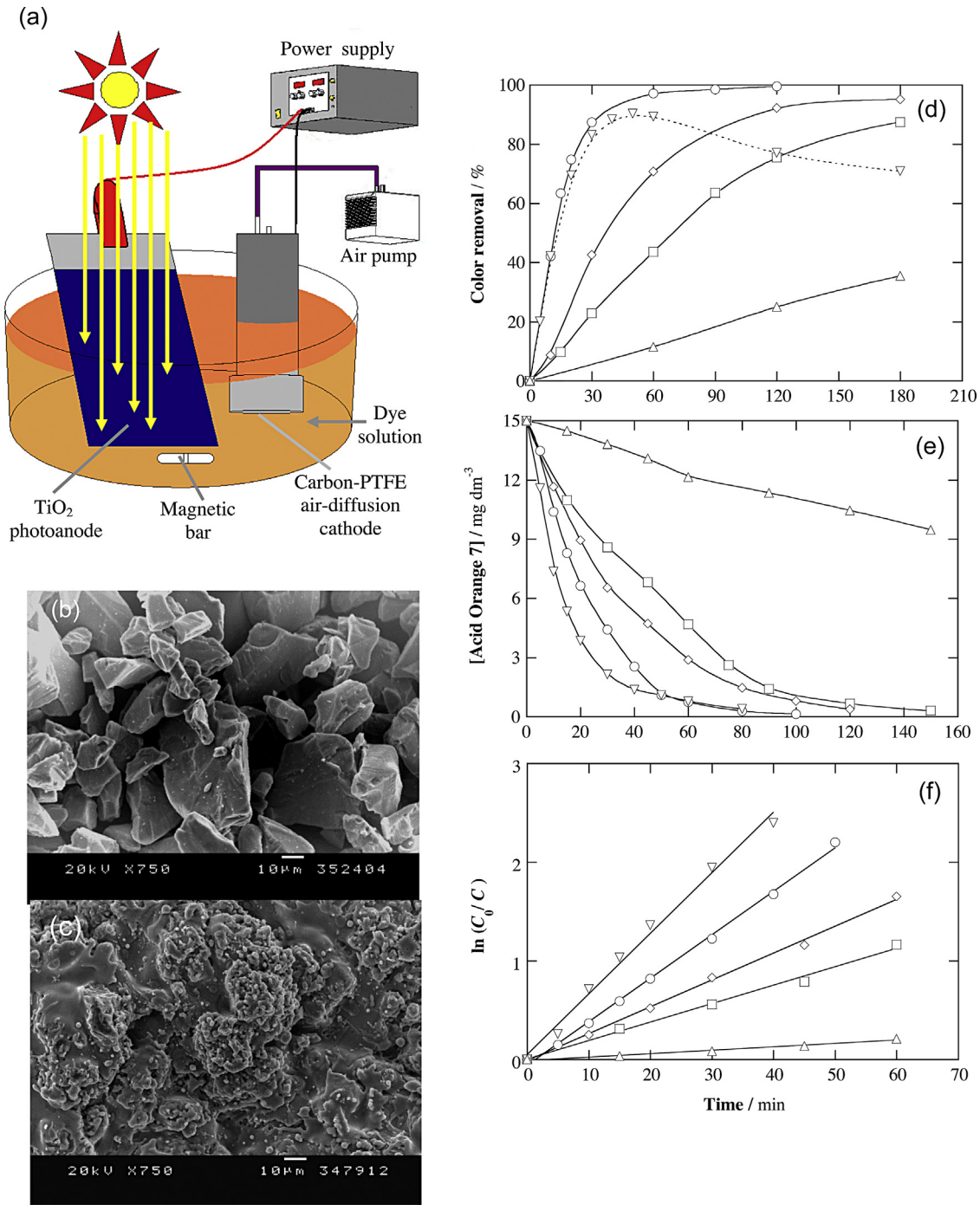

Fig. 18. (a) Experimental set-up used for the degradation by solar photoelectrocatalysis (SPEC) of Acid Orange 7 solutions. The photoelectrochemical reactor contained a TiO_2 photoanode of 5 cm^2 area, prepared by TiO_2 deposition onto stainless steel by atmospheric plasma spray technology, and a 3 cm^2 air-diffusion cathode. SEM images of the free-surface micrograph of: (b) the initial TiO_2 powder and (c) the microparticulated TiO_2 coating prepared by atmospheric plasma spray. (d) Percentage of color removal and (e) dye concentration decay with electrolysis time for the treatment of 100 cm^3 of a 15 mg dm^{-3} Acid Orange 7 solution in 0.05 M Na_2SO_4 at pH 7.0 and 35 °C using (△) solar photocatalysis and SPEC at anodic current density of: (□) 0.25 mA cm^{-2}, (◇) 0.50 mA cm^{-2}, (○) 1.0 mA cm^{-2} and (▽) 2.0 mA cm^{-2}. In plot (f), kinetic analysis of dye concentration assuming a pseudo-first-order reaction.

Adapted from Ref. [192].

persisted longer time, as shows Fig. 19b. A larger accumulation of oxalic acid can be observed, which was rapidly destroyed in 140 min by the efficient photodecomposition of Fe(III)–oxalate complexes by UVA light, whereas persistent tartronic and oxamic acids remained up to 240–300 min due to the larger stability of their Fe(III) complexes. Fig. 19c highlights the predominant release of NH_4^+ ion, along with NO_3^- ion in lesser proportion, during the mineralization of the initial N of the azo dye.

The Khataee's group has described the decolorization of Acid Blue 92 [196] and Direct Red 23 [197] solutions in 0.05 M Na_2SO_4 by PEF using a flow plant with a tank reactor equipped with a BDD or Pt anode and a carbon nanotube (CNT)-PTFE cathode fed with pure O_2 and connected to a cylindrical Pyrex photoreactor with an internal 15 W UVC lamp. In the case of Direct Red 23, for example, the electrolysis of 2 dm^3 of a 30 mg dm^{-3} dye solution with 0.05 mM Fe^{3+} at pH 3.0 and 300 mA for 60 min with a Pt anode yielded 94%

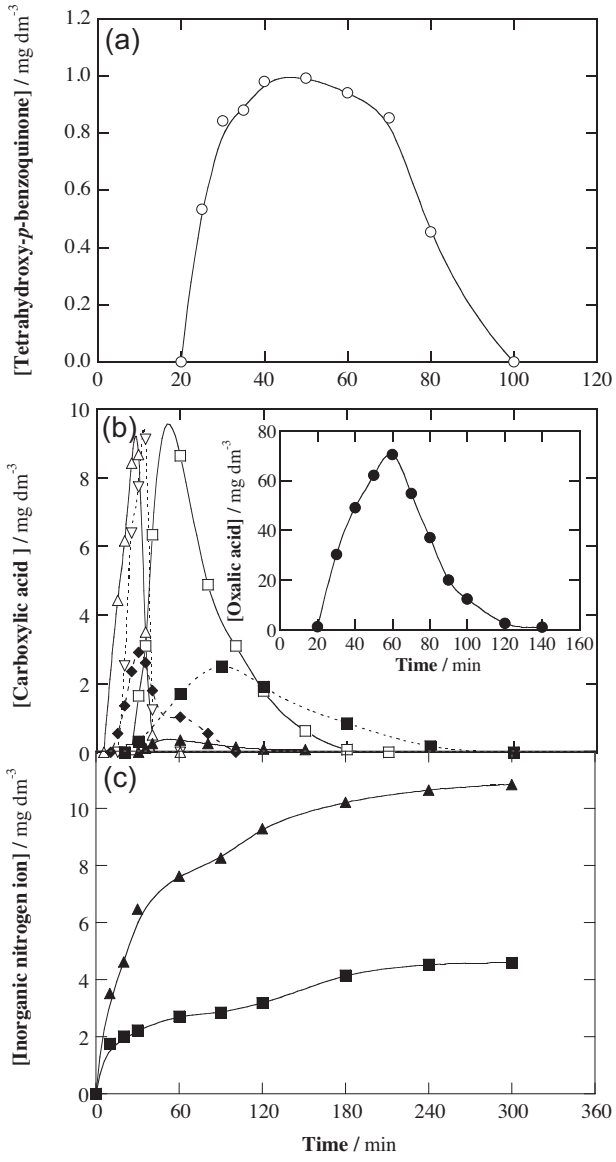

Fig. 19. Time-course evolution for the concentration of: (a) aromatic intermediates, (b) carboxylic acids and (c) inorganic nitrogen ions detected during the PEF degradation of 100 cm^3 of a 244 mg dm^{-3} Acid Red 29 solution in 0.05 M Na_2SO_4 with 0.5 mM Fe^{2+} at pH 3.0, 33.3 mA cm^{-2} and 35 °C using a stirred tank reactor with a BDD/air-diffusion cell of 3 cm^2 electrode area under a 6 W UVA irradiation. In plot (a), (○) tetrahydroxy-*p*-benzoquinone. In plot (b), (▽) malonic, (△) tartaric, (♦) oxalacetic, (▲) fumaric, (□) tartronic, (■) oxamic and (●, in the inset) oxalic acids. In plot (c), (▲) NO_3^- and (■) NH_4^+ ions.
Adapted from Ref. [195].

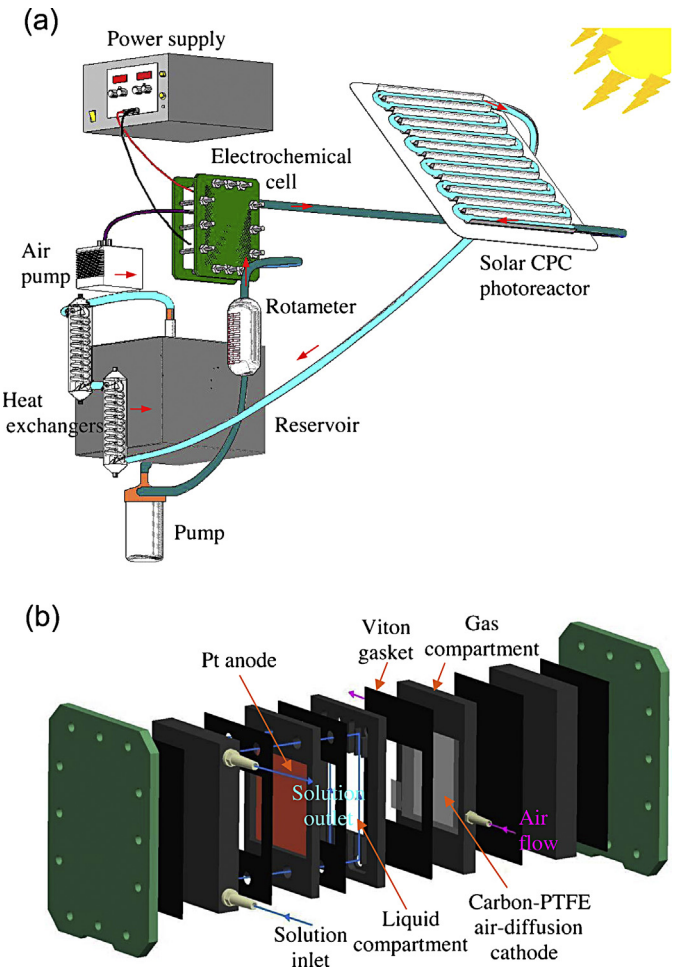

Fig. 20. Schemes of (a) a 10 dm^3 flow plant coupled with a solar compound parabolic collector photoreactor of 1.57 dm^3 irradiated volume used for the SPEF treatment of dye solutions and (b) the one-compartment filter-press Pt/air-diffusion cell of 90.3 cm^2 electrode area.
Adapted from Ref. [202].

decolorization efficiency for PEF, a value much higher than 66% obtained under comparable EF conditions. The superiority of PEF was related to the production of more homogeneous •OH from photolytic reactions (61) and (63) and the photodecomposition of produced Fe(III)–carboxylate complexes by reaction (62). The effect of the operating variables on PEF process was subsequently examined and optimum conditions for decolorization were reached for 10 mg dm^{-3} Direct Red 23, 0.05 mM Fe^{3+}, pH 3.0, 200 mA and liquid flow rate of 10 dm^3 h^{-1}. The same group also investigated the characteristics of the oxalate catalyzed PEF process, consisting in the addition of sodium oxalate and Fe^{3+} to the starting solution to accelerate Fe^{2+} generation via reaction (62), thereby producing more quantity of homogeneous •OH from Fenton's reaction (38). These studies were performed with 800 cm^3 of 2–18 mg dm^{-3} of the dye Basic Red 46 [198] or Basic Blue 3 [199] in 0.05 M Na_2SO_4 with 0.1–0.5 mM oxalate and 0.05–0.25 mM Fe^{3+} at pH 3.0 using a stirred tank reactor with a Pt anode, an O_2-fed CNT-PTFE cathode and an immersed 6 W fluorescent visible lamp by applying 100 mA for 32 min. In both cases, the decolorization efficiency decreased at higher initial dye content and increased with rising initial Fe^{3+} concentration and prolonging electrolysis time, but remained practically unchanged with oxalate concentration. For a 20 mg dm^{-3} solution of each dye with 0.5 mM oxalate and/or 0.15 mM Fe^{3+} treated at 100 mA, the color removal increased in the sequence EF < PEF ≪ PEF/oxalate, demonstrating the greater performance of the latter EAOP.

The Brillas' group has developed the SPEF process with three photoelectrochemical systems: (i) a 100 cm^3 stirred tank reactor with a 3 cm^2 BDD anode and a 3 cm^2 air-diffusion cathode under direct solar radiation [174], (ii) a 2.5 dm^3 flow plant with a BDD/air-diffusion reactor of 20 cm^2 electrode area connected to a planar solar photoreactor of 600 cm^3 irradiated volume [2,39,200,201] and (iii) a 10 dm^3 flow plant equipped with a Pt/air-diffusion cell of 90.3 cm^2 electrode area and a compound parabolic collector (CPC) photoreactor of 1.57 dm^3 irradiated volume (see scheme in Fig. 20 [202]) [174]. The degradation study performed in the stirred tank reactor for a 290 mg dm^{-3} Sunset Yellow FCF solution in 0.05 M Na_2SO_4 and 0.5 mM Fe^{2+} of pH 3.0 by EF, described in Section 6.2, was extended to PEF with 6 W UVA light and SPEF [174]. As can

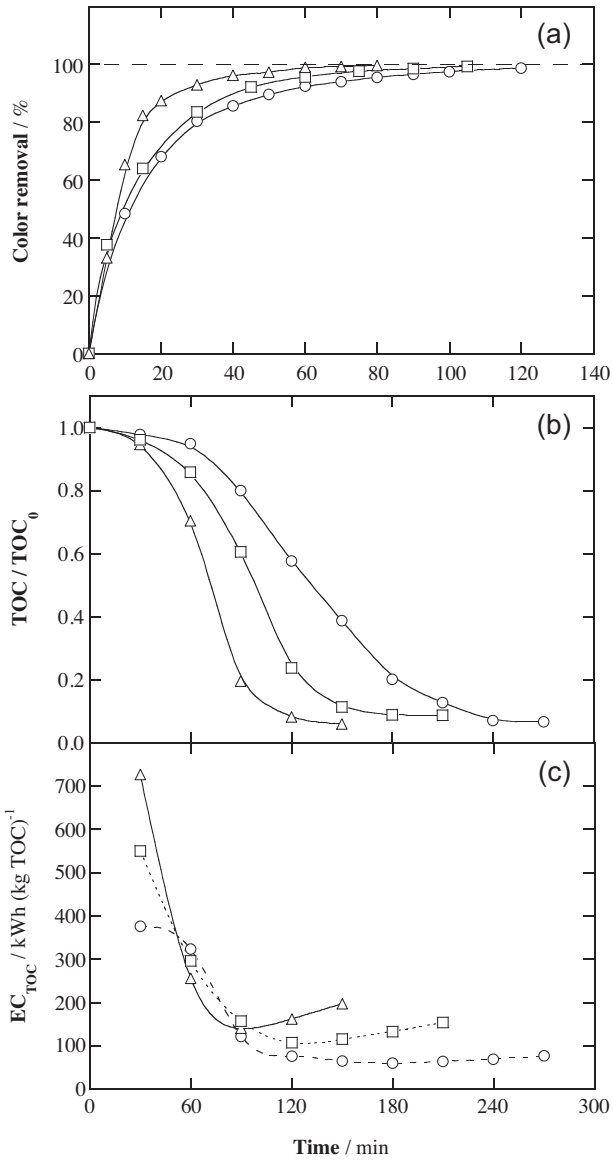

Fig. 21. Effect of current density on the change of: (a) percentage of color removal at λ_{max} = 482 nm, (b) normalized TOC removal and (c) energy consumption per unit TOC mass with electrolysis time for the SPEF treatment of 10 dm^3 of a 290 mg dm^{-3} Sunset Yellow FCF solution in 0.05 M Na_2SO_4 with 0.5 mM Fe^{2+} at pH 3.0 and 35 °C using the flow plant of Fig. 20 at liquid flow rate of 180 dm^3 h^{-1}. Current density: (○) 33.2 mA cm^{-2}, (□) 55.4 mA cm^{-2} and (△) 77.6 mA cm^{-2}.
Adapted from Ref. [174].

be seen in Fig. 16, TOC decayed much more rapidly in both photo-assisted methods, reaching almost total mineralization after 240 and 120 min of electrolysis, respectively. The photolysis of Fe(III) complexes with final oxalic and oxamic acids explained the quicker mineralization found for PEF and SPEF, the latter being more potent owing to the higher UV intensity of sunlight than artificial UVA lamp. Based on these findings, the SPEF process of the Sunset Yellow FCF solution was examined in the 10 dm^3 solar flow plant, where total color removal and almost total mineralization were also quickly reached. The rise in j from 33.2 to 77.6 mA cm^{-2} enhanced the decolorization rate (see Fig. 21a) and TOC removal (see Fig. 21b) by the expected concomitant production of more heterogeneous Pt(•OH) and homogeneous •OH radicals, along with the quicker photodecomposition of Fe(III)–carboxylate species because they are more rapidly generated from the cleavage of aromatic intermediates. Fig. 21c highlights the drop in EC_{TOC} for these trials as j rose. The most economic process was then attained at 33.2 mA cm^{-2}, with a minimum value of 60 kWh (kg TOC)$^{-1}$ at 180 min when the solution was totally decolorized and TOC was reduced by 80%.

The characteristics of the 2.5 dm^3 solar flow plant to the treatment of dyeing solutions has been investigated by the Brillas' group for Disperse Blue 3 [2], Acid Yellow 36 [39], Acid Red 88 and Acid Yellow 9 [200], and Disperse Red 1 and Disperse Red 3 [201]. The treatment of solutions with 50–200 mg dm^{-3} TOC of these dyes in 0.05–0.10 M Na_2SO_4 showed the quickest total decolorization and almost total TOC removal for 0.5 mM Fe^{2+} and pH 3.0 (see Table 6). The increase in j always caused the destruction of more organic matter, but with loss of MCE as a result of the acceleration of parasitic reactions of BDD(•OH) and •OH. In contrast, higher dye content was more slowly removed, but with greater MCE because of the faster reaction of the above radicals with the greater quantity of organics present in the effluent. In all cases, the solution was decolorized at similar rate under comparable EF and SPEF processes owing to the attack of dyes by •OH mainly formed from Fenton's reaction (38). However, the EF treatment led to poor decontamination since Fe(III)–oxalate and Fe(III)–oxamate complexes were slowly destroyed by BDD(•OH), whereas the quick photolytic removal of these species yielded the higher mineralization degree in SPEF. It is also remarkable the study carried out for 200 mg dm^{-3} Disperse Blue 3 solutions with 0.1 M Na_2SO_4 and 0.5 mM Fe^{2+} or 0.5 mM Fe^{2+} + 0.1 mM Cu^{2+} as catalyst at 50 mA cm^{-2} [2]. Fig. 22a depicts the quicker mineralization of SPEF compared to EF for both catalysts, although the use of 0.5 mM Fe^{2+} + 0.1 mM Cu^{2+} slightly improved the performance of both processes. The EC_{TOC} values determined for these trials (see Fig. 22b) usually increased with prolonging electrolysis. At 210 min, about 150 kWh (kg TOC)$^{-1}$ were spent to remove more than 95% TOC by the most potent SPEF regardless of the catalyst utilized. GC–MS analysis of short-time treated solutions allowed the identification of 15 aromatic byproducts coming from •OH oxidation, which include six anthraquinonic derivatives and compounds with two aromatic rings due to intermolecular cyclization or one aromatic ring mainly in the form of phthalic acid products, as can be seen in the proposed reaction pathways of Fig. 22c. Maleic, oxalic, oxamic, pyruvic and acetic acids proceeding form the cleavage of the above aromatics disappeared more quickly in EF and SPEF with 0.5 mM Fe^{2+} + 0.1 mM Cu^{2+}. This was explained by the competitive formation of Cu(II)–carboxylate species that are destroyed much more rapidly with BDD(•OH) than the analogous Fe(III)–carboxylate ones. The initial N of the dye was released in larger extent as NO_3^- than NH_4^+ ion.

8. Combined methods

Many coupled and hybrid electrochemical processes have been proposed aiming developing more powerful processes for dyes removal. They include combined EC, EO, EF and photo-assisted electrochemical methods, as well as the use of microbial fuel cells, which are detailed below.

8.1. Combined EC technologies

Coupling of EC with granular activated carbon (GAC) has been reported [203]. Solutions of 500 cm^3 with 100 mg dm^{-3} Reactive Black 5 and 1 g dm^{-3} NaCl were degraded by EC in a stirred tank reactor with cast iron electrodes of 28 cm^2 area and 100% color removal was found in 8 min operating at pH 7 and 27.7 mA cm^{-2}. However, 61% COD still remained after EC treatment with a high solution toxicity by the presence of generated active chlorine species. Addition of 20 mg dm^{-3} GAC to the resulting solution and further stirring for a long time of 240 min was very positive because COD was reduced up to 7% owing to the adsorption of organics onto

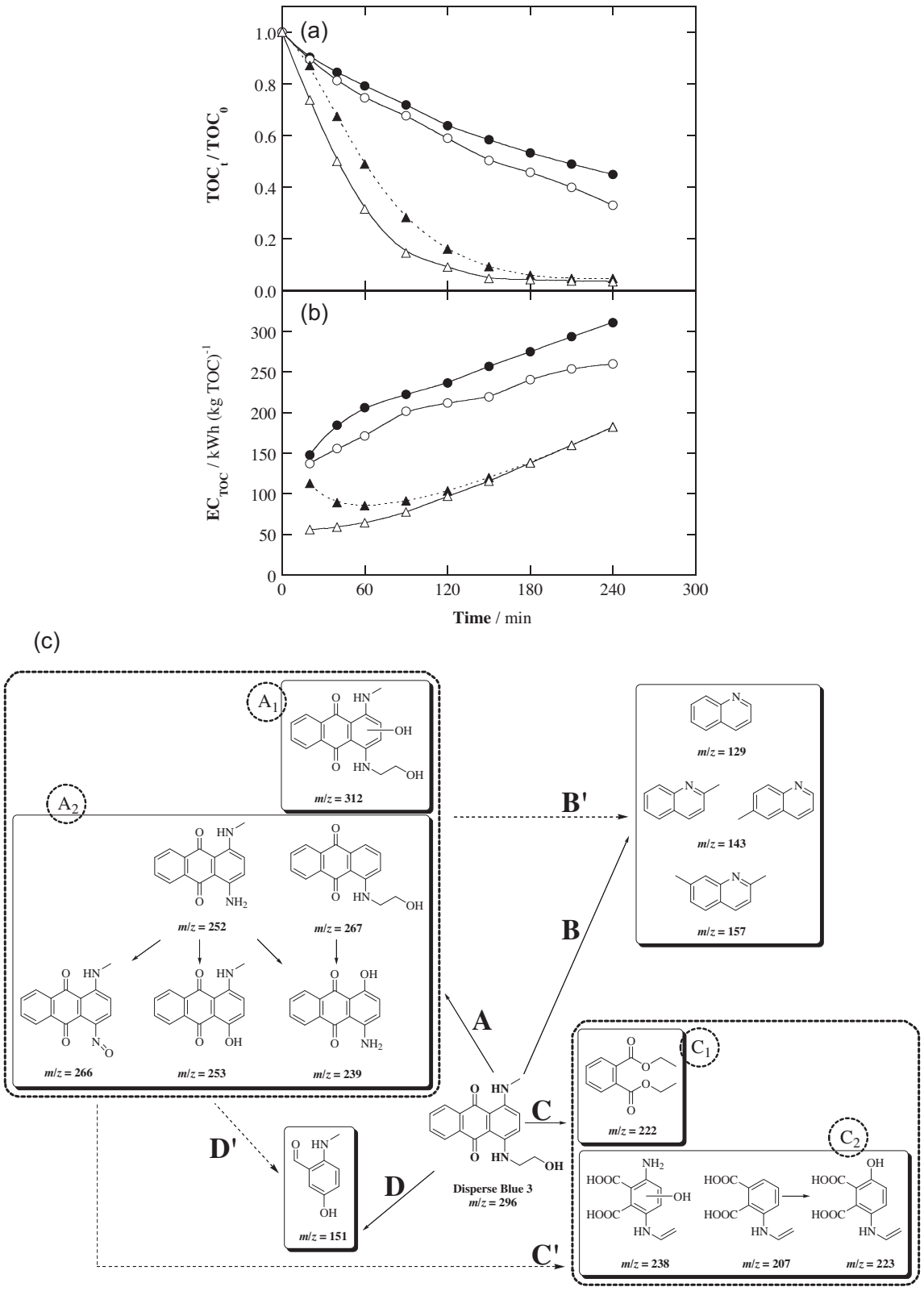

Fig. 22. (a) Normalized TOC abatement and (b) energy consumption per unit TOC mass vs. electrolysis time for the SPEF degradation of 2.5 dm^3 of 200 mg dm^{-3} Disperse Blue 3 solutions with 0.1 M Na_2SO_4 containing (●, ▲) 0.5 mM Fe^{2+} or (○, △) 0.5 mM Fe^{2+} + 0.1 mM Cu^{2+} at pH 3.0 using a flow plant with a BDD/air-diffusion cell of 20 cm^2 electrode area at 50 mA cm^{-2}, 35 °C and liquid flow rate of 200 dm^3 h^{-1}. Process: (●, ○) EF and (▲, △) SPEF. (c) Proposed reaction pathways for the formation of the aromatic by-products identified by GC–MS during the SPEF treatment. Number of aromatic rings: (A) 3, (B and B′) 2 and (C and C′, D and D′) 1.
Adapted from Ref. [2].

GAC. Another very positive aspect of this post-treatment is that the solution was completely detoxified since GAC acted as catalyst to chemically reduce strong oxidants (Cl_2/HClO/ClO^-) to non-toxic products (Cl^-).

Taheri et al. [204] proposed a combined EC/coagulation process to decolorize concentrated solutions of the antraquinone dye Disperse Blue 19 in NaCl. They utilized a stirred tank reactor equipped with 240 cm^2 Al plate electrodes where 2.5 dm^3 of dye solutions were treated at different operating conditions in the presence of poly aluminum chloride as coagulant. From a RSM study with five independent variables, optimum conditions of 162.15 mg dm^{-3} Disperse Blue 19, pH 3.82, 21.5 mA cm^{-2}, electrolysis time of 12.5 min and coagulant dosage of 300 mg were found. Although the coagulant had a very positive effect to accelerate the decolorization process, it increased strongly the operating costs, thereby being doubtful its use in practice.

8.2. Coupled and hybrid EO methods

EO with generation of active chlorine species followed by flash ash adsorption was examined for the decontamination of Methylene Blue solutions [205]. Electrochemical trials were carried out with 500 cm^3 of 100 mg dm^{-3} dye using a stirred tank reactor with 28 cm^2 Ti/IrO_2 electrodes at room temperature. Under optimum conditions of 1 g dm^{-3} NaCl as background electrolyte, pH 7.0 and 42.8 mA cm^{-2}, 99% color removal and 84% COD reduction were achieved in 20 min, but the final solution showed a high toxicity by the presence of active chlorine species. Further treatment with 4 g dm^{-3} fly ash revealed a poor adsorption ability of this material, only yielding <50% COD removal, but total detoxification was feasible by the destruction of active chlorine species. Other authors [206] proposed a coupled treatment in which a supramolecular sorbent was initially used to adsorb azo dye Congo Red from diluted effluents (<10 mg dm^{-3}), followed by its desorption to yield a 30 times more concentrated solution that can be more efficiently treated by EO.

Hybrid systems involving EO with microfiltration [207] or nanofiltration [208] have been recently described for the remediation of wastewaters containing Acid Yellow 36 or Acid Red 73, respectively. In both cases, a suitable membrane was located between the anode and cathode of the electrolytic cell in order to remove the particles in suspension and thus, enhance decontamination. In the case of Acid Yellow 36, for example, a flow plant containing a tubular reactor with a central 9.4 cm^2 Ti/BDD anode surrounded with a ceramic membrane of 1.4 μm porous size, which was encased in a SS tube that also served as cathode, was utilized [207]. Electrolyses of 20 mg dm^{-3} dye solutions in the presence and the absence of 5 mg dm^{-3} kaolin in sulfate medium at pH 3 and 30 mA cm^{-2} for 360 min yielded >94% color removal, 100% COD decay and >93% turbidity removal. These findings demonstrate that the ceramic membrane was very effective to reduce the turbidity of the kaolin particles in suspension and hence, the hybrid system of EO/microfiltration can be useful for the treatment of real dye wastewaters.

The wastewater treatment by sonolysis involves the continuous irradiation with US to produce short-lived ROS (•OH, •O, ...) in cavitational events, which diffuse into the bulk solution to react with soluble organic pollutants [212]. However, sonochemical processes possess so low efficiency that need to be coupled to other methods for practical application. When EO is combined with US, its oxidation ability increases strongly not only by the production of homogeneous •OH from US radiation, but primordially by the faster mass transport of reactants that enhances their oxidation with heterogeneous •OH at the anode and avoids the fouling of electrodes [209,210]. The performance of hybrid EO/US treatment has been assessed for several dyeing solutions. Siddique et al. [209] reported 90% decolorization efficiency and 56% TOC removal for 1 dm^3 of 50 mg dm^{-3} Reactive Blue 19 at pH 8.0 treated by EO in a tank reactor equipped with a PbO_2 anode and a SS cathode, both of 210 cm^2 area, and submitted to an US frequency of 80 kHz and E_{cell} = 10 V for 120 min. In contrast, 13% and 52% color removal was found by applying US and EO alone under comparable conditions, thus confirming the greater effectiveness of the hybrid EO/US process.

Bakheet et al. [211] have developed an electro-peroxone method based on the sparging of a mixture of $O_3 + O_2$ into a contaminated dye solution contained in an electrochemical tank reactor where an O_2-fed carbon-PTFE cathode produces H_2O_2 from reaction (39). Organics can then be destroyed by O_3, heterogeneous •OH formed at the anode surface and homogeneous •OH formed from reaction between electrogenerated H_2O_2 and O_3 as follows:

$$H_2O_2 + O_3 \rightarrow {}^{\bullet}OH + HO_2^{\bullet} + O_2 \quad (64)$$

To assess the performance of this novel hybrid method, 400 cm^3 of 200 mg dm^{-3} Orange II in 0.05 M Na_2SO_4 at pH 3–10 were comparatively treated by ozonation, EO-H_2O_2 and electro-peroxone by injecting 118 mg dm^{-3} O_3. In the electrochemical trials, the tank reactor was equipped with a 1 cm^2 Pt anode and a 10 cm^2 carbon-PTFE cathode and a current between 100 and 500 mA was applied. A poorer performance was found for electro-peroxone in alkaline solutions due to O_3 decomposition by OH^-. At the pH range 3–7, this method led to total decolorization in 4 min and 95.7% TOC decay in 45 min operating at 400 mA, whereas individual ozonation and EO-H_2O_2 treatments gave much lower mineralization, only 55.6% and 15.3% in 90 min, respectively. These results highlight the excellent degradation behavior of electro-peroxone, whose properties should be more extensively studied to clarify its real use for wastewater remediation.

8.3. Peroxi-coagulation and hybrid EF treatments

Peroxi-coagulation consists in the electrochemical treatment of a contaminated acidic solution with a sacrificial Fe anode and a gas-diffusion electrode that generates continuously H_2O_2 from reaction (39). Fe is oxidized to Fe^{2+} by reaction (9), which reacts with H_2O_2 to produce •OH by Fenton's reaction (38) and hence, organics can be oxidized with this radical and/or coagulate with the high amounts of $Fe(OH)_3$ precipitate formed [212–214]. The Khataee's group has investigated exhaustively the decolorization and mineralization of several dyes by peroxi-coagulation [215,216]. The superiority of this method over EC and EF was demonstrated for 250 cm^3 of 20 mg dm^{-3} Basic Yellow 2 in 0.05 M Na_2SO_4 of pH 3.0 using stirred undivided two-electrode tank reactors at 100 mA and 25 °C [215]. A Fe/graphite cell for EC, a Pt/carbon-PTFE one for EF, and Fe/carbon-PTFE and Fe/CNT-PTFE cells for peroxi-coagulation were used. Total decolorization was only reached after 30 min of peroxi-coagulation with the Fe/CNT-PTFE reactor. This quicker process gave 92% TOC reduction after 360 min of electrolysis. GC–MS analysis of treated solutions allowed the identification of soluble products like bis[4-(dimethylamino)phenyl]methanone and 4-dimethylaminobenzoic, *p*-hydroxybenzoic, maleic and oxalic acids. Coagulation of *N*-derivatives with $Fe(OH)_3$ was confirmed by elemental analysis of the precipitate. From these excellent results found for peroxi-coagulation, the treatment with the Fe/CNT-PTFE cell was further extended to aqueous solutions of Basic Blue 3, Malachite Green and Basic Red 46 of pH 3.0 and their optimum degradation conditions were determined by RSM [216].

Wang et al. [217] proposed a novel hybrid EF/MW process based on the flow system schematized in Fig. 23a. A 100 cm^3 solution with 300 mg dm^{-3} Methyl Orange, 0.05 M Na_2SO_4 and 1 mM Fe^{2+} at pH 3.0 and 35 °C was recirculated through a BDD/Ti cell at 180 cm^3 min^{-1}. The MW energy was provided by an oven with 2.45 GHz frequency and 127.5 W power. At 10 mA cm^{-2}, an

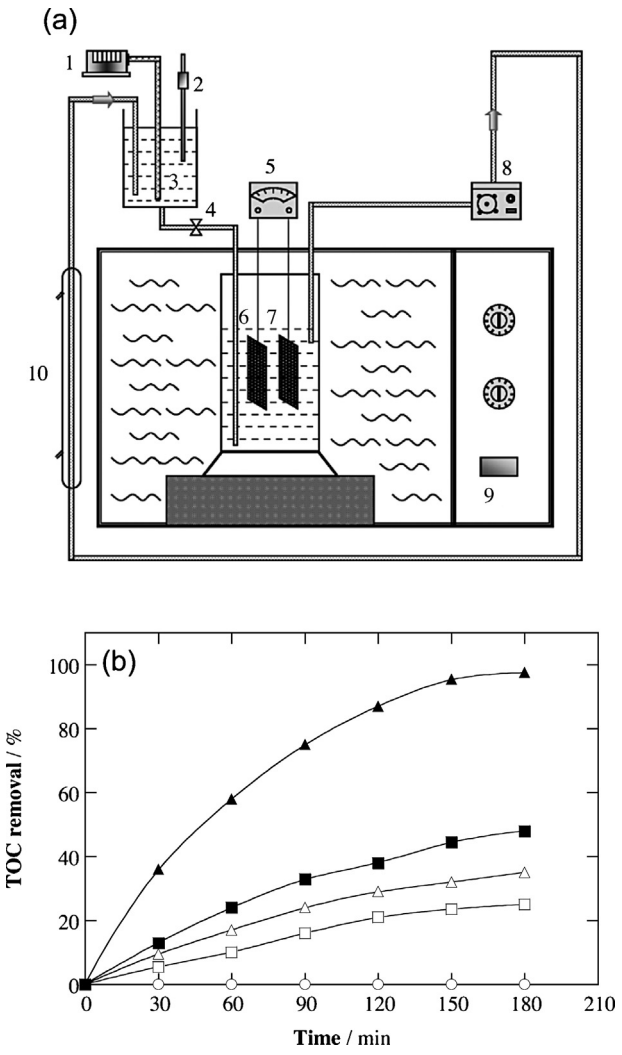

Fig. 23. (a) Experimental set-up of a hybrid EF/Microwave (MW) flow cell. (1) Peristaltic pump, (2) thermometer, (3) liquid buffer, (4) flowmeter, (5) DC regulated power supply, (6) 3 cm^2 Ti bar cathode, (7) 3 cm^2 Si/BDD anode, (8) peristaltic pump, (9) microwave oven and (10) condenser tube. (b) Time-course evolution of 100 cm^3 of 300 mg dm^{-3} Methyl Orange in 0.05 M Na_2SO_4 at pH 3.0, 10 mA cm^{-2}, 35 °C and liquid flow rate of 180 cm^3 min^{-1}. Methods: (○) MW, (□) EO, (△) EF, (■) EO/MW and (▲) EF/MW. In EF and EF/MW methods, the starting solution contained 1 mM Fe^{2+} as catalyst and 500 cm^3 min^{-1} of air flow was bubbled through it.
Adapted from Ref. [217].

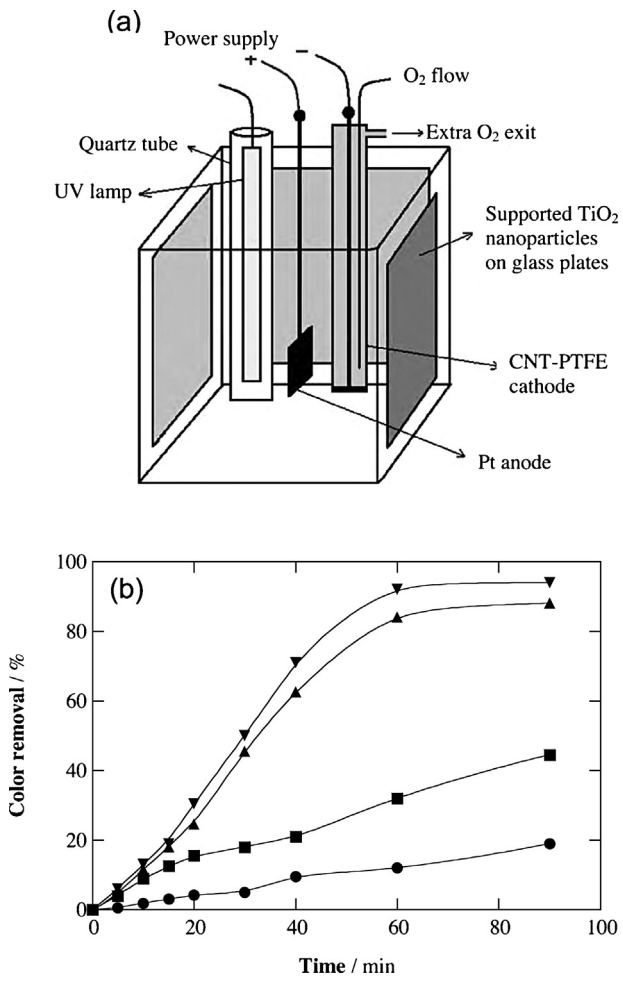

Fig. 24. (a) Sketch of the cubic tank reactor used for the combined PEF/photocatalysis treatment of dyes. A 11.5 cm^2 Pt anode, a 11.5 cm^2 CNT-PTFE O_2-diffusion cathode and a 6 W UVC lamp were placed in the center of the cell, surrounded by TiO_2 nanoparticles onto glass plates covering its four inner walls. (b) Percentage of color removal vs. time for the treatment of 2 dm^3 of a 20 mg dm^{-3} Basic Red 46 solution in 0.05 M Na_2SO_4 with 0.1 mM Fe^{3+} at pH 3.0, 100 mA and 25 °C by: (●) TiO_2/UV, (■) EF, (▲) PEF and (▼) PEF/photocatalysis.
Adapted from Ref. [224].

efficient activation of the BDD anode and Ti cathode surfaces was found under MW irradiation, alleviating the blocking of BDD surface with intermediates to yield more heterogeneous BDD(•OH) and accelerating the Fe^{3+}/Fe^{2+} redox cycles and the cathodic H_2O_2 production to give more homogeneous •OH from Fenton's reaction (38). This behavior improved strongly the dye decay and mineralization of the solution by EF/MW compared to MW, EO, EF and the hybrid EO/MW, as exemplified in Fig. 23b for their TOC abatement. The quickest destruction of detected intermediates such as 2,5-dinitrophenol, *p*-nitrophenol, hydroquinone, *p*-benzoquinone and maleic and oxalic acids confirmed the superiority of EF/MW in dye mineralization.

8.4. Coupled and hybrid photo-assisted electrochemical processes

Coupled methods such as EO followed by PEC [218] and hybrid methods including PEC/EF [219], EO/photocatalysis [220] and PEF/photocatalysis with ZnO [221–223] and TiO_2 [224–227] nanoparticles have been checked as combined photo-assisted electrochemical processes. The good performance of these methods for the destruction of several dye solutions under optimum conditions can be observed in Table 7. For EO + PEC [218], 100 cm^3 of a 500 mg dm^{-3} Methyl Orange solution in 0.1 M Na_2SO_4 at pH 3.0 were electrolyzed in a tank reactor containing a Ti/TiO_2-NTs/SnO_2 anode/photoanode and a Ti cathode at 135 mA. The solution was firstly treated by EO for 90 min up to total decolorization and subsequently, it was degraded by PEC under photoanode illumination with a 300 W UV lamp up to a total time of 600 min yielding 71% TOC removal, a value higher than 59% mineralization obtained by applying single EO. In the case of hybrid PEC/EF [219], a semi-circular quartz glass cylinder reactor equipped with a Bi_2WO_6 photoanode under 300 W tungsten halogen lamp irradiation and a Fe@Fe_2O_3/ACF cathode fed with 5 dm^3 min^{-1} O_2 was utilized to degrade 100 cm^3 of a 10 μM Rhodamine B and 0.05 M Na_2SO_4 solution at pH 6.2 and 0.3 mA for 240 min. TOC was then reduced by 94% in the PEC/EF process, whereas only 78% and 14% mineralization were found for EF with Pt/Fe@Fe_2O_3 cell and PEC with Bi_2WO_6/Pt cell, respectively, under the same conditions. The degradation superiority of PEC/EF was explained by: (i) the better separation of photogenerated e^-_{CB}–h^+_{VB} pairs from reaction (53) by the external current with production of more oxidant holes at

Table 7
Per cent of color removal and TOC decay determined for removing synthetic organic dyes from wastewaters by using combined photo-assisted electrochemical processes under optimum conditions.

Dye[a]	C_0 (mg dm^{-3})	Method	Experimental conditions	% color removal	% TOC decay	Ref.
Ti/TiO_2-NTs/SnO_2 anode and Ti cathode						
Acid Orange 52 (Methyl Orange)	500	EO + PEC	100 cm^3, 0.1 M Na_2SO_4, pH 7, for 1.5 h in EO. 300 W UV lamp, up to 10 h in PEC. Current 135 mA	100	71	[218]
Bi_2WO_6/Fe@Fe_2O_3 cell						
Basic Violet 10 (Rhodamine B)	10[b]	PEC/EF	100 cm^3, 0.05 M Na_2SO_4, pH 6.2, 0.3 mA, 300 W tungsten halogen lamp, for 4 h	100	94	[219]
PbO_2/graphite cell with BiOCl/TiO_2 particles						
Acid Red 87 (Eosin Y)	50	EO/photocatalysis	0.05 M Na_2SO_4, pH 4.0, 1.0 g dm^{-3} BiOCl/TiO_2, 100 mA, 40 W mercury lamp, for 4 h	100	68	[220]
Pt/CNT-PTFE cell with ZnO nanoparticles						
Basic Yellow 28	20	PEF/photocatalysis	2 dm^3, 0.05 M Na_2SO_4, pH 3.0, 0.1 mM Fe^{3+}, 100 mA, 6 W UVC, for 6 h	100	95	[221]
Direct Yellow 12	50	PEF/photocatalysis	2 dm^3, 0.05 M Na_2SO_4, pH 3.0, 0.1 mM Fe^{3+}, 100 mA, 6 W UVC, for 6 h	100	97	[222]
Pt/CNT-PTFE cell with TiO_2 nanoparticles						
Basic Red 46	15	PEF/photocatalysis	2 dm^3, 0.05 M Na_2SO_4, pH 3.0, 0.1 mM Fe^{3+}, 100 mA, 6 W UVC, for 6 h	100	99	[225]
Acid Red 17	18	PEF/photocatalysis	1.5 dm^3, 0.05 M Na_2SO_4 pH 3.0, 0.15 mM Fe^{3+}, 100 mA, 6 W UVC, for 1.5 h	94	–[c]	[226]

[a] Color index (common) name.
[b] μM concentration.
[c] Not determined.

the photoanode and (ii) the extra injection of photoinduced electrons to the Fe@Fe_2O_3 cathode enhancing H_2O_2 production with more generation of •OH. The production of holes as extra oxidant also explains the higher oxidation power of EO/photocatalysis compared to single processes for the degradation of Eosin Y solutions under UV irradiation of BiOCl/TiO_2 nanostructured composites in suspension [220].

The Khataee's group explored the characteristics of PEF/photocatalysis for Basic Yellow 28 [221] and Direct Yellow 12 [222,223] using the cubic undivided cell schematized in Fig. 24a, but with ZnO nanoparticles onto glass plates covering its four inner walls, under vigorous stirring with a magnetic bar. Electrolytic experiments were made with 2 dm^3 of 10–50 mg dm^{-3} dye solutions in 0.05 M Na_2SO_4 with 0.05–1 mM Fe^{3+} at pH 2–6 and between 50 and 500 mA. Optimum conditions were found for 0.1–0.2 mM Fe^{3+} and pH 3.0, whereas the percentage of color and TOC removals, as expected, dropped with increasing dye concentration and rose at higher current. Overall decolorization and almost total mineralization were determined in all cases after 360 min of electrolysis (see Table 7). Comparative ZnO/UV, EF and PEF treatments gave poorer results, corroborating the higher oxidation ability of PEF/photocatalysis with ZnO nanoparticles. This can be attributed to the parallel destruction of organics by: (i) heterogeneous Pt(•OH) and heterogeneous •OH from photogenerated holes on ZnO by reaction (54), (ii) homogeneous •OH formed from Fenton's reaction (38), from photolysis of $Fe(OH)^{2+}$ species by reaction (61) and from UVC photolysis of electrogenerated H_2O_2 by reaction (63), (iii) photoinduced holes produced on ZnO by reaction (53) and (iv) photodecomposition of intermediates under UVC radiation. Hydroxylation products such as 1,2,3,3-tetramethylindoline, 4-methoxybenzenamine and hydroquinone for Basic Yellow 28 and 3-ethoxybenzoic acid, 4-ethoxyphenol, hydroquinone and 4-ethoxybenzenamine for Direct Yellow 12, as well as final carboxylic acids like maleic, propionic, glyoxylic and oxalic, were identified by GC–MS. The Khataee's group also reported the same oxidation characteristics with excellent performance for PEF/photocatalysis with TiO_2 nanoparticles of aqueous solutions of Basic Red 46 [224,225], Acid Red 17 [226] and Acid Yellow 36, Acid Red 14 and Basic Yellow 28 [227] degraded in the cubic cell of Fig. 24a (see Table 7). This method was always more powerful than single TiO_2/UV, EF and PEF processes under comparable conditions, as exemplified in Fig. 24b for a 20 mg dm^{-3} Basic Red 46 solution [224].

8.5. Microbial fuel cells

Several studies have demonstrated the electrochemical reduction of the azo dye Methyl Orange in the cathodic compartment of an undivided MFC with a bioanode [228,229]. The best performance was found for an MFC constituted of two identical chambers of 75 cm^3 capacity equipped with a 20.25 cm^2 carbon-felt electrode and separated by a cation exchange membrane [228]. The anodic compartment was filled with a solution of pH 7.0 with *Klebsiella pneumoniae* strain L17 fed with glucose, while the cathodic compartment contained 0.05 mM Methyl Orange in phosphate buffer of pH 3.0. The transfer of electrons from bacteria respiration to the cathode caused the reduction of the dye at a rate constant of 0.298 μmol min^{-1} with a power density of 34.77 mW m^{-2}. Sulfanilic acid and *N*,*N*-dimethyl-*p*-phenylenediamine formed from the cleavage of the —N=N— bond of Methyl Orange were detected as reduction products. The fact that these compounds are not friendly to the environment is the main drawback for the application of this technology.

9. Conclusions and prospects

There is an increasing incidence in health problems related to environmental issues that originate from inadequate decontamination of industrial wastewaters. This has compelled scientists and engineers to engage innovative technologies to achieve a maximum elimination of organic pollutants at affordable costs. Therefore, it is needed the development of new approaches to degrade synthetic organic dyes by means of an entirely new class of advanced oxidation processes. In that case, the recent advances obtained

with EAOPs such as EO, EO with active chlorine, EF and emerging photo-assisted approaches like PEC, SPEC, PEF and SPEF, suggest that their application to the treatment of industrial effluents should be rapidly developed. The fast decontamination and total oxidation of many dyestuffs due to the great amounts of ROS and other oxidants produced during electrochemical treatments are important profit determinants with the adoption of optimum operating conditions, reactor design and electrocatalytical materials. The interest of electrochemical technologies for destroying dyes from wastewaters has grown exponentially in the last years. Apart from the studies performed with the classical EC, many research groups have dedicated great efforts to clarify the properties of EAOPs as potential alternatives for removing dyes from synthetic and industrial effluents. Electrochemical technologies show a reservoir effect, are often more cost-effective and require less maintenance than other treatment methods. The combination with photovoltaic power supplies allows envisaging the use of electrochemical approaches far from the electrical supply grid. This may be important for its application to industrial effluents in developing countries. The recent combination of electrochemical methods with other treatment technologies like photocatalysis, adsorption, nanofiltration, microwaves and ultrasounds among others, opens new perspectives for an easy, effective and free-chemical remediation of dyestuff effluents.

It is expected that future advances will be performed in the electrochemical reactors at pilot scale when implanted, and combined electrochemical approaches could also be used for wastewater treatment in the industry. The future for these technologies is bright. Initial studies about electrocatalytic materials as well as their catalytic mechanisms are starting to make important contributions to the implementation of a range of new methods and combination of advanced oxidation processes. Several other complementary techniques are emerging and can provide innovative electrocatalytic materials and catalytic pathways for decontamination of effluents. Future developments will rely upon the close collaboration of analytical chemists, engineers, and electrochemists to ensure effective application and exploitation of electrochemical technologies to find new alternatives as pre- or post-treatments methodologies.

References

[1] European Parliament and Council of the European Union, Off. J. Eur. Commun. L327/1 (2000).
[2] R. Salazar, E. Brillas, I. Sirés, Appl. Catal. B: Environ. 115–116 (2012) 107–116.
[3] T. Robinson, G. McMullan, R. Marchant, P. Nigam, Bioresour. Technol. 77 (2001) 247–255.
[4] C.A. Martínez-Huitle, E. Brillas, Appl. Catal. B: Environ. 87 (2009) 105–145.
[5] V. Khandegar, A.K. Saroha, J. Environ. Manage. 128 (2013) 949–963.
[6] D. Brown, Ecotoxicol. Environ. Saf. 13 (1987) 139–147.
[7] K.P. Sharma, S. Sharma, S.P. Sharma, K. Singh, S. Kumar, R. Grover, P.K. Sharma, Chemosphere 69 (2007) 48–54.
[8] E. Forgacs, T. Cserhati, G. Oros, Environ. Int. 30 (2004) 953–971.
[9] X.C. Jin, G.Q. Liu, Z.H. Xu, W.Y. Tao, Appl. Microbiol. Biotechnol. 74 (2007) 239–243.
[10] M. Solís, A. Solís, H.I. Pérez, N. Manjarrez, M. Flores, Process Biochem. 47 (2012) 1723–1748.
[11] M. Sala, M.C. Gutiérrez-Bouzán, Int. J. Photoenergy (2012), http://dx.doi.org/10.1155/2012/629103, ID 629103.
[12] A.B. Koltuniewicz, E. Drioli, Membranes in Clean Technologies. Theory and Practice, vol. 1, Wiley-VCH, Weinheim, Germany, 2008.
[13] F. Fu, T. Viraraghavan, Bioresour. Technol. 79 (2001) 251–262.
[14] I.I. Savin, R. Butnaru, Environ. Eng. Manage. J. 7 (2008) 859–864.
[15] M.C. Gutierrez, M. Crespi, J. Soc. Dyes Col. 115 (1999) 342–345.
[16] O.J. Hao, H. Kim, P.C. Chiang, Crit. Rev. Environ. Sci. Technol. 30 (2000) 449–505.
[17] M.M. Naim, Y.M. El Abd, Sep. Purif. Methods 31 (2002) 171–228.
[18] A.B. dos Santos, F.J. Cervantes, J.B. van Lier, Bioresour. Technol. 98 (2007) 2369–2385.
[19] J. Vijayaraghavan, S.J. Sardhar Basha, J. Jegan, J. Urban Environ. Eng. 7 (2013) 30–47.
[20] M. Klavarioti, D. Mantzavinos, D. Kassinos, Environ. Int. 35 (2009) 402–417.
[21] D. Genders, N. Weinberg (Eds.), Electrochemistry for a Cleaner Environment, Electrosynthesis Company Inc., New York, 1992.
[22] D. Pletcher, F.C. Walsh, Industrial Electrochemistry, 2nd ed., Blackie Academic & Professional, London, 1993.
[23] D. Simonson, Chem. Soc. Rev. 26 (1997) 181–189.
[24] K. Rajeshwar, J.G. Ibanez, Fundamentals and Application in Pollution Abatement, Academic Press, San Diego, CA, 1997.
[25] E. Brillas, P.L. Cabot, J. Casado, in: M. Tarr (Ed.), Chemical Degradation Methods for Wastes and Pollutants Environmental and Industrial Applications, Marcel Dekker, New York, 2003, pp. 235–304.
[26] G. Chen, Sep. Purif. Technol. 38 (2004) 11–41.
[27] M. Panizza, G. Cerisola, Electrochim. Acta 51 (2005) 191–199.
[28] C.A. Martínez-Huitle, S. Ferro, Chem. Soc. Rev. 35 (2006) 1324–1340.
[29] A. Kraft, Int. J. Electrochem. Sci. 2 (2007) 355–385.
[30] M. Panizza, G. Cerisola, Chem. Rev. 109 (2009) 6541–6569.
[31] E. Brillas, I. Sirés, M.A. Oturan, Chem. Rev. 109 (2009) 6570–6631.
[32] Ch. Comninellis, G. Chen (Eds.), Electrochemistry for the Environment, Springer, New York, 2010.
[33] E. Brillas, C.A. Martínez-Huitle (Eds.), Synthetic Diamond Films: Preparation, Electrochemistry, Characterization and Applications, Wiley, Weinheim, 2011.
[34] G.R. de Oliveira, C.K.C. de Araújo, C.A. Martínez-Huitle, D.R. da Silva, Curr. Org. Chem. 16 (2012) 1957–1959.
[35] C. Zhang, Y. Jiang, Y. Li, Z. Hu, L. Zhou, M. Zhou, Chem. Eng. J. 228 (2013) 455–467.
[36] I. Sirés, E. Brillas, M.A. Oturan, M.A. Rodrigo, M. Panizza, Environ. Sci. Pollut. Res. 21 (2014) 8336–8367.
[37] M.A. Oturan, J.-J. Aaron, Crit. Rev. Environ. Sci. Technol. 44 (2014) 2577–2641.
[38] S. Garcia-Segura, F. Centellas, C. Arias, J.A. Garrido, R.M. Rodríguez, P.L. Cabot, E. Brillas, Electrochim. Acta 58 (2011) 303–311.
[39] E.J. Ruiz, C. Arias, E. Brillas, A. Hernández-Ramírez, J.M. Peralta-Hernández, Chemosphere 82 (2011) 495–501.
[40] C. Flox, J.A. Garrido, R.M. Rodríguez, P.L. Cabot, F. Centellas, C. Arias, E. Brillas, Catal. Today 129 (2007) 29–36.
[41] M. Skoumal, C. Arias, P.L. Cabot, F. Centellas, J.A. Garrido, R.M. Rodríguez, E. Brillas, Chemosphere 71 (2008) 1718–1729.
[42] P.K. Holt, G.W. Barton, M. Wark, C.A. Mitchell, Colloids Surf. A: Physicochem. Eng. Asp. 211 (2002) 233–248.
[43] N. Daneshvar, A.R. Khataee, A.R. Amani Ghadim, M.H. Rasoulifard, J. Hazard. Mater. 148 (2007) 566–572.
[44] M.-C. Wei, K.-S. Wang, C.-L. Huang, C.-W. Chiang, T.-J. Chang, S.-S. Lee, S.-H. Chang, Chem. Eng. J. 192 (2012) 37–44.
[45] M. Saravanan, N.P. Sambhamurthy, M. Sivarajan, Clean 38 (2010) 565–571.
[46] U.D. Patel, J.P. Ruparelia, M.U. Patel, J. Hazard. Mater. 197 (2011) 128–136.
[47] C.S. Keskin, A. Özdemir, I.A. Sengil, Water Sci. Technol. 64 (2011) 1644–1650.
[48] C.S. Keskin, E. Kirbaç, A. Özdemir, I.A. Sengil, Fresenius Environ. Bull. 20 (2011) 3206–3216.
[49] B. Merzouk, M. Yakoubi, I. Zongo, J.-P. Leclerc, G. Paternotte, S. Pontvianne, F. Lapicque, Desalination 275 (2011) 181–186.
[50] E. Pajootan, M. Arami, N.M. Mahmoodi, J. Taiwan Inst. Chem. Eng. 43 (2012) 282–290.
[51] M. Taheri, M.R. Alavi Moghaddam, M. Arami, Iran. J. Environ. Health Sci. Eng. 9 (2012) 23–30.
[52] S. Singh, V.C. Srivastava, I.D. Mall, RSC Adv. 3 (2013) 16426–16439.
[53] E.-S.Z. El-Ashtoukhy, N.K. Amin, J. Hazard. Mater. 179 (2010) 113–119.
[54] A. Olad, A.R. Amani-Ghadim, M.S.S. Dorraji, M.H. Rasoulifard, Clean 38 (2010) 401–408.
[55] A. Pirkarami, M.E. Olya, S. Tabibian, J. Environ. Sci. Health A: Toxic/Hazard. Subst. Environ. Eng. 48 (2013) 1243–1252.
[56] P. Durango-Usuga, F. Guzmán-Duque, R. Mosteo, M.V. Vazquez, G. Peñuela, R.A. Torres-Palma, J. Hazard. Mater. 179 (2010) 120–126.
[57] A.R. Amani-Ghadim, S. Aber, A. Olad, H. Ashassi-Sorkhabi, Electrochim. Acta 56 (2011) 1373–1380.
[58] A.R. Amani-Ghadim, A. Olad, S. Aber, H. Ashassi-Sorkhabi, Environ. Prog. Sust. Energy 32 (2013) 547–556.
[59] A.R. Amani-Ghadim, S. Aber, A. Olad, H. Ashassi-Sorkhabi, Chem. Eng. Process. 64 (2013) 68–78.
[60] W. Lemlikchi, S. Khaldi, M.O. Mecherri, H. Lounici, N. Drouiche, Sep. Sci. Technol. 47 (2012) 1682–1688.
[61] A.J. Méndez-Martínez, M.M. Dávila-Jímenez, O. Ornelas-Dávila, M.P. Elizalde-González, U. Arroyo-Abad, I. Sirés, E. Brillas, Electrochim. Acta 59 (2012) 140–149.
[62] S. Velazquez-Peña, I. Linares-Hernández, V. Martínez-Miranda, C. Barrera-Díaz, B. Bilyeu, Fuel 110 (2013) 12–16.
[63] Ch. Comninellis, Electrochim. Acta 39 (1994) 1857–1862.
[64] B. Marselli, J. Garcia-Gomez, P.A. Michaud, M.A. Rodrigo, Ch. Comninellis, J. Electrochem. Soc. 150 (2003) D79–D83.
[65] P.-A. Michaud, M. Panizza, L. Ouattara, T. Diaco, G. Foti, Ch. Comninellis, J. Appl. Electrochem. 33 (2003) 151–154.
[66] D.A. Carvalho, J.H. Bezerra Rocha, N.S. Fernandes, D.R. Da Silva, C.A. Martínez-Huitle, Latin Am. Appl. Res. 41 (2011) 127–133.
[67] S. Song, J. Fan, Z. He, L. Zhan, Z. Liu, J. Chen, X. Xu, Electrochim. Acta 55 (2010) 3606–3613.
[68] M. Weng, Z. Zhou, Q. Zhang, Int. J. Electrochem. Sci. 8 (2013) 290–296.
[69] H. An, H. Cui, W. Zhang, J. Zhai, Y. Qian, X. Xie, Q. Li, Chem. Eng. J. 209 (2012) 86–93.
[70] Q. Li, Q. Zhang, H. Cui, L. Ding, Z. Wei, J. Zhai, Chem. Eng. J. 228 (2013) 806–814.

[71] Z. He, C. Huang, Q. Wang, Z. Jiang, J. Chen, S. Song, Int. J. Electrochem. Sci. 6 (2011) 4341–4354.
[72] F.J. Recio, P. Herrasti, I. Sirés, A.N. Kulak, D.V. Bavykin, C. Ponce-de-León, F.C. Walsh, Electrochim. Acta 56 (2011) 5158–5165.
[73] C. Ahmed Basha, R. Saravanathamizhan, V. Nandakumar, K. Chitra, C.W. Lee, Chem. Eng. Res. Des. 91 (2013) 552–559.
[74] B.D. Soni, J.P. Ruparelia, Proc. Eng. 51 (2013) 335–341.
[75] H. Lin, L. Hou, H. Zhang, Water Sci. Technol. 68 (2013) 2441–2447.
[76] A.B. Isaev, Z.M. Aliev, Russ. J. Appl. Electrochem. 85 (2012) 776–781.
[77] C.C. de Oliveira Morais, A.J. Cabral da Silva, M. Barbosa Ferreira, D. Medeiros de Araújo, C.L.P.S. Zanta, S.S. Leal Castro, Electrocatalysis 4 (2013) 312–319.
[78] R.G. Da Silva, S.A. Neto, A.R. De Andrade, J. Braz. Chem. Soc. 22 (2011) 126–133.
[79] C. Ahmed Basha, J. Sendhil, K.V. Selvakumar, P.K.A. Muniswaran, C.W. Lee, Desalination 285 (2012) 188–197.
[80] F.A. Rodríguez, M.N. Mateo, J.M. Aceves, E.P. Rivero, I. González, Environ. Technol. 34 (2013) 573–583.
[81] H. Zhang, J. Wu, Z. Wang, D. Zhang, J. Chem. Technol. Biotechnol. 85 (2010) 1436–1444.
[82] M.G. Tavares, L.V.A. da Silva, A.M.S. Solano, J. Tonholo, C.A. Martinez-Huitle, C.L.P.S. Zanta, Chem. Eng. J. 204–206 (2012) 141–150.
[83] R. Palani, N. Balasubramanian, Color. Technol. 128 (2012) 434–439.
[84] F.W.P. Ribeiro, S. Do Nascimiento Oliveira, P. De Lima Neto, A.N. Correia, L.H. Mascaro, R. De Matos, E.C.P. De Souza, M.R. De Vasconcelos Lanza, Quim. Nova 36 (2013) 85–90.
[85] P.A. Soloman, C.A. Basha, M. Velan, N. Balasubramanian, Chem. Biochem. Eng. Q. 24 (2010) 445–452.
[86] L. Pang, H. Wang, Z.Y. Bian, Water Sci. Technol. 67 (2013) 521–526.
[87] A.I. del Río, J. Fernández, J. Molina, J. Bonastre, F. Cases, Desalination 273 (2011) 428–435.
[88] A.I. del Río, M.J. Benimeli, J. Molina, J. Bonastre, F. Cases, Int. J. Electrochem. Sci. 7 (2012) 13074–13092.
[89] J. Molina, J. Fernandez, A.I. del Rio, J. Bonastre, F. Cases, Appl. Surf. Sci. 258 (2011) 6246–6256.
[90] A.M. Sales Solano, J.H.B. Rocha, N.S. Fernandes, D.R. Da Silva, C.A. Martínez-Huitle, Oxid. Commun. 34 (2011) 218–229.
[91] G. Rodrigues de Oliveira, N. Suely Fernandes, J. Vieira de Melo, D. Ribeiro da Silva, C. Urgeghe, C.A. Martinez-Huitle, Chem. Eng. J. 168 (2011) 208–214.
[92] M. Jović, D. Stanković, D. Manojlović, I. Andelković, A. Millić, B. Dojćinović, G. Roglić, Int. J. Electrochem. Sci. 8 (2013) 168–183.
[93] M.B. Ferreira, J.H.B. Rocha, J.V. de Melo, C.A. Martinez-Huitle, M.A. Quiroz Alfaro, Electrocatalysis 4 (2013) 274–282.
[94] M. Pepió, M.C. Gutiérrez-Bouzán, Ind. Eng. Chem. Res. 50 (2011) 8965–8972.
[95] P. Kariyajjanavar, J. Narayana, Y. Arthoba Nayaka, J. Environ. Chem. Eng. 1 (2013) 975–980.
[96] M. Rivera, M. Pazos, M.A. Sanromán, Desalination 274 (2011) 39–42.
[97] S.-H. Li, Y. Zhao, J. Chu, W.-W. Li, H.-Q. Yu, G. Liu, Electrochim. Acta 92 (2013) 93–101.
[98] N. Li, S.S. Dong, W.Y. Lv, S.Q. Huang, H.X. Chen, Y.Y. Yao, W.X. Chen, Sci. China Chem. 56 (2013) 1757–1764.
[99] E. Pajootan, M. Arami, Electrochim. Acta 112 (2013) 505–514.
[100] J. Fernández, J. Molina, A.I. del Río, J. Bonastre, F. Cases, Int. J. Electrochem. Sci. 7 (2012) 10175–10189.
[101] Z. Liu, F. Wang, Y. Li, T. Xu, S. Zhu, J. Environ. Sci. 23 (2011) S70–S73.
[102] H.-Z. Zhao, Y. Sun, L.-N. Xu, J.-R. Ni, Chemosphere 78 (2010) 46–51.
[103] Y. Yavuz, R. Shahbazi, Sep. Purif. Technol. 85 (2012) 130–136.
[104] F.L. Migliorini, N.A. Braga, S.A. Alves, M.R.V. Lanza, M.R. Baldan, N.G. Ferreira, J. Hazard. Mater. 192 (2011) 1683–1689.
[105] C. Zhang, J. Wang, H. Zhou, D. Fu, Z. Gu, Chem. Eng. J. 161 (2010) 93–98.
[106] C.A. Martinez-Huitle, E.V. dos Santos, D. Medeiros de Araujo, M. Panizza, J. Electroanal. Chem. 674 (2012) 103–107.
[107] N.E. Rodríguez De León, K. Cruz-González, O. Torres-López, A. Hernández-Ramírez, J.L. Guzmán-Mar, C.A. Martínez-Huitle, J.M. Peralta-Hernández, ECS Trans. 20 (2009) 283–290.
[108] A.M. Sales Solano, C.K. Costa de Araujo, J. Vieira de Melo, J.M. Peralta-Hernandez, D. Ribeiro da Silva, C.A. Martinez-Huitle, Appl. Catal. B: Environ. 130–131 (2013) 112–120.
[109] E. Alvarez-Guerra, A. Dominguez-Ramos, A. Irabien, Chem. Eng. Res. Des. 89 (2011) 2679–2685.
[110] R.E. Palma-Goyes, F.L. Guzmán-Duque, G. Peñuela, I. González, J.L. Nava, R.A. Torres-Palma, Chemosphere 81 (2010) 26–32.
[111] J.H.B. Rocha, A.M.S. Solano, N.S. Fernandes, D.R. da Silva, J.M. Peralta-Hernández, C.A. Martínez-Huitle, Electrocatalysis 3 (2012) 1–12.
[112] S. Moţoc, F. Manea, A. Pop, A. Baciu, G. Burtică, R. Pode, Env. Eng. Manage. J. 12 (2013) 509–516.
[113] C.R. Costa, F. Montilla, E. Morallón, P. Olivi, Electrochim. Acta 54 (2009) 7048–7055.
[114] Y. Yavuz, A. Savaş Koparal, U.B. Öğütveren, J. Chem. Technol. Biotechnol. 86 (2011) 261–265.
[115] C. Ramírez, A. Saldaña, B. Hernández, R. Acero, R. Guerra, S. Garcia-Segura, E. Brillas, J.M. Peralta-Hernández, J. Ind. Eng. Chem. 19 (2013) 571–579.
[116] A. Solano Sales, C. Do Nascimiento Brito, D. Ribeiro Da Silva, C.A. Martínez-Huitle, ECS Trans. 43 (2012) 143–150.
[117] N. Bensalah, M.A. Quiroz Alfaro, C.A. Martínez-Huitle, Chem. Eng. J. 149 (2009) 348–352.
[118] N.E.H. Abdessamad, H. Akrout, L. Bousselmi, Desalination Water Treat. 51 (2013) 3428–3437.
[119] N.E.H. Abdessamad, H. Akrout, G. Hamdaoui, K. Elghniji, M. Ksibi, L. Bousselmi, Chemosphere 93 (2013) 1309–1316.
[120] C. Zhang, J. Wang, T. Murakami, A. Fujishima, D. Fu, Z. Gu, J. Electroanal. Chem. 638 (2010) 91–99.
[121] R. Bogdanowicz, A. Fabiańska, L. Golunski, M. Sobaszek, M. Gnyba, J. Ryl, K. Darowicki, T. Ossowski, S.D. Janssens, K. Haenen, E.M. Siedlecka, Diamond Relat. Mater. 39 (2013) 82–88.
[122] J.M. Aquino, M.A. Rodrigo, R.C. Rocha-Filho, C. Sáez, P. Cañizares, Chem. Eng. J. 184 (2012) 221–227.
[123] H. Akrout, L. Bousselmi, Arab. J. Geosci. 6 (2013) 5033–5041.
[124] M. Zhou, H. Särkkä, M. Sillanpää, Sep. Purif. Technol. 78 (2011) 290–297.
[125] A.M. Sales Solano, J.H. Bezerra Rocha, D. Ribeiro Da Silva, C.A. Martínez-Huitle, M. Zhou, Oxid. Commun. 35 (2012) 751–758.
[126] S. Ammar, M. Asma, N. Oturan, R. Abdelhédi, M.A. Oturan, Curr. Org. Chem. 16 (2012) 1978–1985.
[127] J.M. Aquino, G.F. Pereira, R.C. Rocha-Filho, N. Bocchi, S.R. Biaggio, J. Hazard. Mater. 192 (2011) 1275–1282.
[128] E. Hmani, Y. Samet, R. Abdelhédi, Diamond Relat. Mater. 30 (2012) 1–8.
[129] T. Panakoulias, P. Kalatzis, D. Kalderis, A. Katsaounis, J. Appl. Electrochem. 40 (2010) 1759–1765.
[130] X. Li, D. Pletcher, F.C. Walsh, Chem. Soc. Rev. 40 (2011) 3879–3894.
[131] C.A. Martínez-Huitle, E. Brillas, Angew. Chem. Int. Ed. 47 (2008) 1998–2005.
[132] E. Guinea, F. Centellas, E. Brillas, P. Cañizares, C. Saez, M.A. Rodrigo, Appl. Catal. B: Environ. 89 (2009) 645–650.
[133] L.V. Venczel, C.A. Likirdopulos, C.E. Robinson, M.D. Sobsey, Water Sci. Technol. 50 (2004) 141–146.
[134] H. Bergmann, T. Iourtchouk, K. Schops, K. Bouzek, Chem. Eng. J. 85 (2002) 111–117.
[135] M.E.H. Bergmann, J. Rollin, Catal. Today 124 (2007) 198–203.
[136] K. Rajkumar, M. Muthukumar, Environ. Sci. Pollut. Res. 19 (2012) 148–160.
[137] D.Z. Mijin, M.L. Avramov Ivić, A.E. Onjia, B.N. Grgur, Chem. Eng. J. 204–206 (2012) 151–157.
[138] L. Gomes, D.W. Miwa, G.R.P. Malpass, A.J. Motheo, J. Braz. Chem. Soc. 22 (2011) 1299–1306.
[139] L. Szpyrkowicz, C. Juzzolino, S.N. Kaul, S. Daniele, M.D. De Faveri, Ind. Eng. Chem. Res. 39 (2000) 3241–3248.
[140] L. Szpyrkowicz, R. Cherbanski, G.H. Kelsall, Ind. Eng. Chem. Res. 44 (2005) 2058–2068.
[141] D. Rajkumar, J.G. Kim, J. Hazard. Mater. B136 (2006) 203–212.
[142] D. Rajkumar, B.J. Song, J.G. Kim, Dyes Pigments 72 (2007) 1–7.
[143] C. Boxall, G.H. Kelsall, Inst. Chem. Eng. Symp. Ser. 127 (1992) 59–70.
[144] J.M. Aquino, R.C. Rocha-Filho, N. Bocchi, S.R. Biaggio, J. Appl. Electrochem. 40 (2010) 1751–1757.
[145] H. Akrout, L. Bousselmi, Desalination Water Treat. 46 (2012) 171–181.
[146] J.H.B. Rocha, M.B. Ferreira, N.S. Fernandes, C.A. Martínez-Huitle, ECS Trans. 43 (2012) 127–134.
[147] J.M. Aquino, R.C. Rocha-Filho, M.A. Rodrigo, C. Sáez, P. Cañizares, Water Air Soil Pollut. 224 (2013) 1397–1399.
[148] J.M. Aquino, K. Irikura, R.C. Rocha-Filho, N. Bocchi, S.R. Biaggio, Quim. Nova 33 (2010) 2124–2129.
[149] J.M. Aquino, R.C. Rocha-Filho, N. Bocchi, S.R. Biaggio, J. Environ. Chem. Eng. 1 (2013) 954–961.
[150] J.M. Aquino, R.C. Rocha-Filho, N. Bocchi, S.R. Biaggio, J. Braz. Chem. Soc. 21 (2010) 324–330.
[151] A. Mukimin, K. Wijaya, A. Kuncaka, Sep. Purif. Technol. 95 (2012) 1–9.
[152] F.A. Rodriguez, M.N. Mateo, R. Domínguez, E.P. Riveri, I. González, ECS Trans. 36 (2011) 529–538.
[153] N. Nordin, S.F.M. Amir, Riyanto, M.R. Othman, Int. J. Electrochem. Sci. 8 (2013) 11403–11415.
[154] S. Puttappa, V.T. Venkatarangaiah, Environ. Technol. 32 (2011) 1939–1945.
[155] P. Kariyajjanavar, N. Jogttappa, Y.A. Nayaka, J. Hazard. Mater. 190 (2011) 952–961.
[156] F. Zaviska, P. Drogui, J.F. Blais, G.J. Mercier, J. Appl. Electrochem. 39 (2009) 2397–2408.
[157] A. Oonnittan, M.E.T. Sillanpää, Curr. Org. Chem. 16 (2012) 2060–2072.
[158] A. Wang, Y.-Y. Li, J. Ru, J. Chem. Technol. Biotechnol. 85 (2010) 1463–1470.
[159] H. Lei, H. Li, Z. Li, Z. Li, K. Chena, X. Zhang, H. Wang, Process Saf. Environ. Protect. 88 (2010) 431–438.
[160] H.S. El-Desoky, M.M. Ghoneim, N.M. Zidan, Desalination 264 (2010) 143–150.
[161] N. Djafarzadeh, A. Khataee, M. Khosravi, M.R. Sohrabi, Fresenius Environ. Bull. 21 (2012) 4022–4029.
[162] A. Özcan, M.A. Oturan, N. Oturan, Y. Şahin, J. Hazard. Mater. 163 (2009) 1213–1220.
[163] M. Panizza, M.A. Oturan, Electrochim. Acta 56 (2011) 7084–7087.
[164] G. Zhang, S. Wang, F. Yang, J. Phys. Chem. C 116 (2012) 3623–3634.
[165] B. Kayan, B. Gözmen, M. Demirel, A. Murat Gizir, J. Hazard. Mater. 177 (2010) 95–102.
[166] Y. Fan, Z. Ai, L. Zhang, J. Hazard. Mater. 176 (2010) 678–684.
[167] E. Rosales, M. Pazos, M.A. Longo, M.A. Sanromán, Chem. Eng. J. 155 (2009) 62–67.
[168] E. Rosales, M.A. Sanromán, M. Pazos, Environ. Sci. Pollut. Res. 19 (2012) 1738–1746.
[169] W. He, X. Yan, H. Ma, J. Yu, J. Wang, X. Huang, Desalination Water Treat. 51 (2013) 6562–6571.

[170] Y. Lei, H. Liu, Z. Shen, W. Wang, J. Hazard. Mater. 261 (2013) 570–576.
[171] I. Siminiceanu, C.A. Alexandru, E. Brillas, Chem. Eng. Trans. 21 (2010) 79–84.
[172] C.I. Brînzilă, R. Ciobanu, E. Brillas, Environ. Eng. Manage. J. 11 (2012) 517–523.
[173] S. Garcia-Segura, A. El-Ghenymy, F. Centellas, R.M. Rodríguez, C. Arias, J.A. Garrido, P.L. Cabot, E. Brillas, J. Electroanal. Chem. 681 (2012) 36–43.
[174] F.C. Moreira, S. Garcia-Segura, V.J.P. Vilar, R.A.R. Boaventura, E. Brillas, Appl. Catal. B: Environ. 142–143 (2013) 877–890.
[175] K. Cruz-González, O. Torres-Lopez, A.M. García-León, E. Brillas, A. Hernández-Ramírez, J.M. Peralta-Hernández, Desalination 286 (2012) 63–68.
[176] E. Isarain-Chávez, C. de la Rosa, C.A. Martínez-Huitle, J.M. Peralta-Hernández, Int. J. Electrochem. Sci. 8 (2013) 3084–3094.
[177] O. García, E. Isarain-Chávez, S. Garcia-Segura, E. Brillas, J.M. Peralta-Hernández, Electrocatalysis 4 (2013) 224–234.
[178] L. Wang, J. Hazard. Mater. 171 (2009) 577–581.
[179] M. Magureanu, C. Bradu, D. Piroi, N.B. Mandache, V. Parvulescu, Plasma Chem. Plasma Process. 33 (2013) 51–64.
[180] J. Shang, F. Zhao, T. Zhu, Q. Wang, H. Song, Y. Zhang, Appl. Catal. B: Environ. 96 (2010) 185–189.
[181] J. Shang, Y. Zhang, T. Zhu, Q. Wang, H. Song, Appl. Catal. B: Environ. 102 (2011) 464–469.
[182] Q. Wu, J. Zhao, G. Qin, X. Wang, X. Tong, S. Xue, Water Sci. Technol. 66 (2012) 843–849.
[183] K. Esquivel, L.G. Arriaga, F.J. Rodríguez, L. Martínez, L.A. Godínez, Water Res. 43 (2009) 3593–3603.
[184] K. Esquivel, M.G. García, F.J. Rodríguez, L.A. Ortiz-Frade, L.A. Godínez, J. Appl. Electrochem. 43 (2013) 433–440.
[185] T. Frade, A. Gomes, M.I. da Silva Pereira, A. Lopes, L. Ciríaco, Quim. Nova 35 (2012) 30–34.
[186] M. Zhang, S. Yuan, Z. Wang, Y. Zhao, L. Shi, Appl. Catal. B: Environ. 134–135 (2013) 185–192.
[187] T.T. Guaraldo, T.B. Zanoni, S.I.C. de Torresi, V.R. Gonçales, G.J. Zocolo, D.P. Oliveira, M.V.B. Zanoni, Chemosphere 91 (2013) 586–593.
[188] O. Zhang, B.-Z. Lin, Y.-L. Chen, B.-F. Gao, L.-M. Fu, B. Li, Electrochim. Acta 81 (2012) 74–82.
[189] H. Qu, B. Lin, L. He, X. Fan, Y. Zhou, Y. Chen, B. Gao, Electrochim. Acta 87 (2013) 724–729.
[190] C. Ahmed Basha, R. Saravanathamizhan, P. Manokaran, T. Kannadasan, C.W. Lee, Ind. Eng. Chem. Res. 51 (2012) 2846–2854.
[191] M.M.S. Pupo, L.S. da Costa, A.C. Figueiredo, R.S. da Silva, F.G.C. Cunha, K.I.B. Eguiluz, G.R. Salazar-Banda, J. Braz. Chem. Soc. 24 (2013) 459–472.
[192] S. Garcia-Segura, S. Dosta, J.M. Guilemany, E. Brillas, Appl. Catal. B: Environ. 132–133 (2013) 142–150.
[193] H. Zhang, Y. Li, X. Zhong, X. Ran, Water Sci. Technol. 63 (2011) 1373–1380.
[194] R. Salazar, M.S. Ureta-Zañartu, J. Chilean Chem. Soc. 57 (2012) 999–1003.
[195] L.C. Almeida, S. Garcia-Segura, C. Arias, N. Bocchi, E. Brillas, Chemosphere 89 (2012) 751–758.
[196] A. Khataee, A. Khataee, M. Fathinia, B. Vahid, S.W. Joo, J. Ind. Eng. Chem. 19 (2013) 1890–1894.
[197] A.R. Khataee, B. Vahid, B. Behjati, M. Safarpour, Environ. Progr. Sustain. Energy 32 (2013) 557–563.
[198] A.R. Khataee, M. Zarei, L. Moradkhannejhad, Desalination 258 (2010) 112–119.
[199] A.R. Khataee, M. Zarei, A.R. Khataee, Clean 39 (2011) 482–490.
[200] E.J. Ruiz, A. Hernández-Ramírez, J.M. Peralta-Hernández, C. Arias, E. Brillas, Chem. Eng. J. 171 (2011) 385–392.
[201] R. Salazar, S. Garcia-Segura, M.S. Ureta-Zañartu, E. Brillas, Electrochim. Acta 56 (2011) 6371–6379.
[202] S. Garcia-Segura, L.C. Almeida, N. Bocchi, E. Brillas, J. Hazard. Mater. 194 (2011) 109–118.
[203] S.-H. Chang, K.-S. Wang, H.-H. Liang, H.-Y. Chen, H.-C. Li, T.-H. Peng, Y.-C. Su, C.-Y. Chang, J. Hazard. Mater. 175 (2010) 850–857.
[204] M. Taheri, M.R. Alavi Moghaddam, M. Arami, J. Environ. Manage. 128 (2013) 798–806.
[205] K.-S. Wang, M.-C. Wei, T.-H. Peng, H.-C. Li, S.-J. Chao, T.-F. Hsu, H.-S. Lee, S.-H. Chang, J. Environ. Manage. 91 (2010) 1778–1784.
[206] M. Chen, W. Ding, J. Wang, G. Diao, Ind. Eng. Chem. Res. 52 (2013) 2403–2411.
[207] Y. Juang, E. Nurhayati, C. Huang, J.R. Pan, S. Huang, Sep. Purif. Technol. 120 (2013) 289–295.
[208] L. Xu, Z. Guo, L. Du, J. He, Electrochim. Acta 97 (2013) 150–159.
[209] M. Siddique, R. Farooq, Z.M. Khan, Z. Khan, S.F. Shaukat, Ultrason. Sonochem. 18 (2011) 190–196.
[210] J. Wu, F. Liu, H. Zhang, L. Li, Desalination Water Treat. 44 (2012) 36–43.
[211] B. Bakheet, S. Yuan, Z. Li, H. Wang, J. Zuo, S. Komarneni, Y. Wang, Water Res. 47 (2013) 6234–6243.
[212] B. Boye, M.M. Dieng, E. Brillas, Electrochim. Acta 48 (2003) 781–790.
[213] E. Brillas, B. Boye, M.A. Baños, J.C. Calpe, J.A. Garrido, Chemosphere 51 (2003) 227–235.
[214] P. Ghosh, L.K. Thakur, A.N. Samanta, S. Ray, Korean J. Chem. Eng. 29 (2012) 1203–1210.
[215] M. Zarei, D. Salari, A. Niaei, A. Khataee, Electrochim. Acta 54 (2009) 6651–6660.
[216] M. Zarei, A. Niaei, D. Salari, A.R. Khataee, J. Electroanal. Chem. 639 (2010) 167–174.
[217] Y. Wang, H. Zhao, J. Gao, G. Zhao, Y. Zhang, Y. Zhang, J. Phys. Chem. C 116 (2012) 7457–7463.
[218] K. Zhao, G. Zhao, P. Li, J. Gao, B. Lv, D. Li, Chemosphere 80 (2010) 410–415.
[219] X. Ding, Z. Ai, L. Zhang, J. Hazard. Mater. 239–240 (2012) 233–240.
[220] Z. Liu, X. Xu, J. Fang, X. Zhu, B. Li, Water Air Soil Pollut. 223 (2012) 2783–2798.
[221] M. Iranifam, M. Zarei, A.R. Khataee, J. Electroanal. Chem. 659 (2011) 107–112.
[222] A.R. Khataee, M. Zarei, Desalination 273 (2011) 453–460.
[223] A.R. Khataee, M. Zarei, Desalination 278 (2011) 117–125.
[224] M. Zarei, A.R. Khataee, R. Ordikhani-Seyedlar, M. Fathinia, Electrochim. Acta 55 (2010) 7259–7265.
[225] A.R. Khataee, M. Zarei, R. Ordikhani-Seyedlar, J. Mol. Catal. A: Chem. 338 (2011) 84–91.
[226] A.R. Khataee, M. Zarei, S.K. Asl, J. Electroanal. Chem. 648 (2010) 143–150.
[227] A.R. Khataee, M. Safarpour, A. Naseri, M. Zarei, J. Electroanal. Chem. 672 (2012) 53–62.
[228] L. Liu, F.-B. Li, C.-H. Feng, X.-Z. Li, Appl. Microbiol. Biotechnol. 85 (2009) 175–183.
[229] R.-H. Liu, G.-P. Sheng, M. Sun, G.-L. Zang, W.-W. Li, Z.-H. Tong, F. Dong, M.H.-W. Lam, H.-Q. Yu, Appl. Microbiol. Biotechnol. 89 (2011) 201–208.